University of Southern Queensland

Faculty of Engineering and Surveying

Fracture Toughness of Glass Powder Reinforced Vinyl Ester Resin

A dissertation by

Geoffrey Korowa

In fulfilment of the requirements of

Courses ENG4111 and ENG4112 Research Project

Towards the degree of

Bachelor of Engineering (Mechanical)

Submitted: October, 2009

Abstract

Composite materials are widely used in industry. Composites are used because they utilise a combination of materials which allows cost to be lowered, while at the same time, giving a new material with improved properties.

The aim of this project was to determine which percentage of glass powder (by weight) would give the highest fracture toughness.

Specimens of vinyl ester resin were made, reinforced with glass powder at different percentages (by weight). The percentage composition of glass powder (by weight) was 0 % - 35 % in 5 % intervals. Six specimens of each percentage composition was made, therefore, forty (40) specimens were made. The samples were cured in ambient conditions. After curing, they were post cured in a conventional oven over a period of ten hours, at different temperatures. This ensured the resin had fully cured throughout the specimen. Short bar tests were performed on the specimens. Using the data obtained, the fracture toughness was determined.

Limitations of use

University of Southern Queensland

Faculty of Engineering and Surveying

ENG4111 Research Project Part 1 &
ENG4112 Research Project Part 2

Limitations of Use

The Council of the University of Southern Queensland, its Faculty of Engineering and Surveying, and the staff of the University of Southern Queensland, do not accept any responsibility for the truth, accuracy or completeness of material contained within or associated with this dissertation.

Persons using all or any part of this material do so at their own risk, and not at the risk of the Council of the University of Southern Queensland, its Faculty of Engineering and Surveying or the staff of the University of Southern Queensland.

This dissertation reports an educational exercise and has no purpose or validity beyond this exercise. The sole purpose of the course "Project and Dissertation" is to contribute to the overall education within the student's chosen degree programme. This document, the associated hardware, software, drawings, and other material set out in the associated appendices should not be used for any other purpose: if they are so used, it is entirely at the risk of the user.

Professor Frank Bullen
Dean
Faculty of Engineering and Surveying

Certification

I certify that the ideas, designs and experimental work, results, analysis and conclusions set out in this dissertation are entirely my own efforts, except where otherwise indicated and acknowledged.

I further certify that the work is original and has not been previously submitted for assessment in any other course or institution, except where specifically stated.

Geoffrey Korowa

Student Number: 0050027542

_____

Signature

_____

Date

Acknowledgements

I would like to thank all those involved with the completion of this project, and those who helped and guided me through the various stages.

Firstly, I would like to thank my Supervisor, Dr Harry Ku, whose help made this project as successful as it was. Thank you for your guidance and mentoring through this project. Your advice has made this project a great learning experience to complete my years at university.

I would also like to thanks Mohan Trada, whose technical experience has been a great help in the practical aspect of the project. The knowledge and skills you shared with me will be something I take with me after completing university.

Finally, I would like to thank the Faculty of Engineering and Surveying, as well as the Library for the equipment and resources provided.

Table of Contents

List of Appendices

List of Figures

List of Tables

1 Introduction

1.1 Introduction

This chapter will describe the purpose, background and processes involved in the project. The aim of this project is to find the percentage (by weight) of glass powder to vinyl ester resin, which will give the best fracture toughness.

1.2 Project Topic

Fracture toughness of glass powder reinforced vinyl ester resins post-cured in a conventional oven using short bar tests.

1.3 The Problem

Composites have a long history in industry, and with advances in production techniques, it is found to be an important aspect in the materials engineering field. It is used in a wide range of applications such as civil engineering, transport, aerospace and marine. Civil engineering applications are influenced mainly by cost, while the transport, aerospace and marine applications are mainly influenced by performance (Ku et al., 2008). In all the applications, cost will always play an important role. The cost in producing composites can be reduced with the introduction of fillers. Fillers not only reduce costs but also influence the structural properties of the composites. In this project, vinyl ester resin will be filled with glass powder at different percentages by weight to determine how much glass powder gives the best material properties. The samples will be cured in ambient conditions and then post cured in a conventional oven. The fracture toughness of the samples will be determined after

testing by short bar tests and analysis of the test results has been carried out (Munz, 1981)

1.4 Project Background

Composite materials are widely used in industry. Composites are used because they utilise a combination of materials which allows cost to be lowered, while at the same time, giving a new material with improved properties.

Vinyl ester resins have established and increasing uses in industry. They are regarded for their strong chemical, corrosion and heat resistant properties, as well as their mechanical properties namely fatigue performance and high elongation. The addition of fillers changes structural properties and reduces costs. It can also minimise cracking and decomposition of thick parts of components. The most commonly used filler for vinyl ester resin is Type E fibreglass, however, other materials such as graphite, aramid, olefin, and ceramic fillers may also be used (Blankenship et al., 1989).

1.5 Project Objectives and Aims

Adding glass powder will improve the structural properties of the composite. The aim of this project is to find what percentage of glass powder will give the optimum mechanical property that is fracture toughness. The percentage composition of glass powder (by weight) will be the same as previous studies; these are 0 % - 35 % in 5 % intervals. The samples will also include an accelerator to assist the curing. For an example, take the production of 100 grams of a 10% sample. 10% of the sample i.e. 10 grams, will be powder, and 90% i.e. 90 grams, will be resin with accelerator. The 90 grams will consist of 2% accelerator, i.e.1.8 grams. The success of a test depends on the repeatability of the results; therefore, six specimens will be made for each percentage sample.

In this project, the resin used will be the vinyl ester resin, Hetron 922 produced by Huntsman Composites, a division of Huntsman Chemical Company Australia Pty Ltd (Huntsman Composites, 2001). The accelerator used is methyl ethyl ketone peroxide (MEKP); this is an established and recommended accelerator (Blankenship et al., 1989).

Production of the samples will involve mixing the materials at room temperature. The mixture will then be poured into moulds of specified geometries, and allowed to cure in room temperature. After curing, the samples will be taken out of the moulds and post cured in a conventional oven. They will be post cured for four hours at 50° Celsius, then four hours at 80° Celsius, and finally two hours at 100° Celsius.

To determine the fracture toughness, short bar tests will be used to test the samples. This will involve simply applying a tensile stress at the mouth of the samples and recording the peak loads. The samples will be tested using the Universal Testing Machine. The peak load will be determined, and with the peak load, the fracture toughness can then be found. The results can then be compared to previous studies for verification and comparison.

2 Literature Review

2.1 Introduction

This chapter will describe in detail the relevant literature involved in the undertaking of this project. This chapter will provide details about the materials used, curing and post curing, fracture mechanics and the short bar method, and testing.

The majority of the information in this chapter comes from published sources such as texts, and journals. Other sources of information are USQ study materials and previous reports by students. Also, Material Safety Data Sheets (MSDS) are supplied by companies for use with their products.

2.2 Introduction to Vinyl Ester Resins

Vinyl esters are thermosetting resins that are successfully and continually being used in industrial applications. Its continued utilisation is due to its thermal, mechanical, and chemical resistant properties, which prove to be good quality when compared with its relatively low cost. Vinyl ester resin is formed from the reaction of a multifunctional epoxy resin and ethylenically unsaturated monocarboxylic acid. The product of this reaction is dissolved in styrene and gives a thermosetting liquid with a low viscosity which can be cured by radical polymerisation when peroxides (e.g. MEKP) are introduced. Copolymerisation of the styrene with the unsaturated vinyl ester resin produces a three-dimensional structure which can elongate along the length of the epoxy chain. This allows high elongation under mechanical and thermal stress; it allows high elongation, fatigue resistance, and good thermal resistance (Blankenship et al., (1989).

Properties of vinyl ester resins can vary depending on various factors. These factors include (Blankenship et al., 1989):

1. Epoxy resin structure, which determines mechanical and thermal properties, as well as corrosion;
2. The unsaturated acid, which affects reactivity and chemical resistance; and
3. The diluting monomer, which affects viscosity, reactivity, and chemical resistance

Vinyl esters are more costly than polyesters, and because of this, they are more often used in applications that specifically require superior corrosion, thermal, and fatigue properties. Different techniques are used to manufacture corrosion resistant tanks, piping, ducts, and a wide range of fittings. Aggregate and sand mixtures with vinyl ester resins form strong, chemically resistant polymer concrete used in waste handling applications. High volume fabrication techniques take advantage of vinyl esters low viscosity and adjustable curing time in the production of composites of automotive, industrial and military applications (Blankenship et al., 1989). It is evident from these applications that vinyl esters are a player in the composites field.

2.3 Vinyl Ester Resin Used

The vinyl ester resin used in this investigation is Hetron 922. It was first introduced into the United States in the mid 1960's as a Shell Chemical Co. product, and has since become a well established resin. There are two variations of Hetron 922; these are Hetron 922PAW, used in winter and Hetron 922PAS, used in summer. The main difference between the two is the gel time variation with respect to temperature. Both Hetron 922 PAW and PAS have been developed for exceptional protection in corrosion as well as chemical resistance applications.

Some of the features of Hetron 922 include (Sweet, 2002),

- Excellent corrosion and chemical resistance;
- Excellent impact strength;
- High tensile elongation; and
- FDA compliance for food contact (FDA regulation Title CFR 177.2420)

Some applications include corrosion resistant tanks, pipes, vats, vessels, pumps, and other equipment, as well as coatings and linings.

It is recommended that post curing is done for maximum chemical and heat resistance.

2.4 Vinyl Ester Resin and Catalyst

The curing of vinyl ester resin is attained by radical polymerisation with a peroxide. Methyl Ethyl Ketone Peroxide (MEKP) is an organic peroxide that is commonly used with vinyl ester resin; this is the catalyst (or accelerator) used for the polymerisation of the vinyl ester resin. The ratio of resin to catalyst was selected to be 98% to 2%. This is recommended for boat layups at moderate temperatures, i.e. 20° to 25°C (Sweet, 2002).

2.5 Glass Powder

Glass powder is made of fused inorganic oxides, and is spherical and non-porous. They are used to improve the performance and reduce viscosity in paints and coatings. Glass powder is also a common lightweight additive in plastic components. Glass powder is chemically inert, meaning they do not react with chemicals, and also has very low oil absorption. Table 2.1 shows typical properties of glass powder.

Table 2.1: Typical properties of Glass Powder

Typical Properties	
Shape	Spherical
Colour	White
Composition	Proprietary Glass
Density	1.1 g/cc and 0.6g/cc
Particle Size	Mean Diameter 11 and 18 microns
Hardness	6 (Moh's Scale)
Chemical Resistance	Low alkali leach/insoluble in water
Crush Strength	>10,000 psi

The addition of glass powder to epoxy, compounds, fibreglass reinforced plastics, and urethane castings lowers costs and also gives weight reduction. It also improves impact resistance. Glass powder hollow spheres have insulating properties and improve thermal shock and heat affected areas.

2.6 Glass Powder Used

Glass powder is the filler used in this project. The glass powder used is SPHERICAL® 60P18 Hollow Glass Spheres, manufactured by Potters Industries Inc. Table 2.2 gives properties of SPHERICAL® 60P18 Hollow Glass Spheres.

Table 2.2: Properties of SPHERICAL® 60P18 Hollow Glass Spheres

True Density (g/cc)		0.60
	Mean volume	16-20
Particle Size (µm)	D10	6-10
	D50	15-19
	D90	28-32
Working Pressure	10 Volume % Loss	8,000psi
Appearance		White powder
Composition		Fused Inorganic Oxides
Shape		Spherical, Non-Porous

2.7 Fracture Toughness

Fracture toughness is the ability of a material containing a flaw to withstand an applied load. Unlike the results of an impact test, fracture toughness is a quantitative property of a material (Askeland, 1998). Once calculated, fracture toughness can be used to determine the load a structure can withstand before it fails catastrophically as a result of fracture. A typical fracture toughness test may be done by applying a tensile force to a specimen with a known geometry and size. Figure 2.1 shows a tensile force being applied to two blocks, one with an edge flaw, (a), and one with an internal flaw, (b). The flaws are where the stress is intensified when they are applied to the materials (Askeland, 1998).

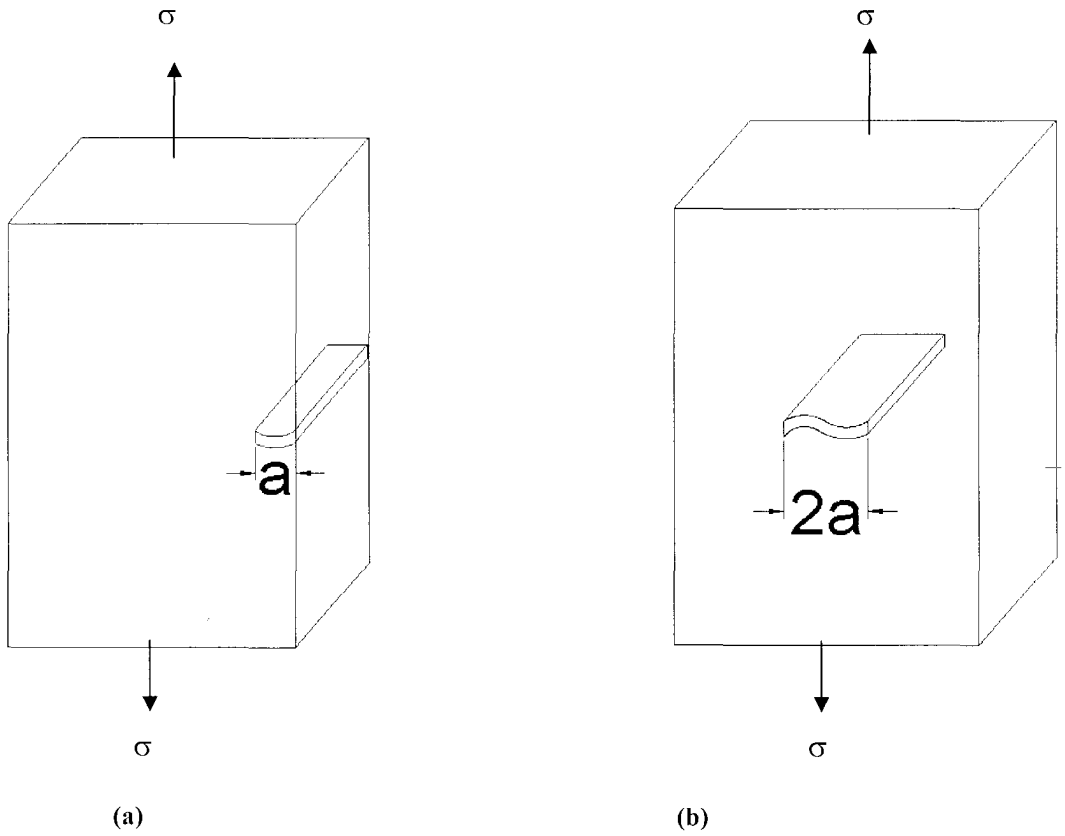

Figure 2.1: Schematic Drawing of Fracture Toughness Specimens with Edge and Internal Flaws

Applying fracture mechanics to figure 2.1, the stress intensity factor, K, is defined as,

$$K = f\sigma\sqrt{\pi a} \tag{1}$$

where f is the geometry factor of the specimen and flaw, σ is the applied stress, and a is the flaw size. If the dimension of the flaw size is known, tests can be performed to determine the K value which causes a crack to grow and fail. This is known as the critical stress intensity factor, and is given as,

$$K_c = f\sigma_c\sqrt{\pi a} \tag{2}$$

The critical stress intensity factor, K_c, of a material is defined as its fracture toughness, and has the units MPa $\sqrt{m}$; K_c is the K required to propagate a crack (Ku et al., 2006; 2007; 2008).

For specimens where the width is assumed 'infinite', the geometry factor, f = 1; for samples with 'semi-infinite' width, f = 1.1 (Askeland 1998). Fracture toughness of thin specimens will depend on the specimen thickness, but as thickness increases, the thickness will have less effect on the fracture toughness.

2.8 Plane Strain Fracture Toughness

Plane strain exists when a specimen's thickness is large enough that the crack's size will not influence the specimens fracture toughness. In plane strain, there will be no resulting strain perpendicular to the front and back faces of the sample. This means the load will be purely a tensile load, also known as mode I loading (Juvinall & Marshek, 2001). The fracture toughness will become the plane strain fracture toughness, i.e. K_c will be K_{Ic}.

$$K_{Ic} = f\sigma\sqrt{\pi a} \tag{3}$$

Brittle materials have low K_{Ic}, while ductile materials have high K_{Ic} values. Plane strain fracture toughness is an important property and can be affected by a number of factors including, temperature, microstructure, and strain rate. K_{Ic} decreases with increase strain rate, and decrease temperature (Askeland 1998).

2.9 Short Rod and Short Bar Method

2.9.1 Introduction to Short Rod and Short Bar Method

The fracture toughness of a material is determined using the ASTM standard, ASTM E 399-78. This standard requires the maximum load a material can take before failure. The short rod or short bar method is the preferred method of finding the peak load a specimen reaches before breaking. The short rod and short bar methods were mainly developed to determine the fracture toughness of brittle materials (Barker, 1977). The short rod method uses a circular cross section specimen, while the short bar method has a rectangular cross section. Selection of the geometry to be used depends on manufacturing equipment available. It may be used on a number of materials including metals, ceramics, polymers and rocks (Barker, 1981). This method is preferred because it uses a real crack, as well as reducing the size of the specimen. The short rod and short bar methods reduce the cost of testing and also eliminates residual stresses since no fatigue pre-cracking is required (Barker, 1980).

2.9.2 Short Rod and Short Bar Geometry

There are four configurations for the geometry of the short rod and short bar methods; two for short rod, and two for short bar method. These different geometries allow the accurate calculation of the peak load for different production methods of the specimens. The geometries are shown in figures 2.2(a), 2.2(b), 2.3(a) and 2.3(b). Figures 2.2(a) and 2.2(b) show the short rod and short bar geometries with straight chevron slots. These are made by feeding the saw blade through the specimen. Figures 2.3(a) and 2.3(b) show short rod and short bar geometries with curved chevron slots. These slots have been made by plunging the saw blade into the specimen (Barker, 1981).

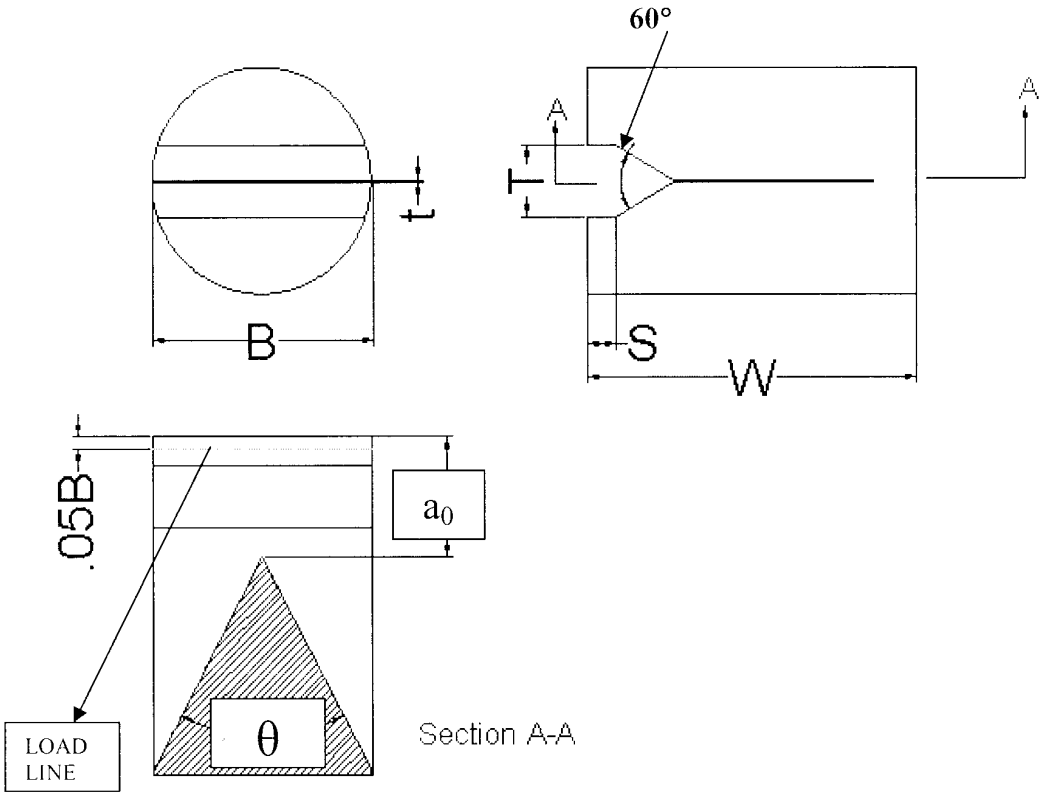

SYMBOL	DEFINITION	VALUE	TOLERANCE
B	DIAMETER	B	
W	LENGTH	1.5B	± .010B
a_0	INITIAL CRACK LENGTH	0.513B	± .005B
θ	SLOT ANGLE	55.2°	± 1/2°
T	SLOT THICKNESS	SEE TABLE III (of Barker, 1981)	
S	GRIP GROOVE DEPTH	.130B	± .010B
T	GRIP GROOVE WIDTH	.313B	± .005B
R	RADIUS OF SLOT CUT	SEE FIGURE 4 (of Barker, 1981)	± 2.5

Figure 2.2(a): Short Rod Specimen with straight chevron slots.

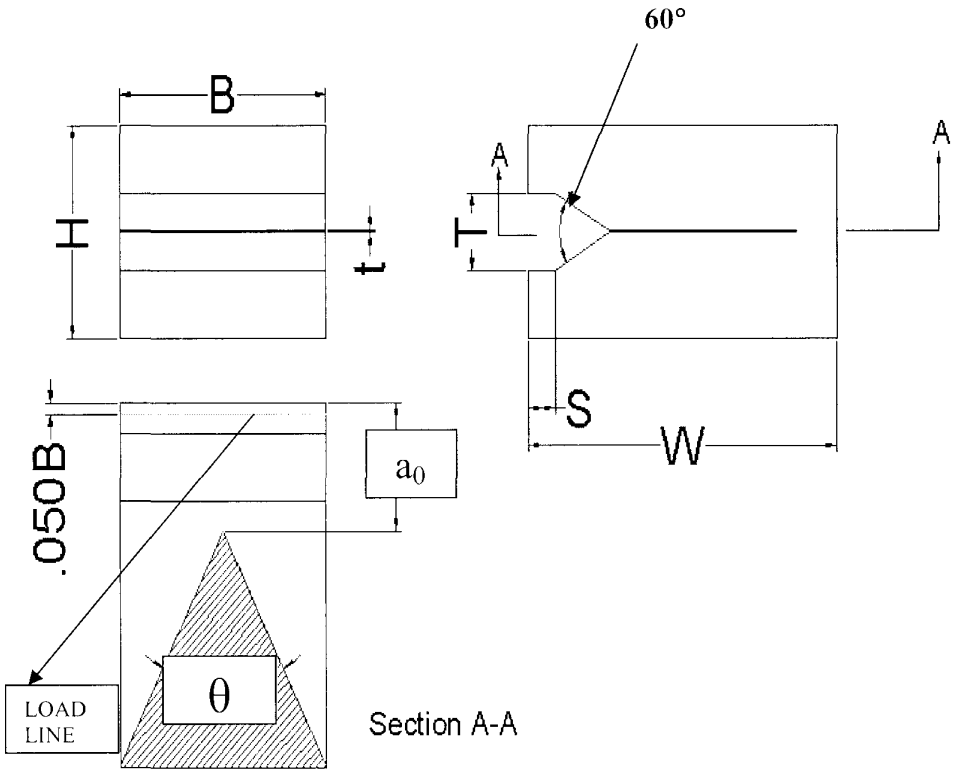

SYMBOL	DEFINITION	VALUE	TOLERANCE
B	BREADTH	B	
W	LENGTH	1.5B	± .010B
H	HEIGHT	.870B	± .005B
a_0	INITIAL CRACK LENGTH	.513B	± .005B
θ	SLOT ANGLE	55.2°	± 1/2°
T	SLOT THICKNESS	SEE TABLE III (of Barker, 1981)	
S	GRIP GROOVE DEPTH	.130B	± .010B
T	GRIP GROOVE WIDTH	.313B	± .005B
R	RADIUS OF SLOT CUT	SEE FIG 4 (of Barker, 1981)	±2.5B

Figure 2.2(b): Short Bar Specimen with straight chevron slot.

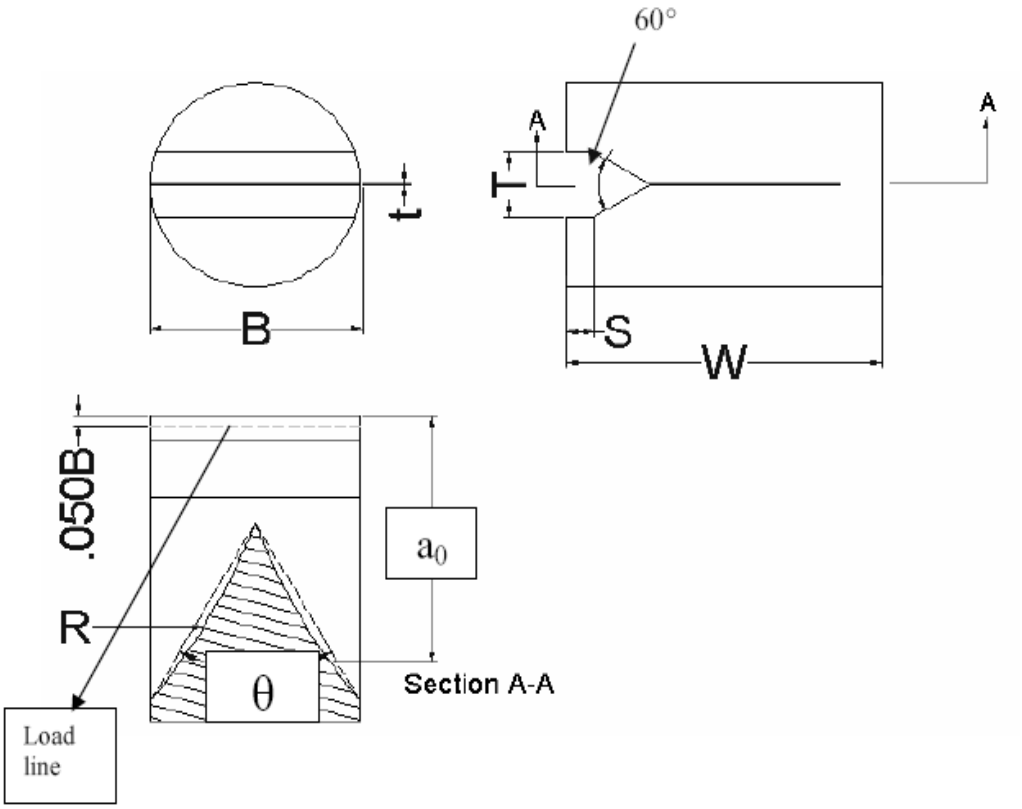

SYMBOL	DEFINITION	VALUE	TOLERANCE
B	DIAMETER	B	
W	LENGTH	1.5B	± .010B
a_0	INITIAL CRACK LENGTH	.513B	± .005B
θ	SLOT ANGLE	55.2°	± 1/2°
T	SLOT THICKNESS	SEE TABLE III (of Barker, 1981)	
S	GRIP GROOVE DEPTH	.130B	± .010B
T	GRIP GROOVE WIDTH	.313B	± .005B
R	RADIUS OF SLOT CUT	SEE FIG 4 (of Barker, 1981)	

Figure 2.3(a): Short Rod Specimen with curved slot.

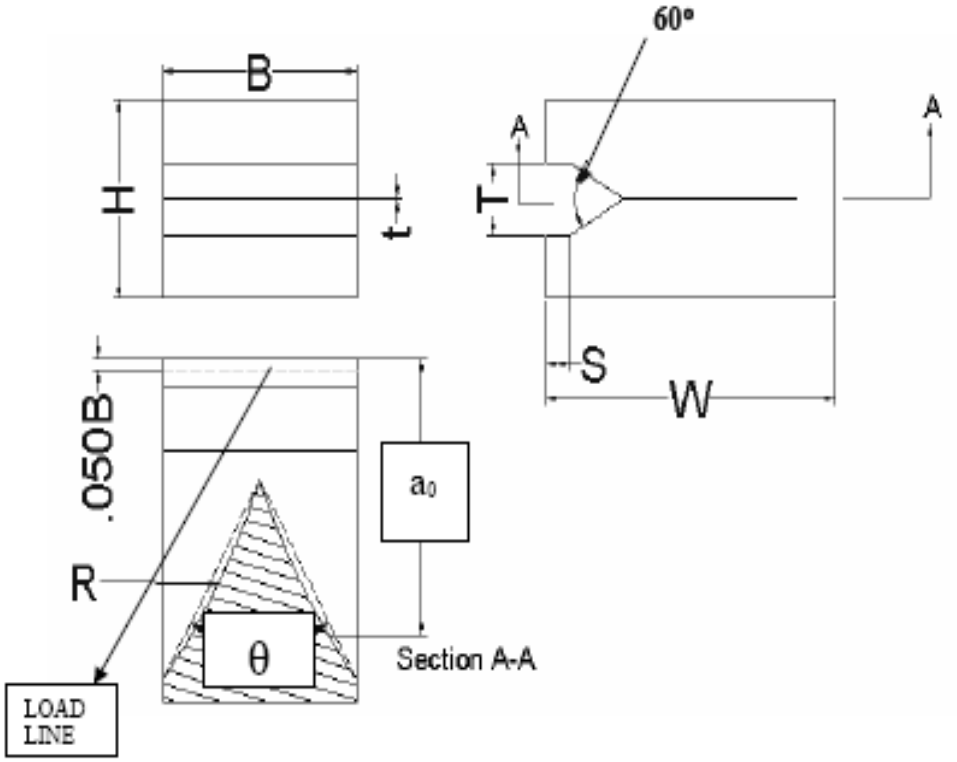

SYMBOL	DEFINITION	VALUE	TOLERANCE
B	BREADT	B	
W	LENGTH	1.5B	± .010B
H	HEIGHT	.870B	± .005B
a_0	INITIAL CRACK LENGTH	.513B	± .005B
ANG	SLOT ANGLE	55.2°	± 1/2°
T	SLOT THICKNESS	SEE TABLE III (of Barker, 1981)	
S	GRIP GROOVE DEPTH	.130B	± .010B
T	GRIP GROOVE WIDTH	.313B	± .005B
R	RADIUS OF SLOT CUT	SEE FIG 4 (of Barker, 1981)	

Figure 2.3(a): Short Rod Specimen with curved slot.

Figure 2.4 shows a more detailed diagram of the cross section of the short bar specimen.

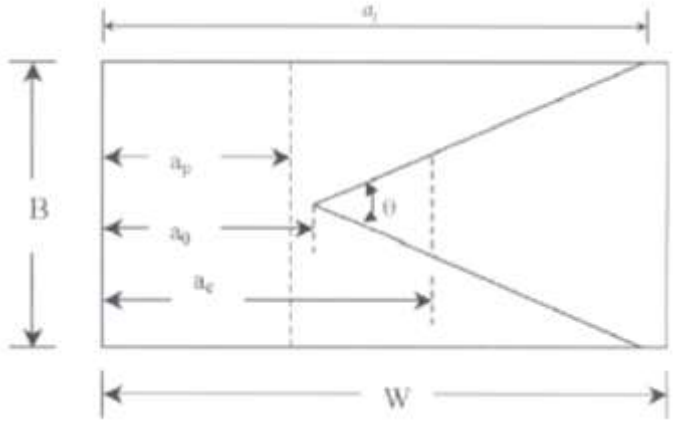

Figure 2.4: Cross-section dimensions of short bar specimen

2.9.3 Short Rod and Short Bar Calibration

The plan views of the short rod and short bars are identical. The short bar specimen's height (0.870B) was selected so the compliance derivative with respect to the crack length would be equivalent to that of the short rod specimens. Therefore, the short rod and short bar calibrations should be equal. Barker (1979) carried out experiments that showed that the two specimens can be considered to be equal. It is also necessary to have equal calibrations for the straight and curved chevron slot specimens. This can be done accurately by superimposing the plan views of the two configurations on top of each other, and adjusting the slot configurations until the straight edge and slot edge are tangential to each other at the location of the critical crack length, a_c, as shown in figure 2.5. This is where the fracture toughness measurement is taken, thus the crack is near the location where the fracture toughness measurement is to be taken. Both configurations have approximately the same crack-front width, rate of change of crack-front width, and compliance derivative, which causes their calibrations to essentially be equivalent (Barker 1981).

When machining the chevron slots in a curved specimen, it is much easier to do so by measuring the distance to the point of the chevron slot, a_o, and the angle θ (Figure 2.4) than to see directly whether the slots pass through the tangent points correctly. Therefore, the values of a_o and θ have been calculated as a function of the diameter of the saw blade used to cut out the slots. By using these dimensions, the specimen calibration is virtually always constant, regardless of specimen size. Figure 2.6 shows the functions plotted against each other.

Slot thickness plays an important role in the determination of the samples plane strain fracture toughness. For a material to be in plane strain there must be no forces acting perpendicular to the force applied. Therefore, any crack which intersects a lateral surface cannot be in perfect plane strain; any lateral surface is in plane stress rather than plane strain. However, the condition changes from plane stress to plain strain as distance from the free surface increases (Barker, 1981). Hertzberg (1976) determined that the non-plane strain region detrimental because metal tougher in plain stress than in plane strain. Thus, any attempt to measure plain strain fracture toughness in specimens with non plain strain regions at the sides of the cracks can result in high values of fracture toughness. One can see that reducing non plane strain regions can be done by not allowing not allowing the crack to intersect the lateral surface at all, but by using the thin slots (such as those in short bar specimens) to guide the crack. To determine the magnitude that non plane strain effects had on the short rod specimens, a study was carried out to test the effects of slot thickness, and sharpness of the slot bottom. The test involved two aluminium and three steel materials in a range of crack sizes, and crack tip variations. The results of the study indicated the effect on the specimen calibration, the slot configuration with slot thickness had. The slot configuration study showed that the properly designed slots significantly improved the amount of plane strain constraint along the crack front. Table 2.3 shows the summary of the slot geometry study.

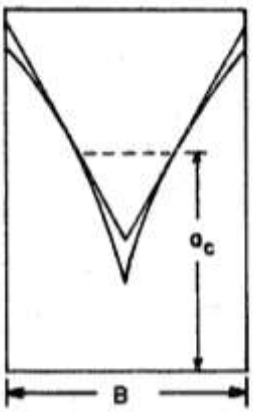

Figure 2.5: Curved and straight chevron slots superimposed. Tangent at critical crack length, a_c

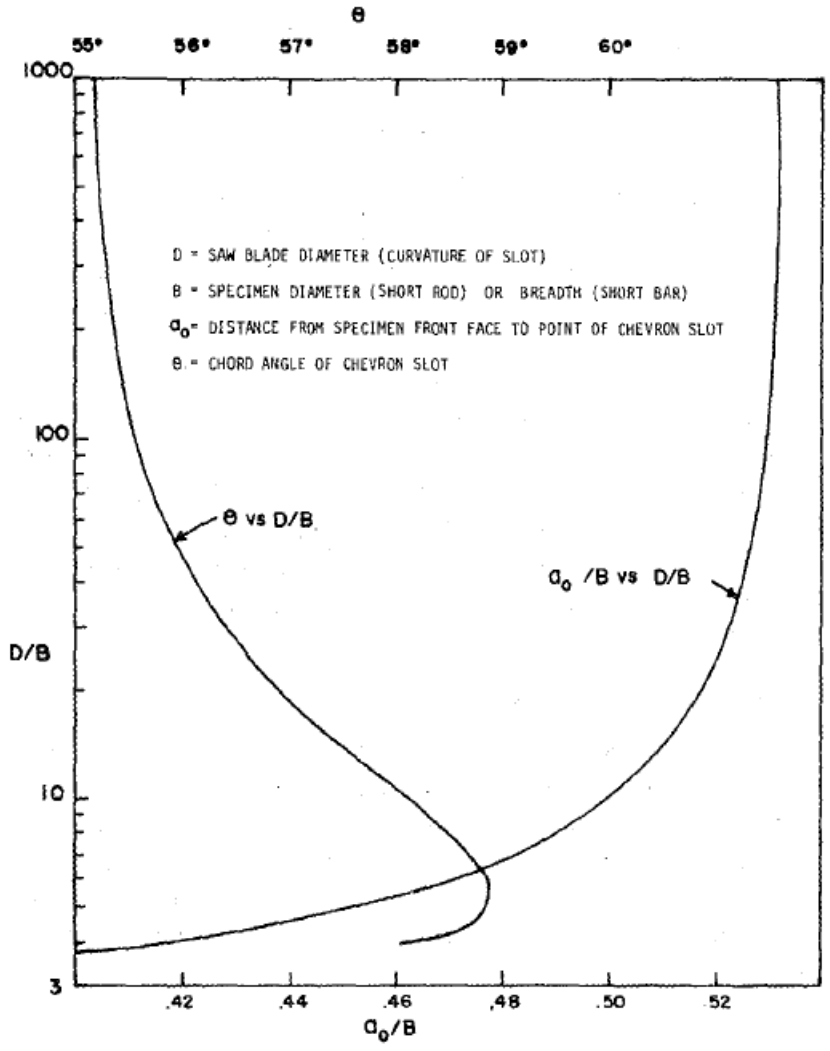

Figure 2.6: Chevron angle θ and initial crack length a_o for curved chevron slot specimens

Table 2.3: Summary of slot geometry study results (Barker, 1981)

SLOT CONFIGURATION	SLOT THICKNESS (mm)	EFFECT ON SPECIMEN CALIBRATION	PLANE-STRAIN CONSTRAINT*
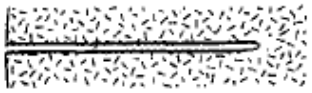	0.38	0	Excellent
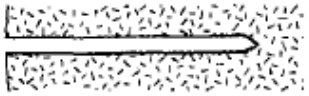	0.8	-1%	Excellent
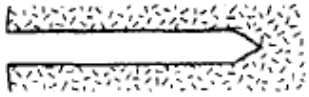	1.6	-3%	Excellent
	0.38	0	Excellent
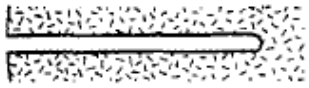	0.8	-1%	Good
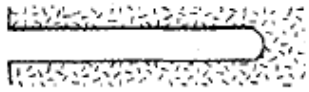	1.6	-3%	Poor
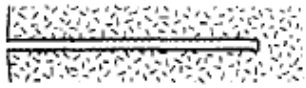	0.38	0	Good
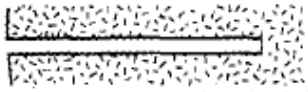	0.8	-1%	Poor
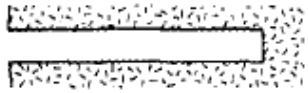	1.6	-3%	Poor

* Excellent = less than +2% effect on the measurement
Good = less than +5% effect on the measurement
Poor = more than +5% effect on the measurement

2.9.4 Short Bar Testing

This project will use the short bar method. The short bar test requires an initial load to be applied at the mouth of the specimen which causes the crack to initiate at the

tip of the chevron slot. The load is applied continually at the specified rate, until the length of the crack reaches the critical crack length, a_c. This is the breaking point of the specimen, and is the point where the peak load occurs. The load should decrease after this point. Figure 2.7 shows the cross section of the specimen along with the variation of load versus crack length.

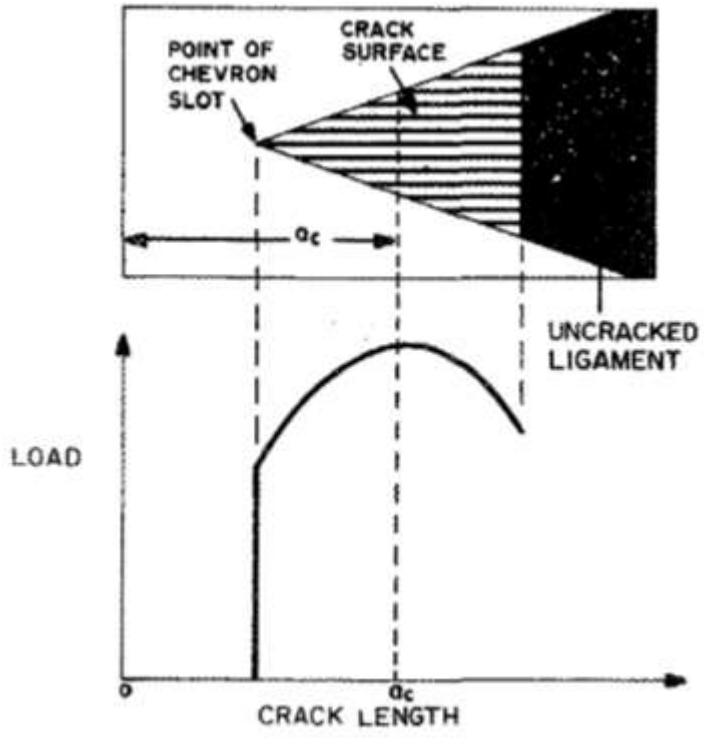

Figure 2.7: Load applied vs. crack length

2.10 Determining Fracture Toughness

Determining fracture toughness using the short bar method is done using basic fracture mechanics, and the assumptions of linear elastic fracture mechanics. The plane strain critical stress intensity factor of a material, using the short bar method, K_{IcSB}, is defined as (Munz, 1981),

$$K_{IcSB} = \frac{F_{max} Y_m^*}{B\sqrt{W}}$$

where F_{max} = Peak load

Y_m^* = Compliance calibration according to ASTM E-399-78

B = Sample breadth

W = Sample width

The compliance calibration, Y_m^*, is calculated according to ASTM E-399-78. It is given by the equation (Munz, 1981),

$$Y_m^* = \{-0.36 + 5.48\omega + 0.08\omega^2 + (30.65 - 27.49\omega + 7.46\omega^2)\,\alpha_0$$

$$+ (65.90 + 18.44\omega + 9.76\omega^2)\,\alpha_0^2\} \left\{\frac{(\alpha_1 - \alpha_0)}{(1 - \alpha_0)}\right\}^{\frac{1}{2}}$$

where $\omega = \frac{W}{H}$; $\alpha_0 = \frac{a_0}{W}$; $\alpha_1 = \frac{a_1}{W}$.

The values of a_0 and a_1 are shown in Figures 2.2(a), 2.2(b), 2.3(a) and 2.3(b).

2.11 Curing and Post Curing

The samples will be cured at room temperature. For this, promoters (or accelerators) must be added to the resin to induce decomposition of the peroxides forming free radicals. This will ensure an adequate rate of curing. Certain metallic soaps and tertiary amines are effective accelerators; however, the most common is methyl ethyl ketone peroxide (MEKP). If a sufficient exothermic reaction is achieved, green strength develops rapidly. With this is mind, post-curing will give optimum properties. A strong exotherm can result in cracking and possibly also decomposition. An alternative would be to use benzyl peroxide and dimethyl aniline;

this also gives faster curing times and is less sensitive to moisture effects (Blankenship et al., 1989).

2.12 Scanning Electron Microscope Analysis

2.12.1 Introduction to Scanning Electron Microscopy

Scanning electron Microscopy enables detailed imaging and analysis of surfaces of specimens. Samples usually need preparation before they may be examined due to the size and functional requirements of the scanning electron microscope (SEM). Ideally, samples should be clean, dry, conductive, and able to generate a signal. The size of a sample should ideally be one to two centimetres in diameter; samples large than this should be cut to smaller sizes. Samples with biological origins require more preparation than samples with non-biological samples; however, some non-biological specimens such as water pipes may contain traces of micro-organisms, thus classing that specimen as biological.

2.12.2 Cleaning Sample surfaces

Scanning electron microscopy analyses the surface of samples, so a good surface is important. A surface may be altered by undesired deposits of debris, silt, oil, wax, etc, so unless these deposits are important in the analysis, they will have to be removed. Removal of these deposits can be done by buffer rinse, solvent wash, physical removal, or enzymatic treatment. The method depends on the characteristics of the deposit and the sample.

2.12.3Dehydration of Samples

Any water in a sample will evaporate in the SEM causing damage to the sample, as well as contaminating the microscope; therefore, water has to be removed. There are a number of methods of removing water from a sample.

Air drying is suitable for most samples obtained from aqueous environments. However, if micro-organisms are present in the sample, they must be treated as biological and treated accordingly.

Solvent drying will dehydrate the sample and replace the water with the solvent. Ethanol, methanol and acetone are commonly used solvents. The solvents may be air dried, depending on the nature of the samples.

Critical point drying is the standard method for drying biological samples. It may also be used in some non-biological samples. Special equipment known as a critical point dryer is required.

Freeze drying is a less common method. Special equipment is required. The samples are frozen to -80 degrees Celsius and placed in a vacuum at low pressure, where the ice turns into vapour and is removed by the vacuum. This method is slow.

2.12.4 Coating Samples

When using scanning electron microscopy, the sample surface must be electrically and thermally conductive. Conductivity can be improved by coating the sample with a thin film of metal or carbon. This layer is usually 10-25 nm thick. A carbon coating is used if elemental analysis, while topographical imaging uses gold, platinum, or gold/palladium coatings.

Heat can build up from the electron beam and may damage the sample. Charge can also build up and repel the incident electron beam resulting from a loss of signal from the sample. The charge build up can result in bursts and deflections of the

electron beam and cause charging or flaring. The coating must be continuous to prevent the build up of charges in a sample. Samples consisting of lower atomic number elements (i.e. less reactive elements) tend to have insufficient secondary electrons and a metal coating is a good source of these electrons to give a good signal.

Sputter coating is used to gold coat samples. It allows all exposed areas of the sample to be coated, as it is a non-directional coating method.

Vacuum evaporation coating is used to carbon coat samples. It is a directional method and only coats the surfaces in direct line with the evaporative source. This method is therefore suitable for flat surfaces.

2.12.5 Sputter Coating

Sputter coating occurs in a low vacuum where an inert gas (e.g. Argon) is exposed into a high voltage field, typically between 1-3 kilovolts. The Argon gas molecules become ionised and become attracted to a metal target, typically gold foil. This gold foil creates the gold coating. Gold atoms become dislodged from the gold foils target, and interact with the argon, forming a cloud. The gold atoms deposit on the sample, coating it evenly. Figures 2.8 and 2.9 show the setup of the sputter coater, and a representation of the sputter coater chamber.

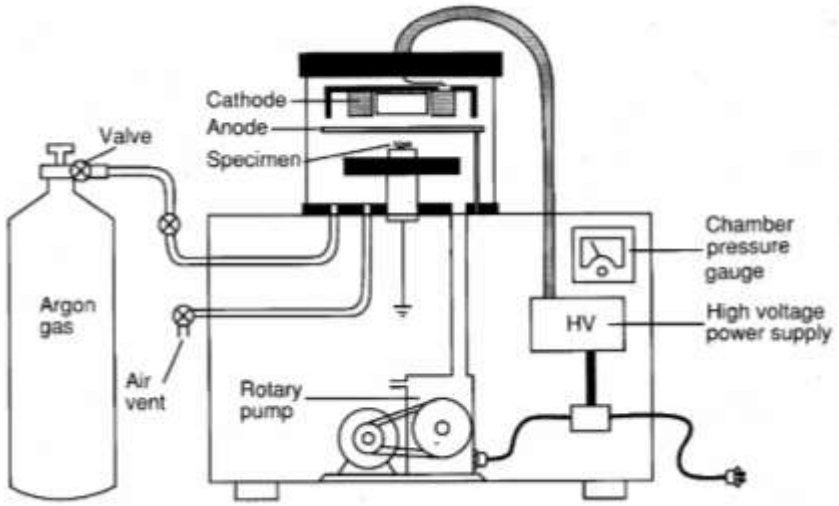

Figure 2.8: Setup of the Sputter Coater

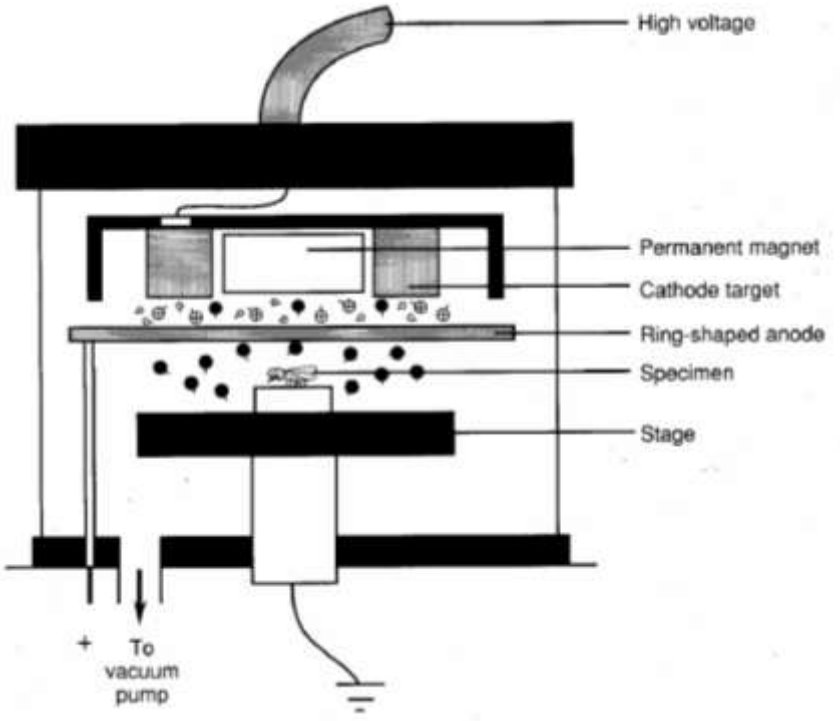

Figure 2.9: Sputter Coater chamber with a specimen

2.13 Works of Others

Similar work has previously been done, where the fracture toughness of different composite specimens were determined. The materials used in the previous composite are different. The resin and filler were phenol formaldehyde and envirospheres (E-spheres), abbreviated, PF/E-SPHERES (X %) where X was the percentage by weight of filler. Although a different composite was used, the method used to find the fracture toughness was the same as in this study. The short bar test was used in both studies to determine the fracture toughness of the composites. The results are provided to give a comparison on the studies. Table 2.4 shows the results of the fracture toughness of different percentages by weight of SLG reinforced phenolic resin. These results are plotted in Figure 2.8.

Table 2.4: Fracture toughness of different percentages by weight of slg reinforced phenolic resin

Percentage by weight of slg	0	15	20	25	30	35
Fracture toughness MPa√m	8.72	10.5	12.5	9.62	8.82	8.12
(Standard deviation)	(1.94)	(0.80)	(0.16)	(0.24)	(0.36)	(0.67)

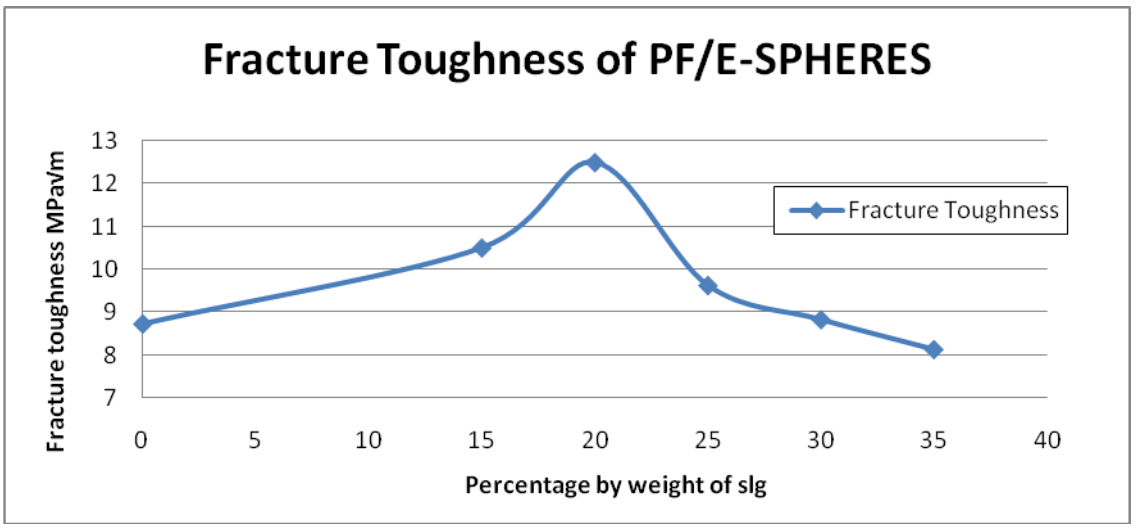

Figure 2.10: Fracture toughness of PF-E-SPHERES with varying percentages by weight of slg

[Ku, H, Rogers, D, Davey, R, Cardona, F and Trada, M 2007]

3 Project Methodology

3.1 Introduction

This chapter will outline the process involved in the preparation, production, curing and post-curing, testing, and microscopic analysis of the samples. The underlying method implemented in this project was intentionally kept similar to previous years methods for the purpose of obtaining repeatable results. These processes were demonstrated in reports previously done by students, which were provided by the supervisor as a guide. Elements such as the materials, mould, and post curing were among the aspects kept constant. Production techniques have improved to give the best possible samples with the least possible defects. Production technique is something that can change, but the main aim of the specimen production was kept in sight.

3.2 Mould and Mould Preparation

The mould used in this project was the same as the mould used in previous year projects. This was to ensure the repeatability of results. The mould is made of Poly-vinyl chloride (PVC) which is essentially a plastic. The advantage of this is that it is tough, easy to construct, will hold its shape during curing, and has a slightly slippery surface allowing the cured mould to be removed with ease.

The mould consists of seventeen separate parts. One bottom plate, two side plates, seven separating pieces (including two end pieces), one covering piece, and six triangular pieces attached to the covering piece, which create the chevron slot openings. This mould does not include the chevron slots. The chevron slots are made of cardboard, and are glued onto the triangular pieces and positioned into the mould spaces. They are positioned so they divide most of the mould space in two. They, in

effect, represent the cracks in materials. The final mould (ready for sample production) is the combination of the mould, and the chevron sots.

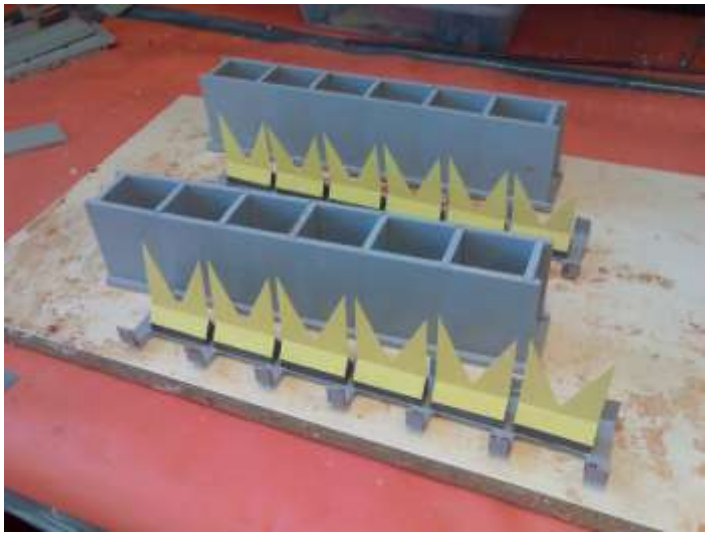

Figure 3.1: Total mould assembly with chevron slots

Before the mould is assembled, it was important to prep them. Prepping the moulds includes cleaning them and lubricating them. Cleaning the mould is very important. Because other students use the same moulds, this means they have different materials left on them. Cleaning these materials will ensure there will be no contamination in the specimens being made. The moulds were cleaned by scraping off older dry flakes left over from previous castings, and wiping clean and dry using a paper towel. After the moulds were cleaned, they were lubricated. Lubrication can be done by two methods; using canola spray or applying wax. Canola spray is the easier method, however, it has disadvantages. If too much is applied, the excess will affect the specimens shape and composition during curing. For this reason, waxing the moulds was seen to be the best option for lubrication. The wax had to be rubbed on to form a thin film; this meant there was minimal effect on the specimen's geometry.

3.3 Sample Production

During the casting process, a mould casts six specimens, all of the same percentage by weight of glass powder. These six specimens in the mould make up a sample. Therefore, eight samples are made, with each sample containing six specimens. The samples made will range from 0% glass powder to 35% glass powder, in increments of 5%.

3.4 Measuring materials

Before handling any of the materials, it was essential that their Material Safety Data Sheets (MSDS) were read and understood. Wearing the appropriate Personal Protective Equipment (PPE) was also required. Before bringing out the materials, their weights had to be determined. The samples varied from 0% glass powder to 35% glass powder, in increments of 5%. The accelerator or MEKP was to be 2% by weight to resin. Since the density of MEKP is 1 cc (i.e. 1 gram equals 1 millilitre), it was quite easy to extract an accurate amount. For a mould of this size, 900 grams of material had to be used. This weight decreased however, as the percentage of glass powder increased. At 35% glass powder, 800 grams of material was being mixed.

Table 4.1 shows the different percentages of weight of glass powder to resin, as well as accelerator. Reading off this table, the materials are measured in separate containers. It is important to zero the scale before adding the materials into the containers. Once the measured amounts are obtained, they are ready to be mixed.

Table 3.1: Percentages by weight

Percentage	Composite (g)	Resin (g)	MEKP (ml)	Glass Powder (g)
0	900	882.0	18.0	0
5	900	837.9	17.1	45
10	900	793.8	16.2	90
15	900	749.7	15.3	135
20	800	627.2	12.8	160
25	800	588.0	12.0	200
30	800	548.8	11.2	240
35	800	509.6	10.4	280

3.5 Mixing the Materials

Mixing of the materials is a very important process. This is the stage which can alter the structure of the specimens. The resin and glass powder were mixed together first, this had to be done slowly to minimise any formation of air bubbles in the mixture. If air bubbles formed in this stage, they would be in the specimen after curing, thus creating areas of localised stress concentration during testing. Mixing slowly in a figure eight motion around the container was found to be an adequate method; it allowed the glass powder to blend in with the resin, while the slow speed minimised the formation of air bubbles. After the resin and glass powder had been mixed together, the accelerator was ready to be mixed in. The accelerator had to be mixed in at a quicker rate than the resin and glass powder. This is because the accelerator

will actually start the curing process, making the mixture more viscous. When all three are mixed in together, the mixture can be poured into the mould.

Figure 3.2: Mixing the materials

The mixing was done in the ventilation chamber with the exhaust fan turned on. This allowed most of the fumes to escape the work environment. The windows were also opened to allow a flow of fresh air through the room.

Figure 3.3: Samples in the ventilation chamber

3.6 Filling the Mould

Filling the mould can be a delicate process. Because the chevron slot in no rigid, it can move around when the mixture is poured into the mould, and slant toward one side of the mould. It is ideal for the chevron slot to remain fixed in the centre of the mould. This will give better, more reliable results from testing. To minimise this slanting, the mixture was poured in at an even rate from both sides of the slot. The mixture is also poured along the length of the mould at the same time, that is, all mould spaces are filled in at the same time, instead of one at a time. This is because the mixture seeped through the separating plates, into the next mould space. It was important not to overfill the moulds, as this would make it more difficult to remove the cured specimens. As well as this, it meant that the specimen's geometry would not be suitable for testing, and thus need alteration.

3.7 Curing and Sample Removal

The samples were left to cure in ambient conditions for three days. After this, they were removed from the mould. Removal from the mould, for some of the specimens, proved to be a bit hard. This was due to the fact that the resin had seeped through gaps in the mould assembly and had set. This made it hard to remove certain plates. The whole assembly had to be dismantled in order to remove the specimens. Once the specimens were removed, they were ready for post-curing.

3.8 Post-Curing

The samples are to be post-cured in a conventional oven over a course of ten hours. The oven was programmed using a Eurotherm 3200 Series Controller, to heat the specimens at 50 degrees Celsius for four hours, then 80 degrees for four hours, then 100 degrees for two hours. Using the controller allowed the oven to control itself,

without interaction from anyone. It was observed however, to make sure the temperature did change after the prescribed time. All the specimens were able to fit into the oven at the one time, but care had to be taken to make sure they were evenly spaced. This meant the specimens could be evenly heated to the required temperature, without any uneven temperature regions.

Please note, care should always be taken when using the oven, as the temperature in the oven is high. The temperature on the controller was always checked before opening the oven door. The oven and specimens were allowed to cool before retrieving the specimens from the oven.

The oven was made by Steridium, which are commonly installed with Eurotherm controllers. The Eurotherm 3200 Series Controller user manual was used to program the controller to the desired requirements. The programming instructions may be seen in Appendix B.

Figure 3.4: Specimens in conventional oven

Figure 3.5: Eurotherm programmer

3.9 Short Bar Tests

3.9.1 Preparation for Testing

A number of moulds were overfilled during specimen production, making the specimen's chevron slot openings longer than desired. These parts had to be filed down in order to fit into the testing machine and give more accurate results. The specimens were fixed into a vice and the necessary parts were filed down to the required lengths, as shown in Figures 4.6. A face mask had to be worn as because of the dust that was created from the filing.

Figure 3.6: Filing down a specimen to required length

3.9.2 Testing

The testing of the specimens was done using the MTS 810 Materials Testing System. The Machine was fitted with the appropriate parts to apply the load to a short bar specimen. The specimen was loaded into the machine as shown in Figure 4.7. The height of the fitting was adjusted so the edge of the specimen sat flush against it. Rubber bands were used to hold the specimens in place.

With the specimen in place, the safety shield was pulled down, and the load was applied using the computer program. The opening load was applied at the mouth of the chevron slot at a rate of 1mm per second (Munz, 1981). As the load increased, its progress was monitored on the computer screen. The critical crack length was reached when the load was seen to significantly decrease, as in Figure 2.7. Once this was reached, the program could be stopped, and the load taken off. The results were then saved onto disc, and the results printed. The next sample could now be done.

The result that was required from the testing was the maximum load; this would be used in the calculation of the specimen's fracture toughness.

Figure 3.7: Specimen loaded onto MTS 810

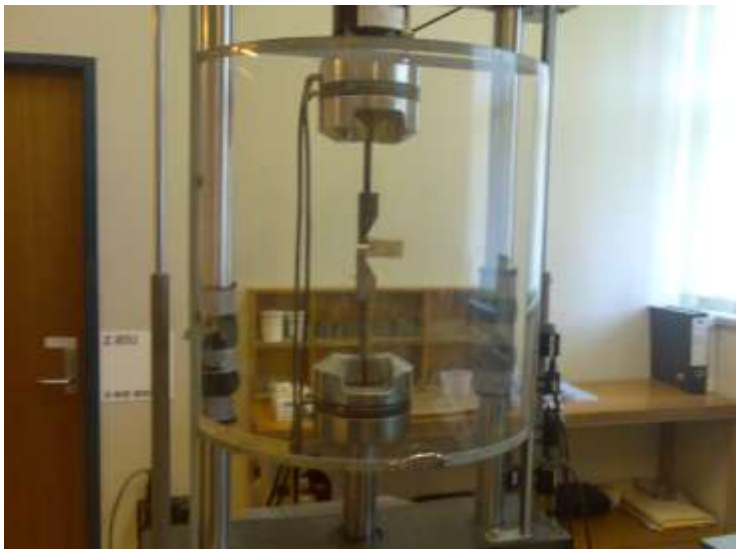

Figure 3.8: The MTS 810 during short bar test

3.9.3 Data Retrieved

Figure 3.9 Shows the raw data obtained from the testing. Looking at the figure, the point of interest is point F. This is the peak load, and will be used in the fracture toughness calculation.

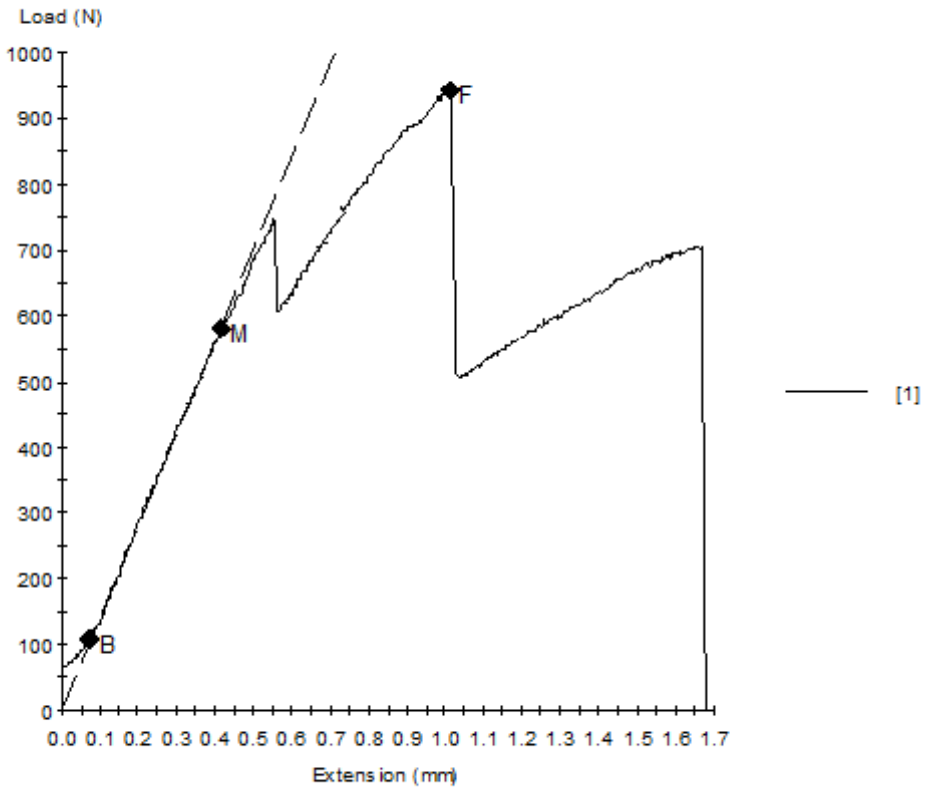

Specimen Results:

Name	Value	Units
Thickness	26.000	mm
Width	50.000	mm
Area	1300	mm^2
Peak Load	943	N
Peak Stress	0.73	MPa
Break Load	943	N
Break Stress	0.73	MPa
Elongation At Break	1.012	mm
Stress At Offset Yield	0.467	MPa
Load At Offset Yield	606.952	N

Figure 3.9: Raw data obtained from the testing

3.10 Microscopic Analysis

To further investigate the effects the glass powder had on the vinyl ester resin, the use of a scanning electron microscope was implemented. As USQ does not have a scanning electron microscope (SEM), the microscope analysis was done at Queensland University of Technology (QUT) in Brisbane.

3.10.1 Sample Preparation

The samples had to be prepped in order to fit into the SEM. They were prepared to the specifications for a dry, non-conductive sample without surface residue.

The samples were prepared simply by cutting them to the required size. For short bar specimens, a 10 mm strip had to be cut down the centre of the specimen, which contained the length of the crack surface, as this was the surface to be investigated. Refer to Figure 4.9. The specimens were then gold coated. This was necessary as the specimens had to be heat and charge conductive. The sputter coating method was used to coat the specimens. This took some time due to the specimens size; the larger the specimen, the longer it took. Sputter coating allowed the whole surface of the specimen to be coated. Refer to Figure 4.10. After coating the specimens, they were ready to be examined. The specimens were put into the SEM where their surface was magnified to50, 200, 1000 and 2000 times. This allowed a more detailed view of the fracture surface, as well as the locations of fracture lines.

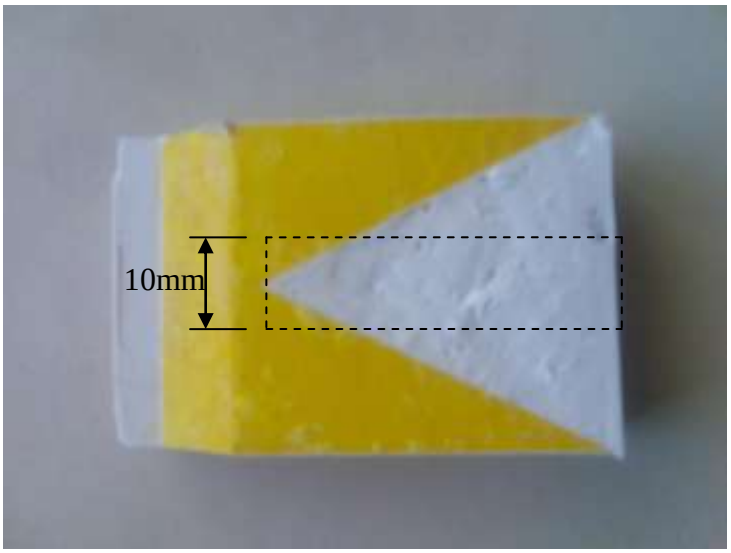

Figure 3.10: The required geometry for SEM analysis

Figure 3.11: Gold coated specimens after sputter coating

3.11 Improvements in Methodology

There are a number of aspects that can be improved in the methodology. The main improvement one can see is to do with the removal of the specimens from the moulds after they have been cured. In the current method, the wet mixture seeped through cracks and hardened, making the mould plates hard to remove. This could be

improved by making the mould from fewer pieces, or using a material that is more flexible. However, this will make it more expensive, and may not be worth investing in. Another solution would be to construct the mould, filling in the gaps along the plate slots with plasticine or something similar. This would stop the wet mixture from seeping through the gaps. The plasticine may react with or may be eaten away by the mixture, so this may not be suitable and would have to be investigated.

3.12 Conclusion

This chapter described the steps taken in the practical aspects of the project which included making the specimens, post curing and test preparation, testing, and finally a further analysis of the specimens fracture surface using scanning electron microscopy. Improvements were also suggested at the end of the chapter.

4 Consequential Effects

4.1 Introduction

In the project, risks are present which have to be identified and minimised. If the proper precautions are not taken, the consequences may include serious injury, damage to the environment, and damage to property. This chapter will analyse the potential dangers involved in the project, and steps taken to manage them.

4.2 Identification

In the production and testing of the samples, there are several risks that have to be identified in order to be eliminated or minimised. The materials used to create the samples themselves pose a danger. These materials can cause harm if not handled correctly. The samples require a chemical reaction to occur, hence heat may be involved. If the quantities used are incorrect, the reaction may prove violent or even explosive in an extreme case. The post curing process involves the use of an oven. The temperature will reach 100° Celsius; this can cause serious injury if negligence occurs. Finally, the testing of the specimens may cause injury. There are other dangers that are not so obvious that may cause injury or damage as well.

4.3 Preparation

Like any professional workplace, USQ takes measures to prevent injury occurring to people using its facilities; prevention of harm to people and damage to property is an important aspect. Before starting any practical work, a work permit must be granted. This will outline the work area, equipment, procedures, and special precautions. It may be revoked at any time. As well as a work permit, a material safety data sheet (MSDS) must be read and understood by the student. These provide all precautions to be taken, e.g. personal protective equipment (PPE), exposure limits, safe handling information, etc. As well, there is first aid information in case of an emergency. Students are also shown how to proceed when making samples. Correct techniques are demonstrated to eliminate any confusion.

The engineering block is equipped with the necessary facilities to do the project. A ventilation chamber with an exhaust fan is at hand and its use is necessary for the

mixing of the samples. The testing machine is fitted with a shield. This will protect form any flying chips resulting from the tensile testing.

4.4 Risks

Any activity that has risks involved has the potential to cause harm. After being identified, the appropriate action can be taken to minimise the likelihood of an accident occurring.

Resin

Hazards

- Hetron 922PAS and PAW will have adverse effects if in contact with eyes.
- Contact with skin will cause irritation and may also have adverse effects.
- Prolonged exposure to fumes will have adverse effects on respiratory system.

Recommendations

- Wear safety glasses.
- Wear rubber gloves.
- Limit exposure time, wear respirator, open windows.

Accelerator

Hazards

- MEKP corrosive to eyes. Will cause blindness if not treated immediately.
- Corrosive to skin. Will cause burning if not treated immediately.
- Harmful if swallowed.

Recommendations

- Wear safety glasses.
- Wear rubber gloves.
- Do not swallow.

Glass Powder

Hazards

- Adverse effects on respiratory system if inhaled.

Recommendations

- Wear respirator when handling and filing.

Reaction of resin and accelerator

Hazard

- Reaction may be violent if wrong amounts of accelerator used.

Recommendation

- Consult MSDS for recommended amounts before mixing.

Testing

Hazard

- Chip may fly from specimen during testing.

Recommendation

- Close shield on testing machine when testing.

Laboratory Dangers

Hazards

- Risk of trip or slip in lab.
- Spills present on work areas.

Recommendations

- Keep laboratory.

This information can be tabulated into a risk assessment sheet. It will make it easier to refer to certain aspects of the project to undertake the project safely. Table 4.1 shows the risk assessment sheet for this project.

Table 4.1: Risk Assessment

Description of Hazard	Risk Level	People at risk	Parts of Body	Control Measures
Inhalation of fumes	High	People in room	Respiratory system, brain	Wear respirator, open windows, turn on exhaust fan, avoid long periods of exposure
Skin contact with resin and catalyst	Medium	Person mixing	Skin	Wear gloves, wear covered shoes, wear long sleeve shirt
Resin and catalyst touching eye	Medium	Person mixing	Eye	Wear safety glasses
Potentially violent chemical reaction	Low	People in room	Body parts exposed to reaction	Wear PPE, mix behind shield
Flying chip from test specimen	Low	People in room	All exposed parts	Close shield when testing
Trip or slip in lab	Low	People in room	Whole body	Keep lab tidy

5 Results and Discussion

5.1 Introduction

This chapter will analyse and discuss the results obtained from the short bar tests carried out. By using fracture mechanics with assumptions of linear elastic fracture mechanics, the fracture toughness was calculated. Comparison of the results to previous works will also be done. This will give an indication of whether the results are practical. Further to this, microscopic analysis will be done using Scanning Electron Microscopy (SEM). This will assist in determining reasons for failure as well as factors that improve fracture toughness.

5.2 Short Bar Test

Table 5.1 shows the raw data obtained from the short bar tests. Peak load was the only data obtained from the short bar test that was needed for the calculation of fracture toughness. From looking at the graphs, the peak loads are the highest point reached during the duration of the testing. The results of all the testing is given in Appendix A.

Table 5.1: Peak Load

	F_{max} (N)							
Percentage	**0**	**5**	**10**	**15**	**20**	**25**	**30**	**35**
Specimen 1	557	757	755	943	853	829	806	796
Specimen 2	741	786	903	927	809	819	775	709
Specimen 3	505	829	765	856	846	802	762	725
Specimen 4	645	750	779	940	804	887	765	765
Specimen 5	615	783	792	953	809	943	761	790
Specimen 6	743	815	791	977	811	812	903	752

5.3 Fracture Toughness

The fracture toughness of the specimens is calculated using the formula,

$$K_{IcSB} = \frac{F_{max} Y_m^*}{B\sqrt{W}}$$

F_{max} is the peak force obtained from testing. The breadth, B, is given by design as 50 millimetres; the width, W, is determined to be 74 millimetres from actual measurements of the specimens. The compliance calibration, Y_m^*, is given by the formula,

$$Y_m^* = \{-0.36 + 5.48\omega + 0.08\omega^2 + (30.65 - 27.49\omega + 7.46\omega^2)\,\alpha_0$$

$$+ (65.90 + 18.44\omega + 9.76\omega^2)\,\alpha_0^2\} \left\{\frac{(\alpha_1 - \alpha_0)}{(1 - \alpha_0)}\right\}^{\frac{1}{2}}$$

where $\omega = \frac{W}{H}$, $\alpha_0 = \frac{a_0}{W}$ and $\alpha_1 = \frac{a_1}{W}$. a_0 and a_1 (as shown in figure 2.2(b)) were measured as 72 and 26 millimetres respectively. The height, H, equals 38 millimetres. It was therefore determined that,

$$\omega = \frac{W}{H} = \frac{74}{38} = 1.95$$

$$\alpha_0 = \frac{a_0}{W} = \frac{26}{74} = 0.35$$

$$\alpha_1 = \frac{a_1}{W} = \frac{72}{74} = 0.97$$

From this, the compliance calibration was calculated to be $Y_m^* = 17.524$ (as shown in Appendix C). The fracture toughness of glass powder reinforced vinyl ester resin (VE/Glass Powder) at different percentages by weight was then calculated and is given in Table 5.2. Standard deviation is given in brackets.

Table 5.2: Fracture Toughness

	Fracture Toughness (MPa√m)							
Percentage	**0**	**5**	**10**	**15**	**20**	**25**	**30**	**35**
Fracture Toughness (Standard Deviation)	31.12 (3.92)	31.71 (1.06)	31.63 (0.66)	38.62 (0.76)	33.49 (0.88)	33.23 (0.46)	31.53 (0.77)	31.61 (0.85)

For visual representation, the results were plotted to provide a better comparison of the fracture toughness calculated. A five percent (5%) marker was included. This allowed unusually higher and lower measurements to be omitted from calculating fracture toughness. The fracture toughness of varying percentages of VE/Glass Powder post cured in a conventional oven is given in Figure 5.1.

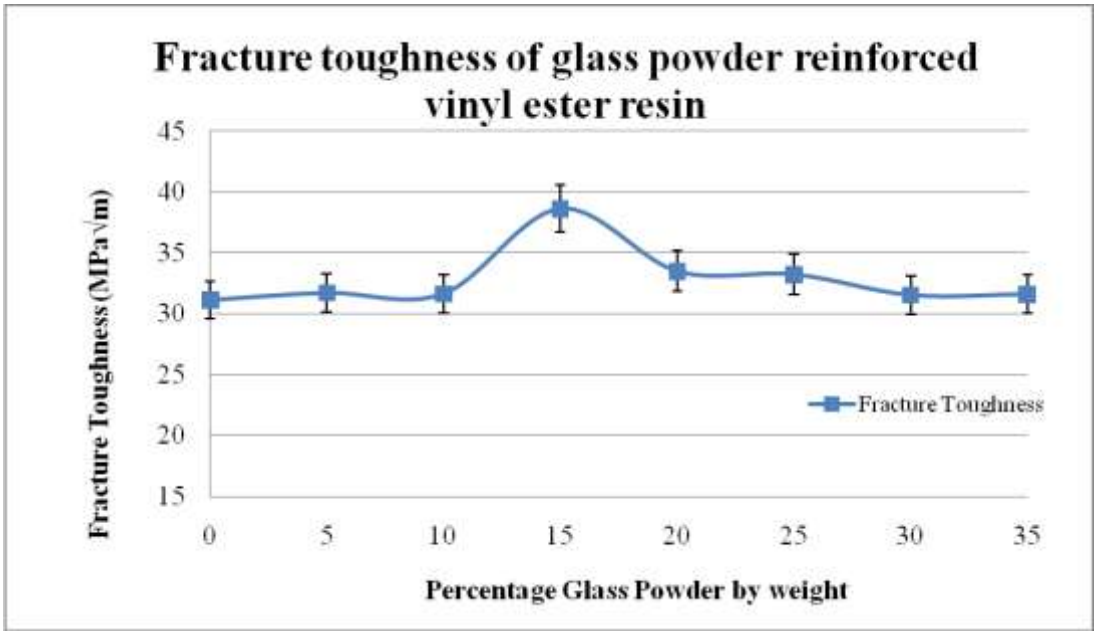

Figure 5.1: Fracture toughness of glass powder reinforced vinyl ester resin.

From Figure 5.1, it can be seen that the fracture toughness of VE/Glass Powder was highest at 15%. The fracture toughness was 38.62 MPa√m. The fracture toughness

for the different percentages of glass powder showed little variation. At neat resin (0% glass powder), gave the lowest fracture toughness, which was 31.12 MPa√m. For 5 % and 10%, the fracture toughness was 31.71 and 31.63 MPa√m respectively. From 0% to 10%, the fracture toughness remained steady and increased directly to 38.63 MPa√m at 15%. The fracture toughness then decreased to 33.49 MPa√m at 20%. It decreased slightly to 33.23 MPa√m at 25%. Again, the fracture toughness remained constant for these two readings. At 30% and 35%, the result again slightly decreased to 31.53 MPa√m and 31.61 MPa√m respectively. The results obtained showed little variation; apart from 15% glass powder, the fracture toughness remained between 31 MPa√m and 34 MPa√m for the other percentages of glass powder.

5.4 Comparison to Previous Works

Comparison of the results to previous work is a good indication of the viability of the fracture toughness measurements calculated. A previous study conducted investigated the fracture toughness of phenol formaldehyde composites. Ku et al. (2008) used envirospheres slg reinforced phenolic resin (PF/E-Spheres). The fracture toughness was determined using the same method (i.e. the short bar method) ensuring similar testing conditions for both studies. Table 5.3 shows the fracture toughness of PF/E-Spheres at varying percentages. Figure 5.2 shows a comparison of this and the previous studies results.

Table 5.3: Fracture toughness of different percentage by weight of SLG reinforced phenolic resin

Percentage by weight of slg	0	15	20	25	30	35
Fracture toughness MPa√m	8.72	10.5	12.5	9.62	8.82	8.12
(Standard deviation)	(1.94)	(0.8)	(0.16)	(0.24)	(0.36)	(0.67)

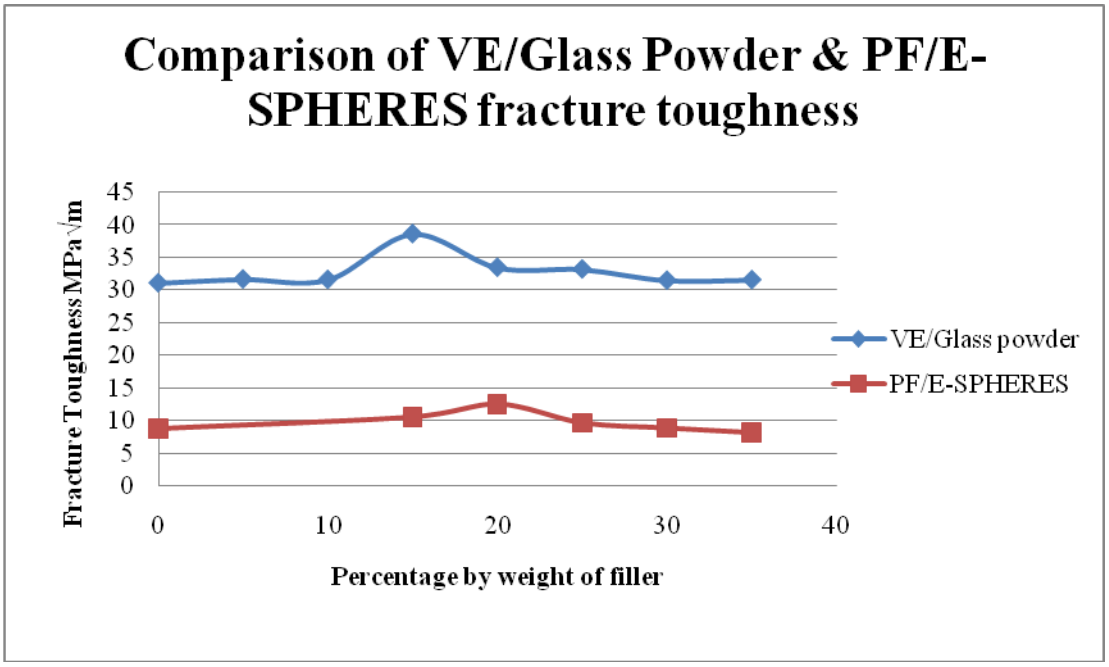

Figure 5.2: Fracture toughness of PF/E-SPHERES with varying percentage by weight of slg

It can be seen that the results from both studies follow a similar trend. The fracture toughness starts low at neat resin before rising to a maximum at 20% by weight. It then drops back down.

5.5 Scanning Electron Microscopy (SEM) Analysis

SEM analysis made it possible to view the fracture surface of the specimens to determine the characteristics that contributed to their behaviour. Characteristics that influenced behaviour include voids, gaps around the glass powder, brittle/ductile zones. Apart from these, other features are to be observed; features such as elongation of fractured surfaces, signs of brittle and ductile fracture, fracture lines, and debris.

SEM was done on a 0% and 20% specimen to help understand how the addition of the filler affected the behaviour of the resin.

5.5.1 0% Glass Powder

Figure 5.3 is an image of a specimen of 0% glass powder, or neat resin. The four locations indicated (positions 1, 2, 3, and 4) were studied. No details can be seen yet, as this image is only 19 times magnifications.

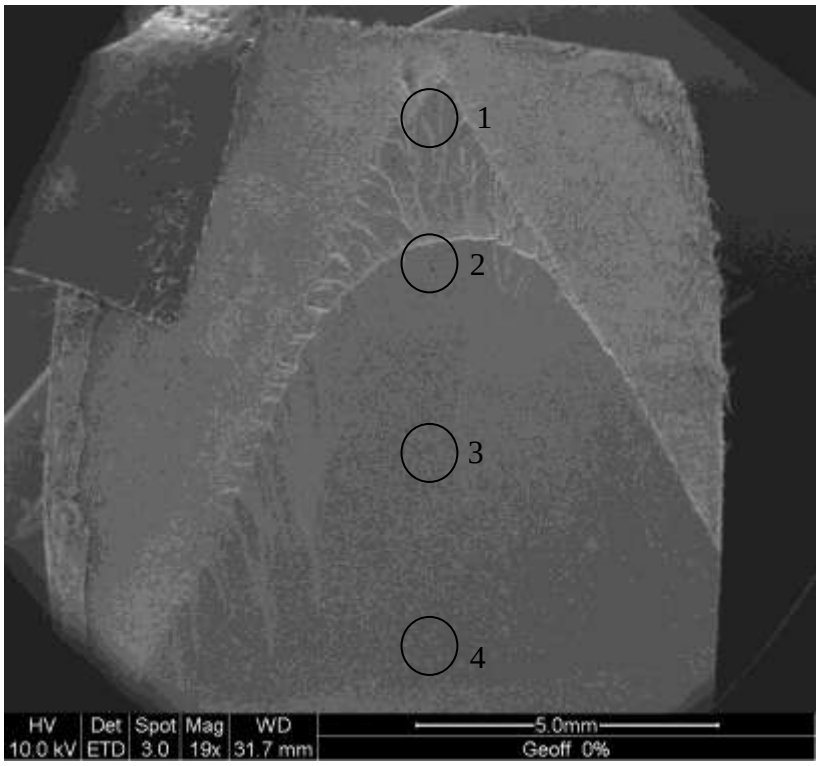

Figure 5.3: Locations of SEM analysis, 0% glass powder

Figure 5.4 shows neat resin at position 1 at 200 times magnification. At this location, we can see fracture lines along which fracture occurs. The smooth straight lines indicate brittle fracture. Looking at Figure 5.3, we can see that this only occurs at the tip of the fracture surface where crack propagation is initiated.

Figure 5.5 shows neat resin at position 1 at 1000 times magnification. We can see more clearly the fracture line, and also smaller lines that represent the propagation of

the crack. We can also see that there is a considerable amount to debris on the surface.

Figure 5.6 shows neat resin at position 1 at 2000 times magnification. The debris can be seen more easily at this magnification.

Figure 5.7 shows neat resin at position 2 at 200 times magnification. This image shows the fracture line where failure of the specimen occurred. The top part shows the surface of the crack propagation, while the lower shows the surface of sudden catastrophic failure.

Figure 5.8 and 5.9 shows neat resin at position 2 at 1000 and 2000 times magnification respectively. It can be seen that the surface is mainly formless. There is however an area where there is an empty hole. There is also debris on the surface.

Figure 5.10, 5.11, and 5.12 shows neat resin at position 3 at 200, 1000, and 2000 times magnification. The surface is mostly plain; however, as in position 2, there is an area with empty holes.

Figure 5.13, 5.14, and 5.15 shows neat resin at position 4 at 200, 1000, and 2000 times magnification. It is seen that the surface is quite plain.

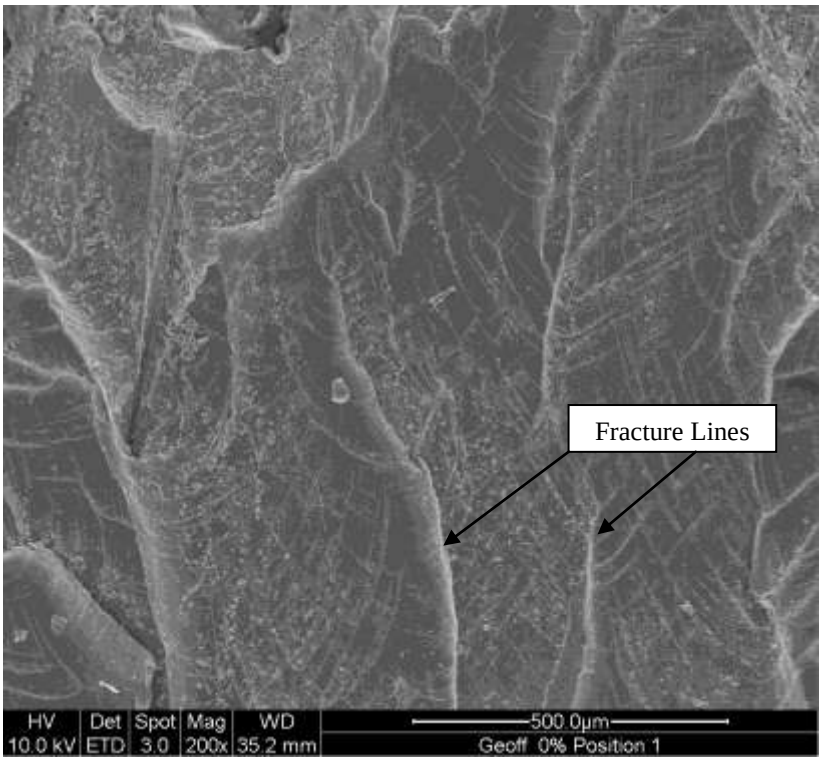

Figure 5.4: Position 1 at 200x magnification, 0% glass powder

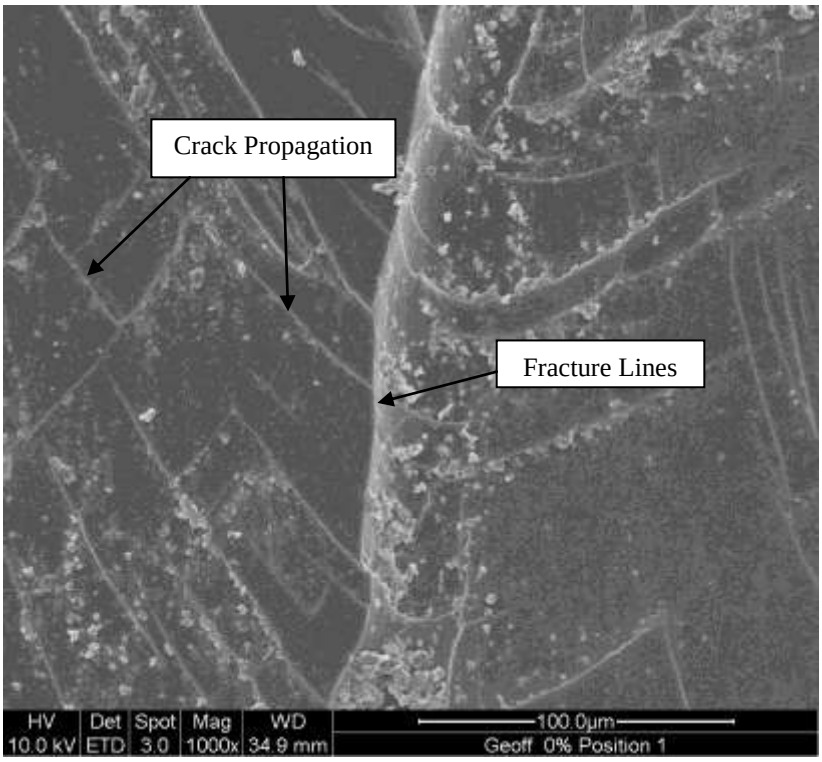

Figure 5.5: Position 1 at 1000x magnification, 0% glass powder

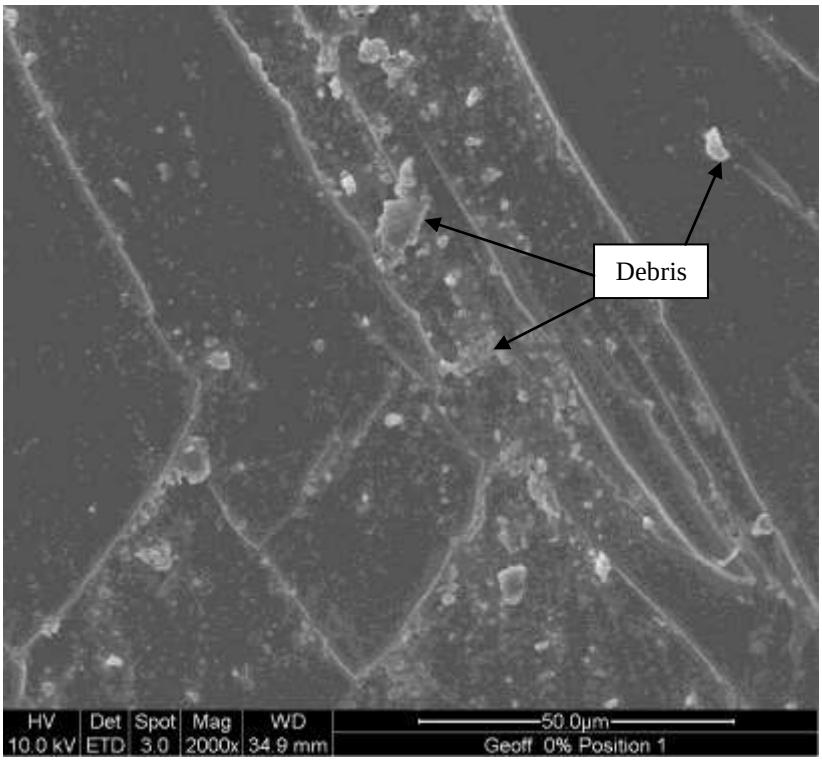

Figure 5.6: Position 1 at 2000x magnification, 0% glass powder

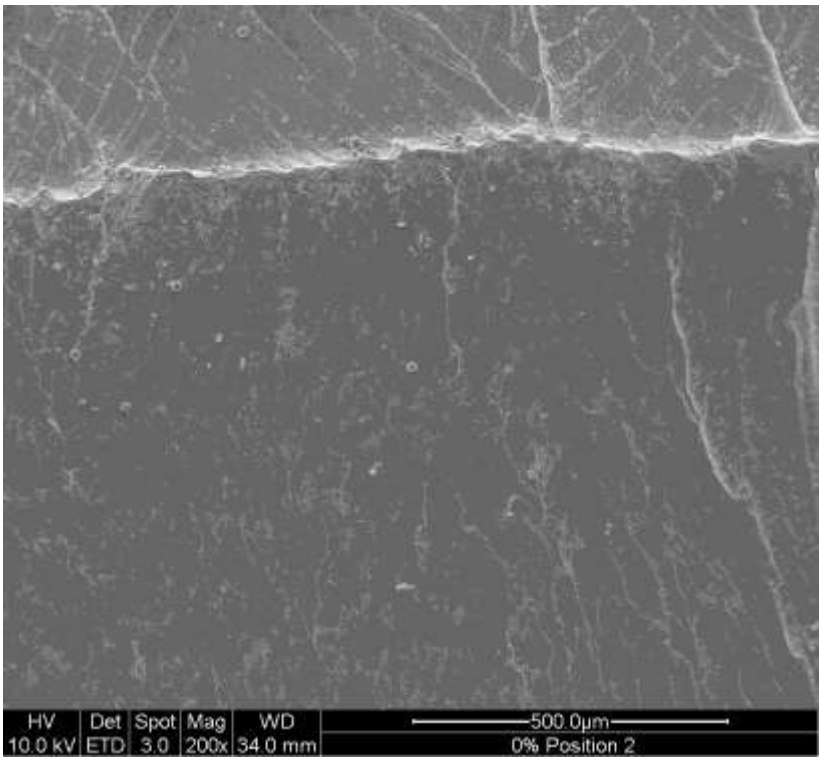

Figure 5.7: Position 2 at 200x magnification, 0% glass powder

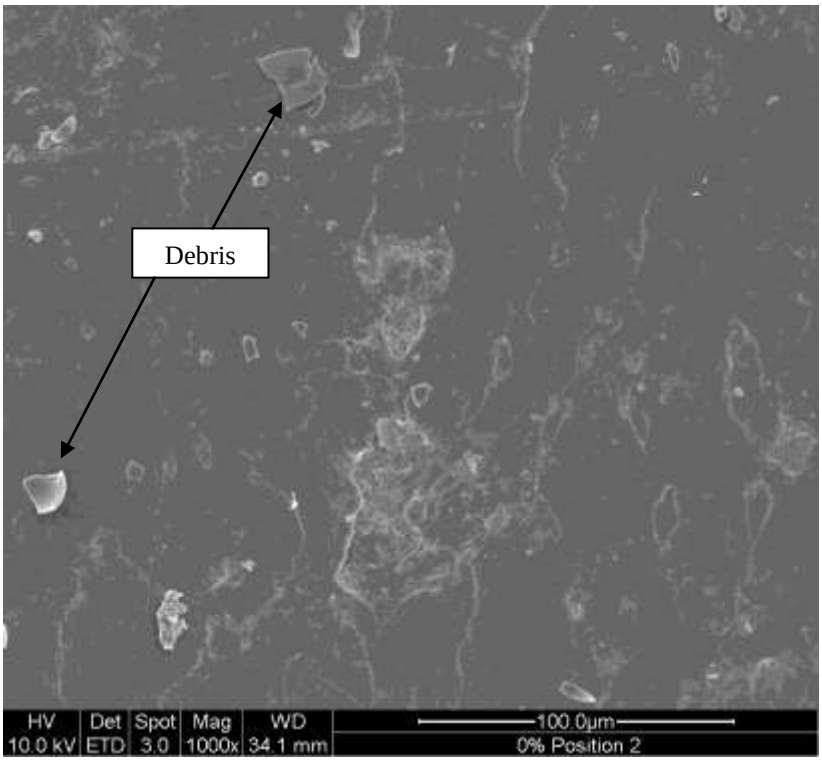

Figure 5.8: Position 2 at 1000x magnification, 0% glass powder

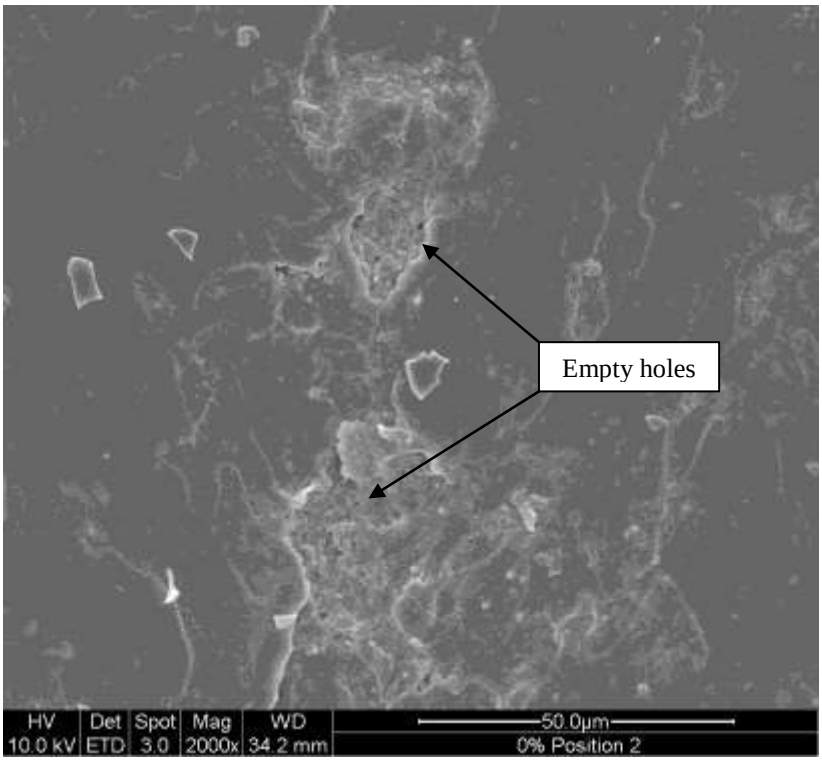

Figure 5.9: Position 2 at 2000x magnification, 0% glass powder

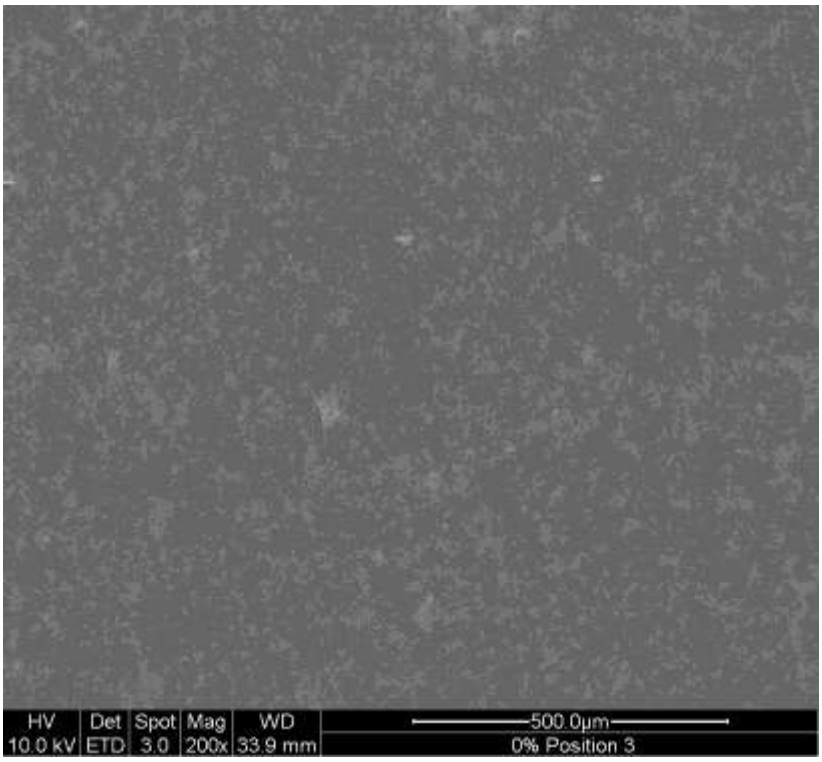

Figure 5.10: Position 3 at 200x magnification, 0% glass powder

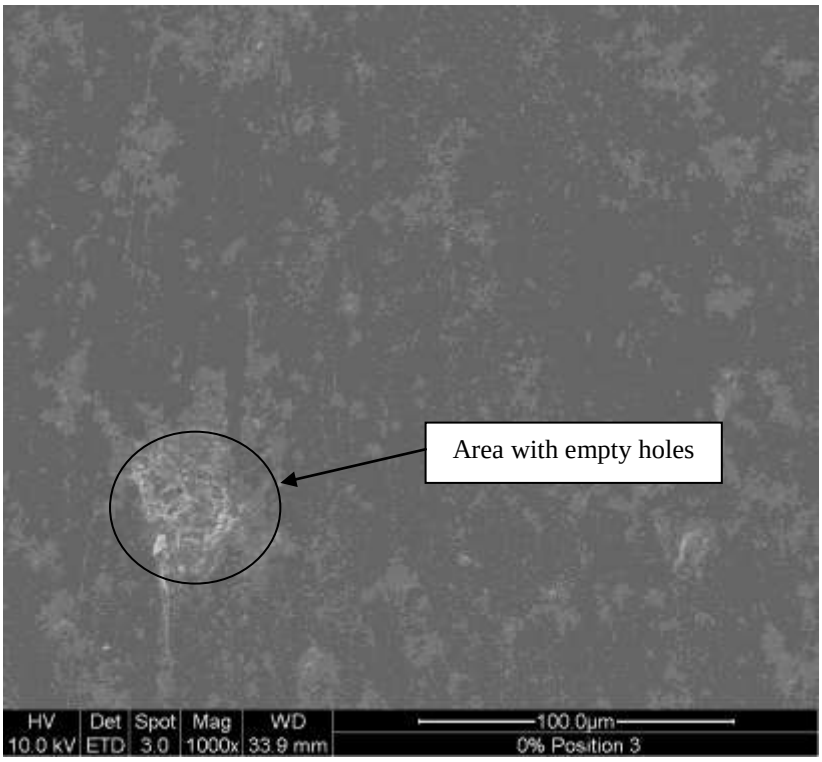

Figure 5.11: Position 3 at 1000x magnification, 0% glass powder

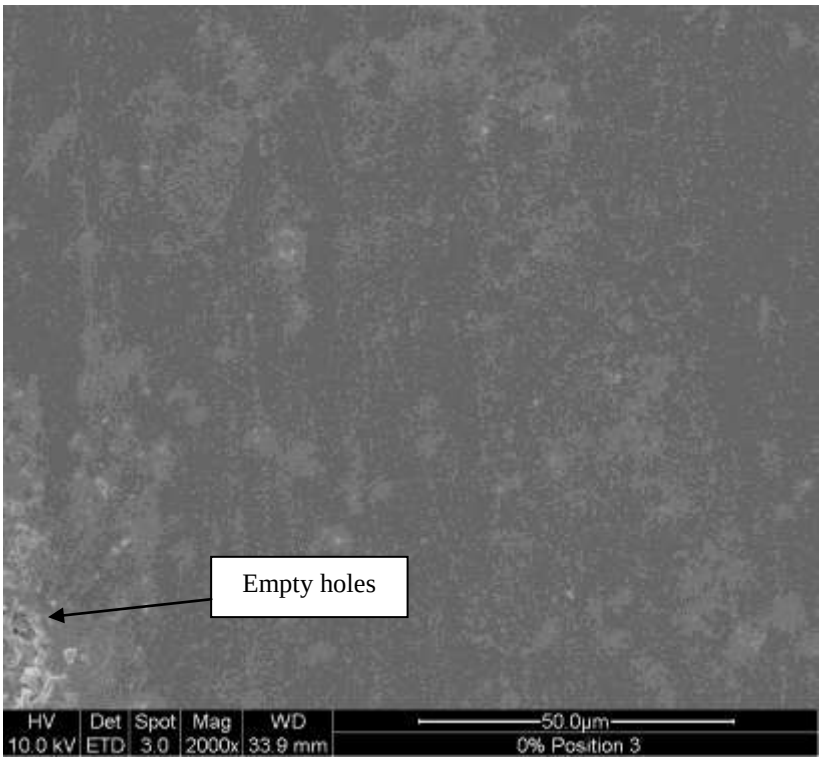

Figure 5.12: Position 3 at 2000x magnification, 0% glass powder

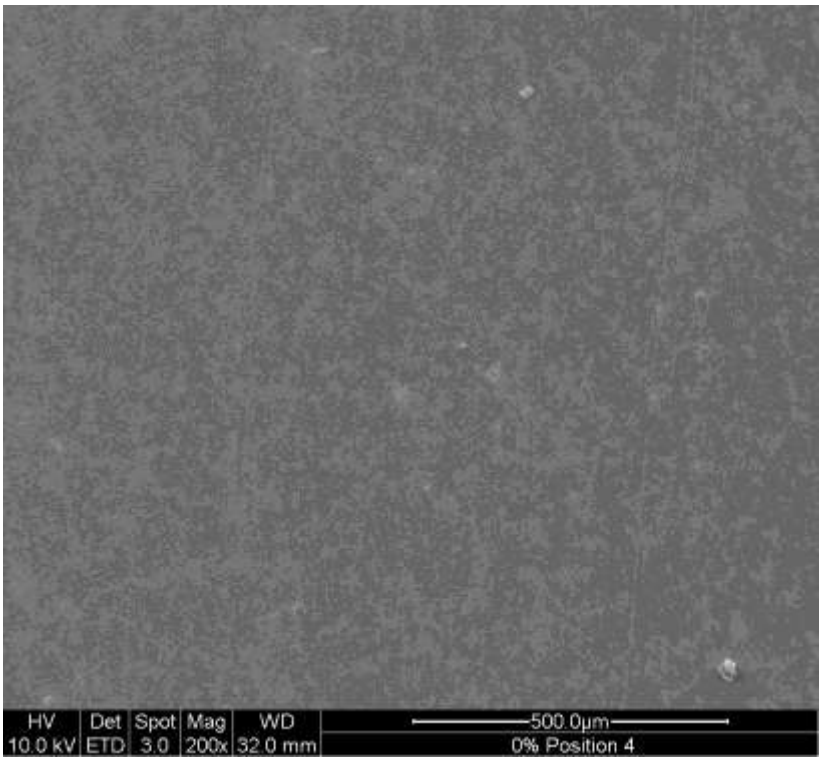

Figure 5.13: Position 4 at 200x magnification, 0% glass powder

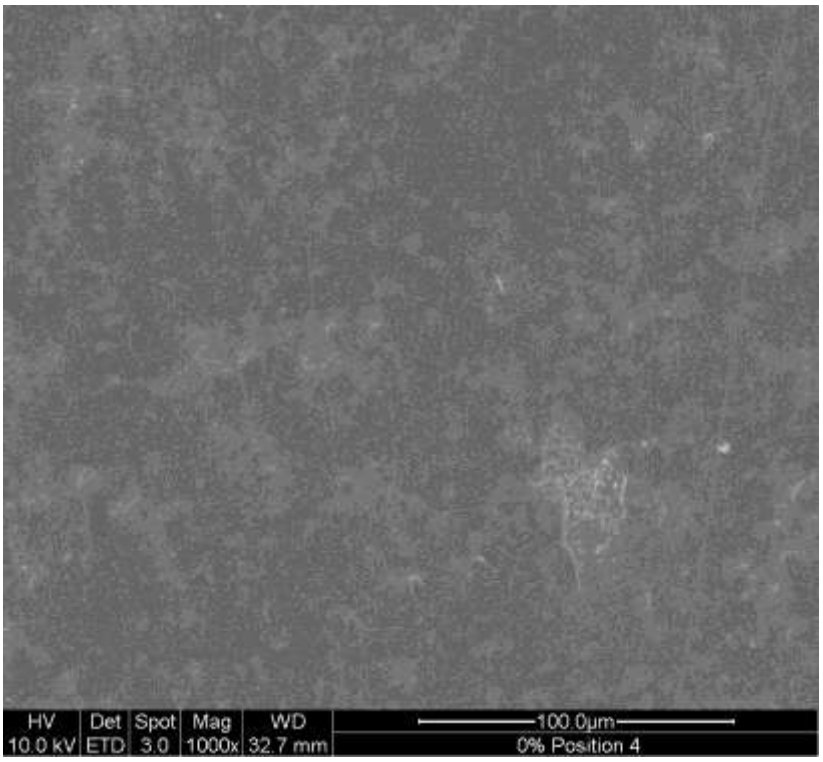

Figure 5.14: Position 4 at 1000x magnification, 0% glass powder

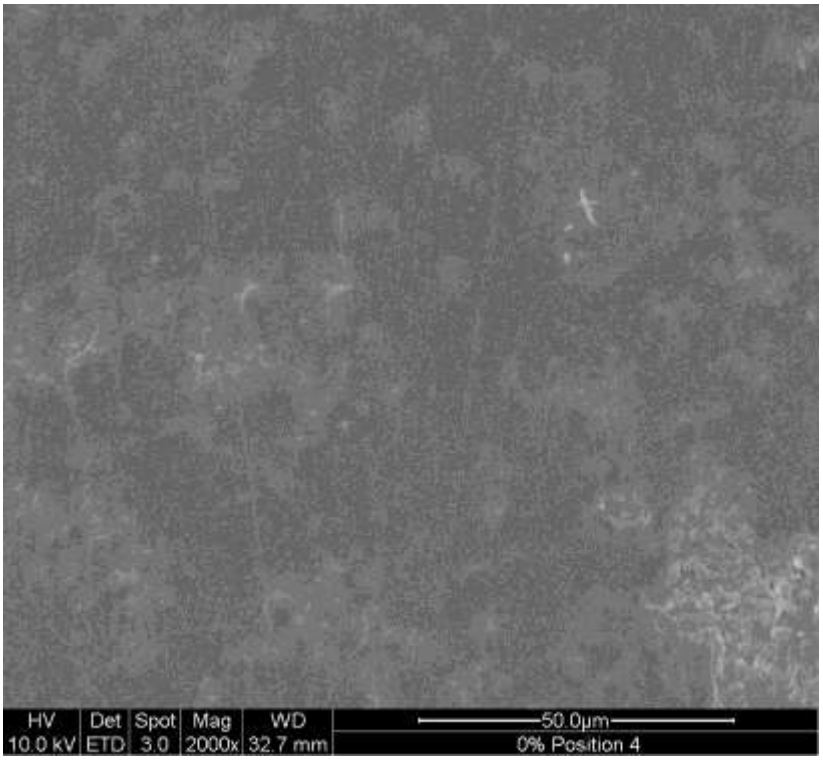

Figure 5.15: Position 4 at 2000x magnification, 0% glass powder

5.5.2 20% Glass Powder

Figure 5.16 shows a specimen of 20% glass powder. As in the neat resin, four locations (positions 1, 2, 3, and 4) were studied using SEM. From this magnification, it can be see that there are air bubbles (or voids) on the fracture surface. These may have formed during the reaction of the resin and accelerator.

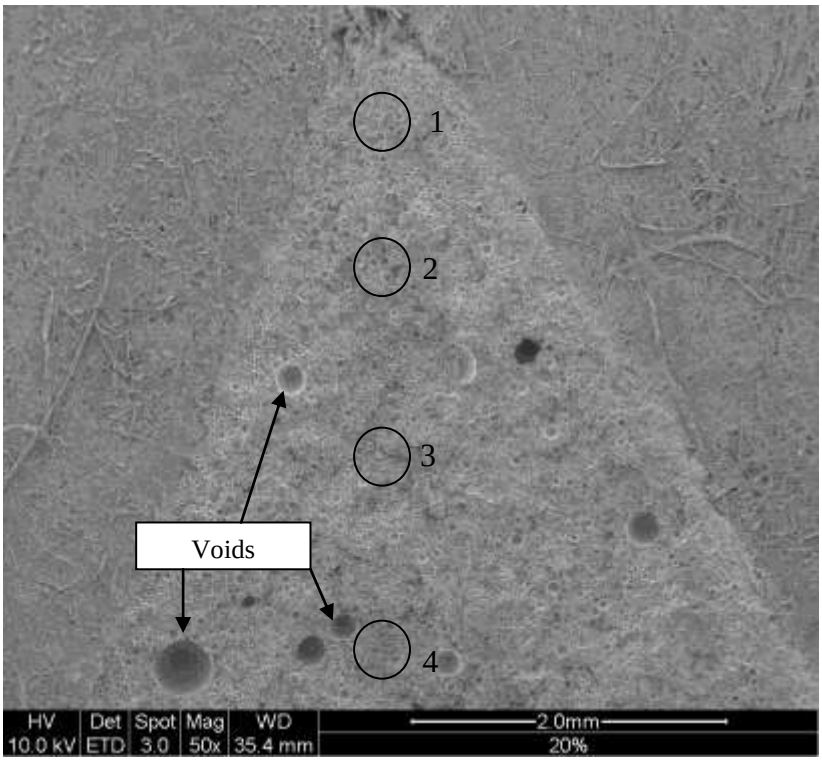

Figure 5.16: Locations of SEM analysis, 20% glass powder

Figure 5.17 shows a specimen of 20% glass powder at position 1, magnified to 200 times. From the image, it can be seen that the glass powder is of varying sizes. At this magnification, it is difficult to see in detail the interaction between the resin and glass powder.

Figure 5.18 shows a specimen of 20% glass powder at position 1, magnified to 1000 times. At this magnification, we can view the surface in more detail. The image shows that there are voids in the specimen. These generally appear to be larger than

the glass powder. The image also shows glass powder that has broken. We also see that there are gaps around the glass powder particles.

Figure 5.19 shows a specimen of 20% glass powder at position 1 magnified to 2000 times. At this magnification, it is possible to see the fracture surface.

Figure 5.20 shows a specimen of 20% glass powder at position 2 magnified to 200 times. In this image, we can see a large empty hole. We can also see the fracture line on the lower left of the image. The darker shadow indicates the direction the fracture line travels in.

Figure 5.21 shows a specimen of 20% glass powder at position 2 magnified to 1000 times. From the image, it can be seen that the glass powder particles range roughly from 5 microns to 80 microns.

Figure 5.22 shows a specimen of 20% glass powder at position 2 magnified to 2000 times. In this image, we can see that part of the surface seems to have been peeled before fracture. This could indicate some ductile behaviour did occur.

Figures 5.23, 5.24, and 5.25 shows a specimen of 20% glass powder at position 3 magnified to 200, 1000, and 2000 times respectively.

Figure 5.24 contains a number of voids, as well as fracture lines. We can see that some of the fracture lines run along the edges of the voids, suggestive of stress concentration areas.

Figure 5.25 shows an area containing a crevice. It also shows a surface that has cracks through it. This may be indicative of brittle fracture.

Figure 5.26 shows a specimen of 20% glass powder at position 4 magnified to 50 times. This image shows a considerable number of voids and holes. Further investigation will reveal these features influence the behaviour of the specimen.

Figure 5.27 shows a specimen of 20% glass powder at position 4 magnified to 200 times. From this image, we can start to see fracture lines on the surface.

Figure 5.28 shows a specimen of 20% glass powder at position 4 magnified to 1000 times. From this image, we can see the fracture lines. It can be seen that they occur between and around the glass powder and voids.

Figure 5.29 shows a specimen of 20% glass powder at position 4 magnified to 2000 times. This figure gives a more detailed image of the fracture surface. This image gives conclusive evidence that the fracture lines originate from the glass powder particles as shown in the figure. We can see that in certain locations, cracks have originated from crevasses from dislodged glass powder particles.

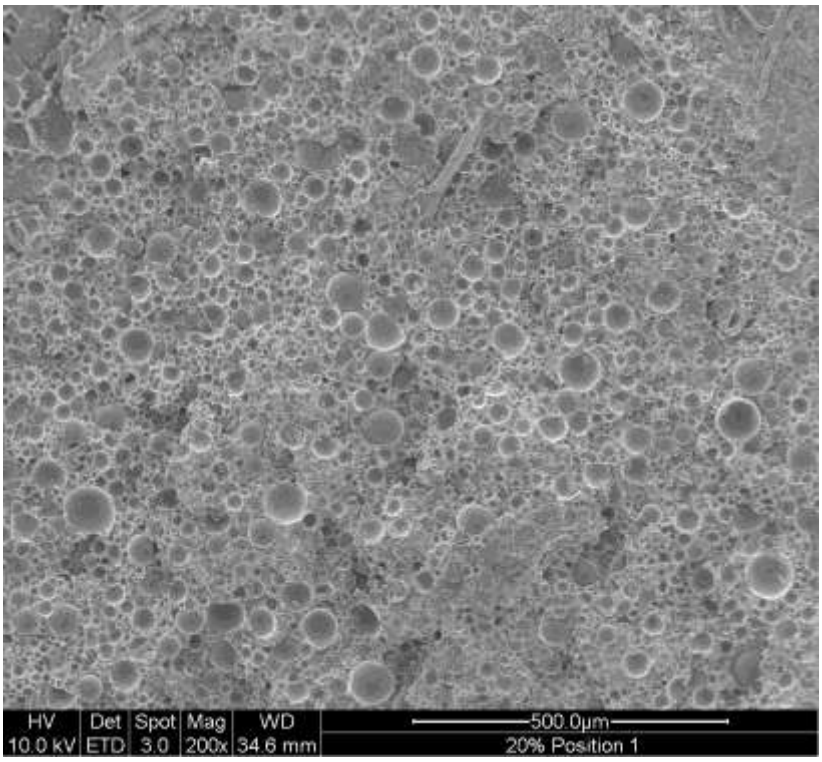

Figure 5.17: Position 1 at 200x magnification, 20% glass powder

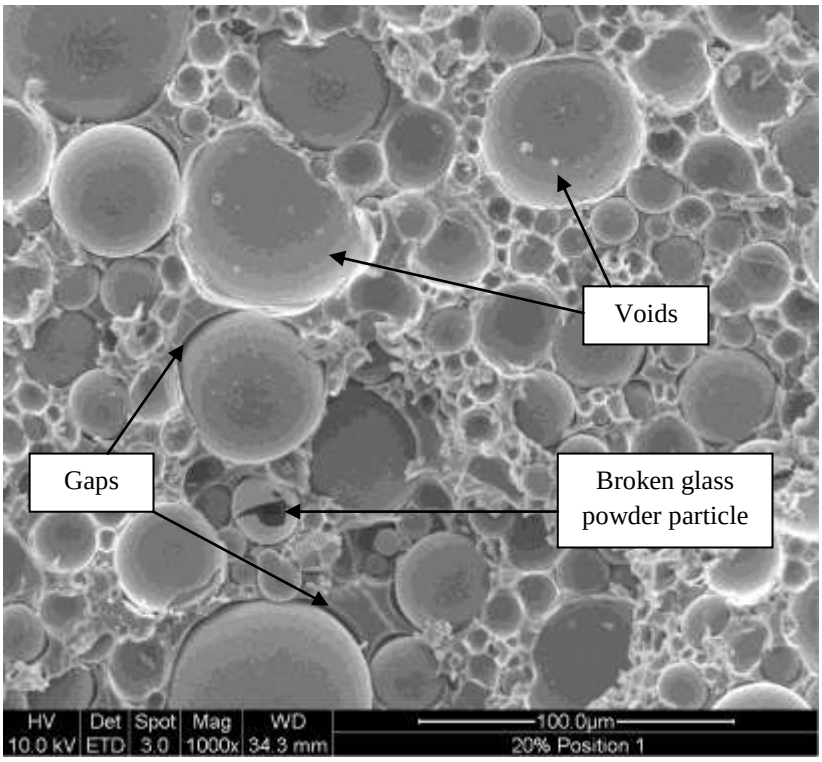

Figure 5.18: Position 1 at 1000x magnification, 20% glass powder

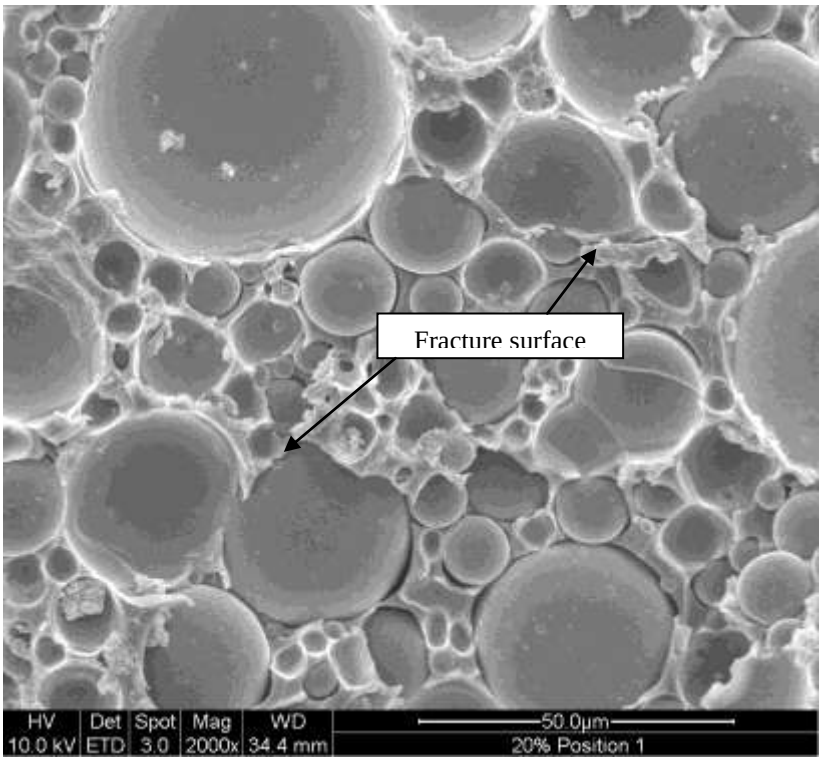

Figure 5.19: Position 1 at 2000x magnification, 20% glass powder

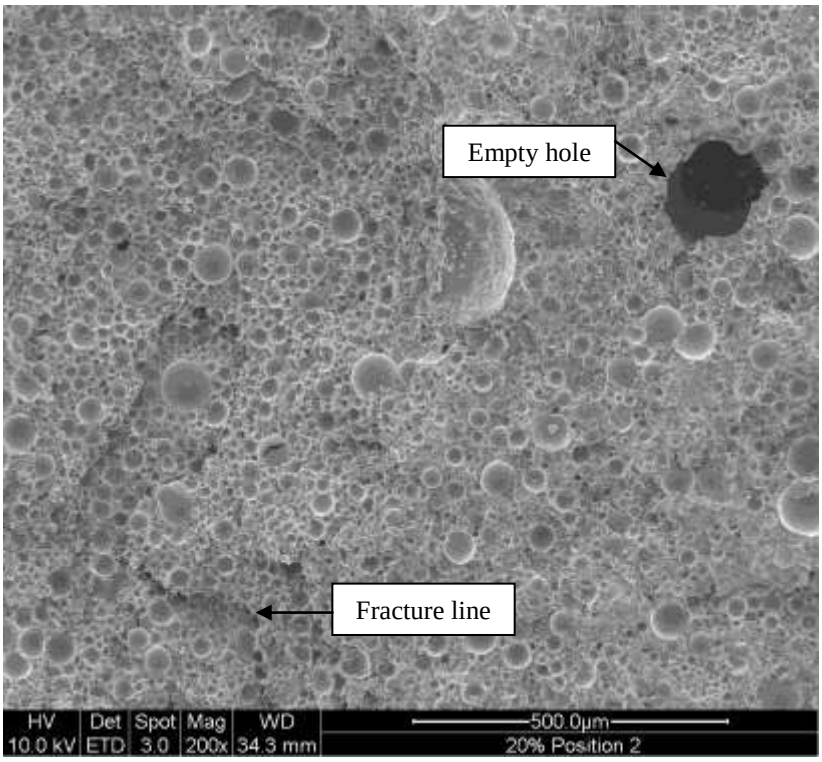

Figure 5.20: Position 2 at 200x magnification, 20% glass powder

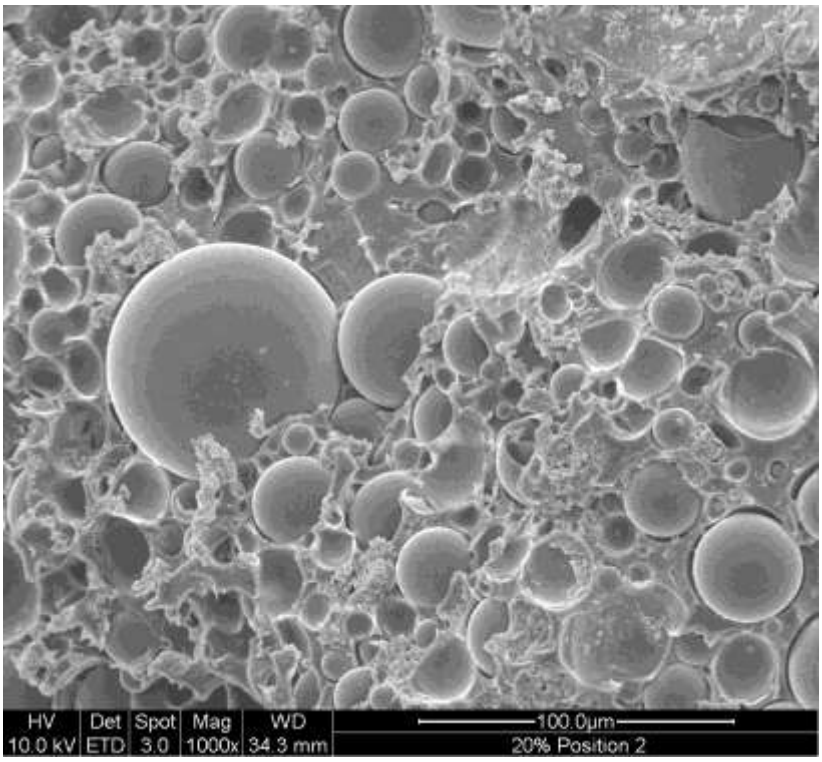

Figure 5.21: Position 2 at 1000x magnification, 20% glass powder

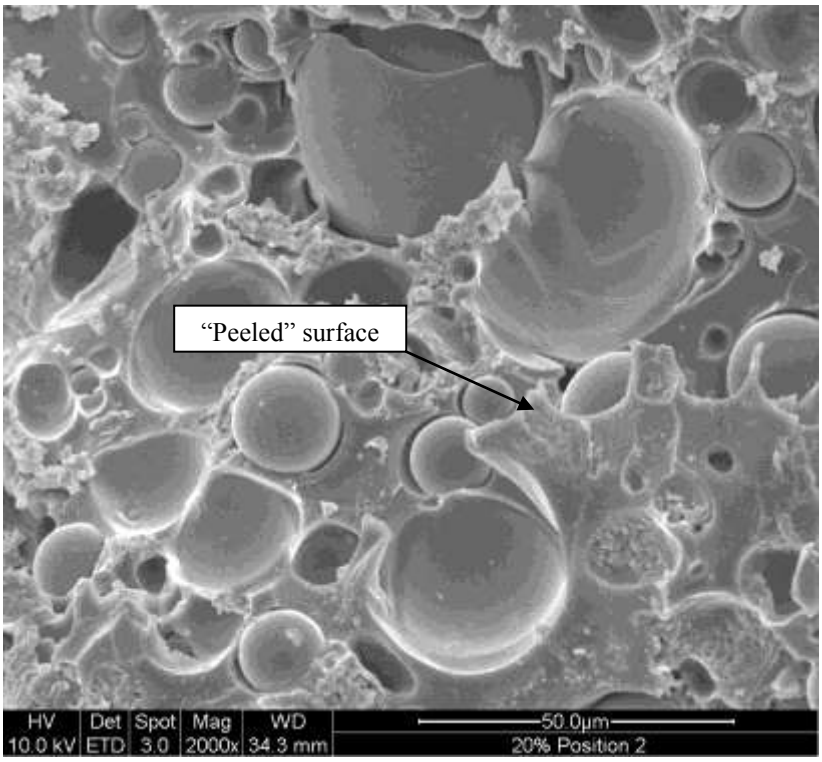

Figure 5.22: Position 2 at 2000x magnification, 20% glass powder

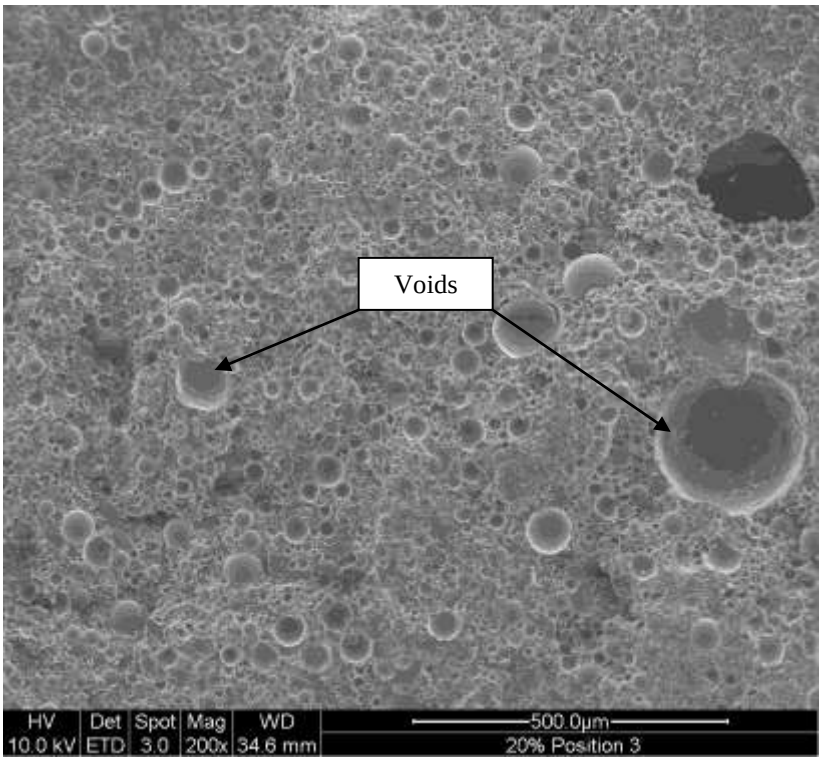

Figure 5.23: Position 3 at 200x magnification, 20% glass powder

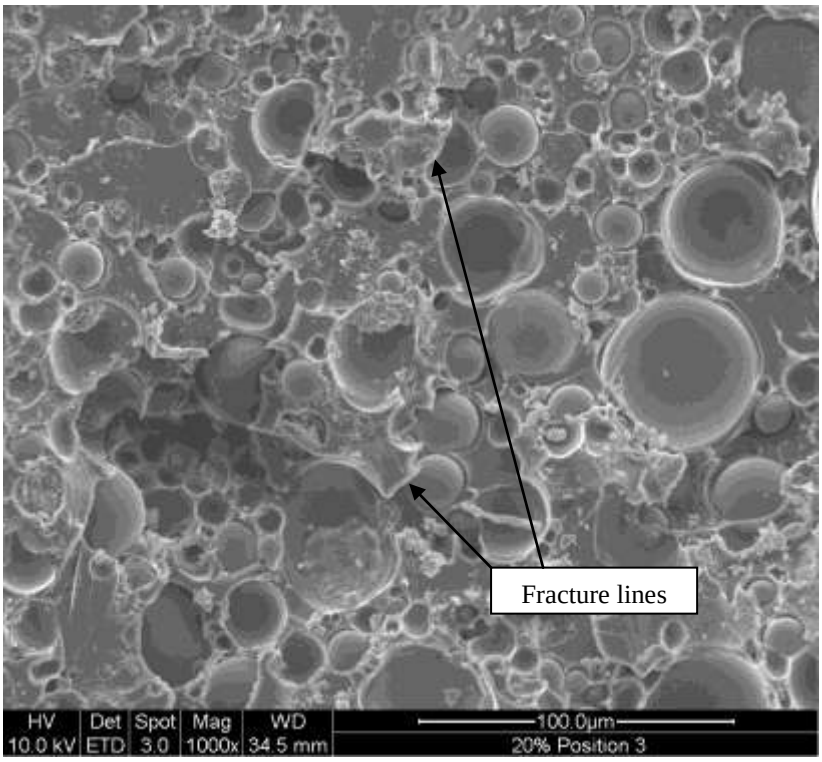

Figure 5.24: Position 3 at 1000x magnification, 20% glass powder

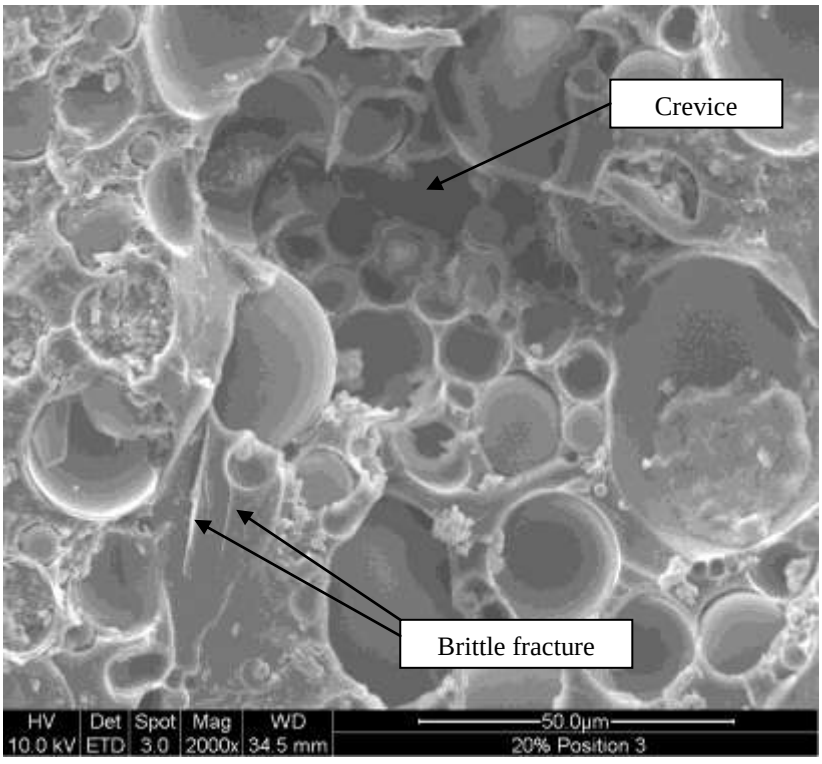

Figure 5.25: Position 3 at 2000x magnification, 20% glass powder

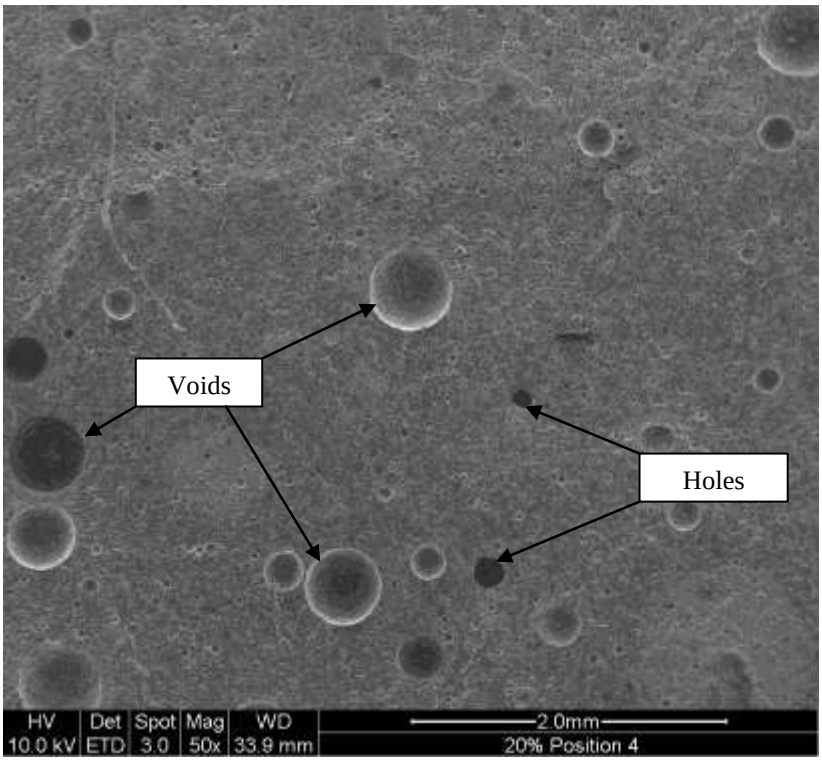

Figure 5.26: Position 4 at 50x magnification, 20% glass powder

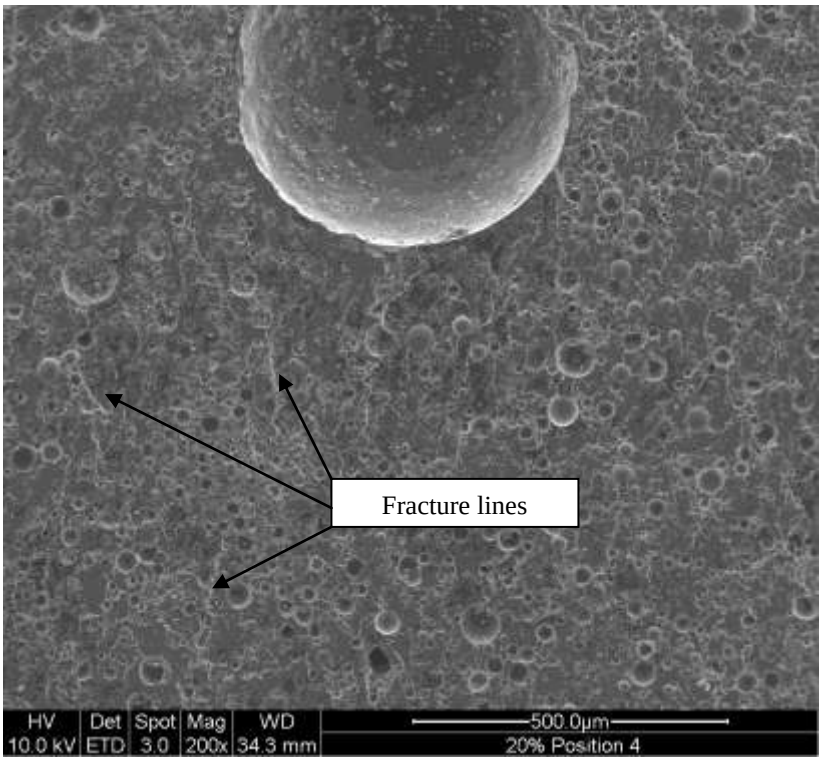

Figure 5.27: Position 4 at 200x magnification, 20% glass powder

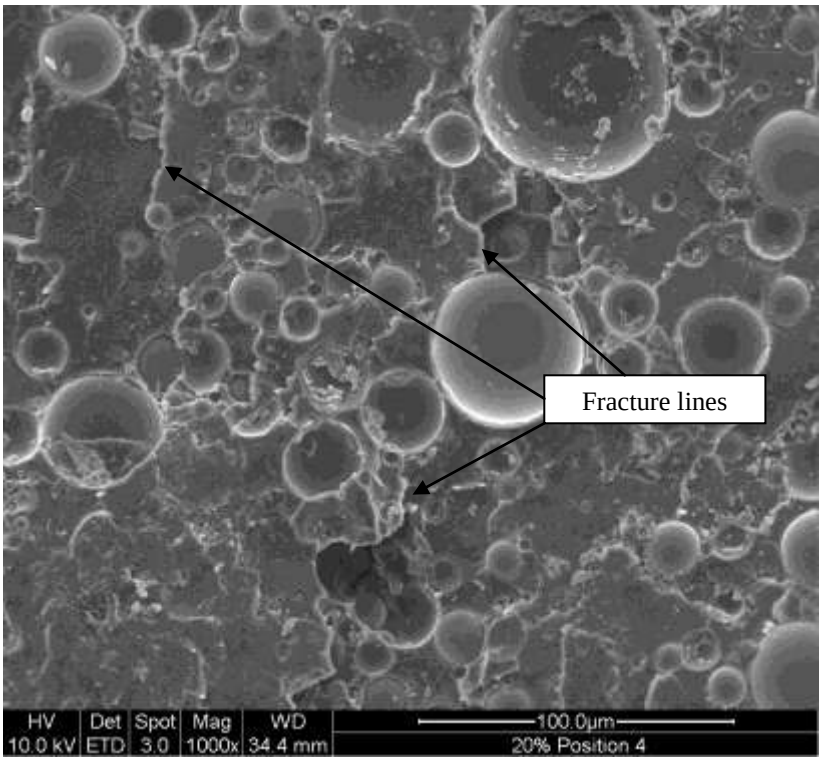

Figure 5.28: Position 4 at 1000x magnification, 20% glass powder

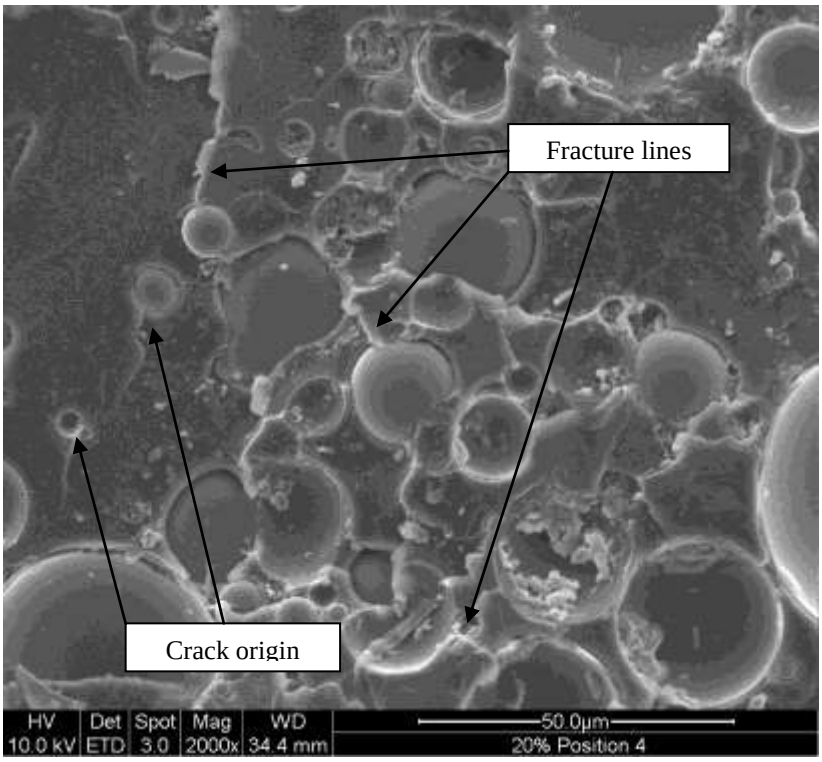

Figure 5.29: Position 4 at 2000x magnification, 20% glass powder

5.6 Conclusion

The analysis of the results has given the fracture toughness of each sample. The use of SEM has allowed a detailed analysis at the fractured surfaces of two selected specimens. This allowed us to draw conclusions as to what influenced the behaviour of the samples.

A comparison to other studies has concluded that the results were comparable. Trends and values were particularly important, as well as materials used. Encouraging comparisons gave more confidence in my results.

The fracture toughness of glass powder reinforced vinyl ester resin is the highest at 15% glass powder by weight. Comparison to previous results supported the data. SEM analysis indicated that crack propagation occurred around the glass powder particles and voids, and it was also at these locations where some cracks originated, thus playing an important role in the behaviour of the specimens.

6 Conclusion

6.1 Introduction

This chapter is the conclusion of the report. It will essentially answer what the project set out to investigate; that is, what percentage by weight of glass powder gives vinyl ester resin the highest fracture toughness? This chapter will briefly discuss the results, SEM analysis, the project on a whole, and outline any future work.

6.2 Fracture Toughness

After obtaining the results and analysis, it was concluded that the fracture toughness of glass powder reinforced vinyl ester resin was highest at 15 percent (by weight of glass powder). Comparison to other studies gave confidence in the results obtained, as trends and values were comparable, even for different combinations of materials.

6.3 SEM Analysis

The SEM analysis gave detailed pictures of the fracture surface of specimens; one of neat resin (0% glass powder), and one at 20% glass powder. It was concluded that fracture occurred through the resin, rather than through the glass powder. There were gaps around numerous glass powder particles allowing the particles to become easily dislodged, leaving craters on the specimen's surface. These craters, along with air bubbles (or voids) in the specimen created areas of stress concentration where cracks originated from. It was also seen that there were areas of brittle as well as ductile behaviour.

6.4 Conclusion and Further Work

This project has comprehensively established that glass powder improves the fracture toughness of vinyl ester resin. The best percentage by weight of glass powder to vinyl ester resin was 15 percent.

For the future, an investigation into the corrosion properties of glass powder reinforced vinyl ester resin would be beneficial. Since vinyl ester resin is known for its corrosion resistance, a study into the effects of adding a filler such (as glass powder) to the resin would be valuable.

References

Baker, L M, Compliance calibration of a family of short rod and short bar fracture toughness specimens 1983, Vol. 17, No. 4, pp. 289-312.

Barker, L M, Short Rod and Short Bar Fracture Toughness Specimen Geometries and Test Methods for Metallic Materials," *Fracture Mechanics: Thirteenth Conference. ASTM STP* 743 1981, pp. 456-475.

Blankenship, L T, White, M N, Puckett, P M, Vinyl ester resins: Versatile resins for composites 1989, pp. 234-245.

Bozzola, J J, Russell, L D, Electron Microscopy. Principles and Techniques for Biologists. (first edition 1992; second edition 1998) Jones and Bartlett Publishers.

Charalambides, M N, Williams, J G, Fracture Toughness Characterization of Phenolic Resin and Its Composite 1995, Vol. 16, No. 1, pp. 17-28.

Chemwatch, Material Safety Data Sheet for Methyl Ethyl Ketone Peroxide, 2000, pp.1-2.

Fu, S Y, Feng, X Q, Lauke, B, Mai, Y W, Effects of particle size, particle/matrix interface adhesion and particle loading on mechanical properties of particulate-polymer composites 2008.

Huntsman Composites, Technical Data Sheet, Hetron® 922PA vinyl ester resin, 2001, pp.1-2.

Juvinall, R C, Marshek, K M, 2001, Fundamentals of Machine Component Design, Fourth Edition 2006,Wiley and Sons Inc.

Ku, H, Cheng, Y M, Snook, C, Baddeley, D, Drop weight impact test fracture of vinyl ester composites: micrographs of pilot study 2005, Vol. 39, No. 18, pp. 1607-1620.

Ku, H, Rogers, D, Davey, R, Cardona, F, Trada, M, Fracture toughness of phenol formaldehyde composites: pilot study 2008, Vol. 17, No. 1, pp. 85-90.

Liang, J Z, Yang, Q Q, Mechanical properties of carbon black-filled high-density polyethylene antistatic composites 2009, Vol. 28, No. 3, pp.295-304.

Munz, D, Determination of fracture toughness of high strength aluminium alloys with chevron notched short rod and short bar specimens 1981, Vol. 15, No. 1-2, pp.231-236.

Potters Industries Inc, Material safety data sheet, Spherical hollow glass spheres 2007, pp. 1-4.

Robinette, E J, Ziaee, S, Palmese, G R, Toughening of vinyl ester resin using butadiene-acrylonitrile rubber modifiers 2004, pp. 6143-6154.

Sweet, J R, Methyl Ethyl Ketone Peroxide, 2002, pp.1-2.

Appendix A – Project Specification

University of Southern Queensland
Faculty of Engineering and Surveying

ENG 4111/4112 Research Project
PROJECT SPECIFICATION

Project title:	**Fracture toughness of glass powder reinforced vinyl ester resin post cured in a conventional oven using short bar tests.**
Student:	Geoffrey Korowa – 0050027542
Supervisor:	Dr. Harry Ku
Co-Supervisor:	
Sponsorship:	

Project Synopsis:

In this project, a number of samples of vinyl ester resin specimens will be made with each sample containing different percentages by weight of glass powder as a filler. The samples will be post-cured and tested to find fracture toughness. The results can then be analysed to develop behavioural trends and formulas that predict material behaviour in relation to filler composition.

Timelines:

1. Familiarization of equipment and literature reviews.
   Begin : 9th December 2008
   Completion : 7th January 2009
   Approx. Hours : 60 hours

2. Preparation of a cast/mould for short bar tests.
   Begin : 13th January 2009
   Completion : 19th January 2009
   Approx. Hours : 10 hours

3. Casting of components.
   Begin : 20th January 2009
   Completion : 10th February 2009
   Approx. Hours : 25 hours

4. Post-Curing and preparation of specimens.
   Begin : 16th February 2009
   Completion : 17th February 2009

Approx. Hours : 15 hours

5. Carry out fracture toughness tests.
   Begin : 24th February 2009
   Completion : 26th February 2009
   Approx. Hours : 15 hours

6. Analysis of results.
   Begin : 15th March 2009
   Completion : 1st May 2009
   Approx. Hours : 60 hours

7. Outline conclusion.
   Begin : 9th May 2009
   Completion : 30th May 2009
   Approx. Hours : 20 hours

8. Discuss thesis outline with supervisors.
   Begin : 15th June 2009
   Completion : 17thJuly 2009
   Approx. Hours : 10 hours

9. Initial draft of thesis – draft form for supervisor to check over

   Begin : 1st August 2009
   Completion : 13th September 2009
   Approx. Hours : 60 hours

10. Final draft of thesis – to incorporate changes suggested by supervisor.

    Begin : 19th September 2009
    Completion : 3rd October 2009
    Approx. Hours : 15 hours

11. Complete the thesis in requested format.

    Begin : 3rd October 2009
    Completion : 25th October 2009
    Approx. Hours : 20 hours

AGREED:

_____ (student) _____ (Supervisor)

(Date)___/___/___

Appendix B – Raw Data

24/02/2009

Sample ID: Geoff-0%G-1.mss
Specimen Number: 1
Tagged: False

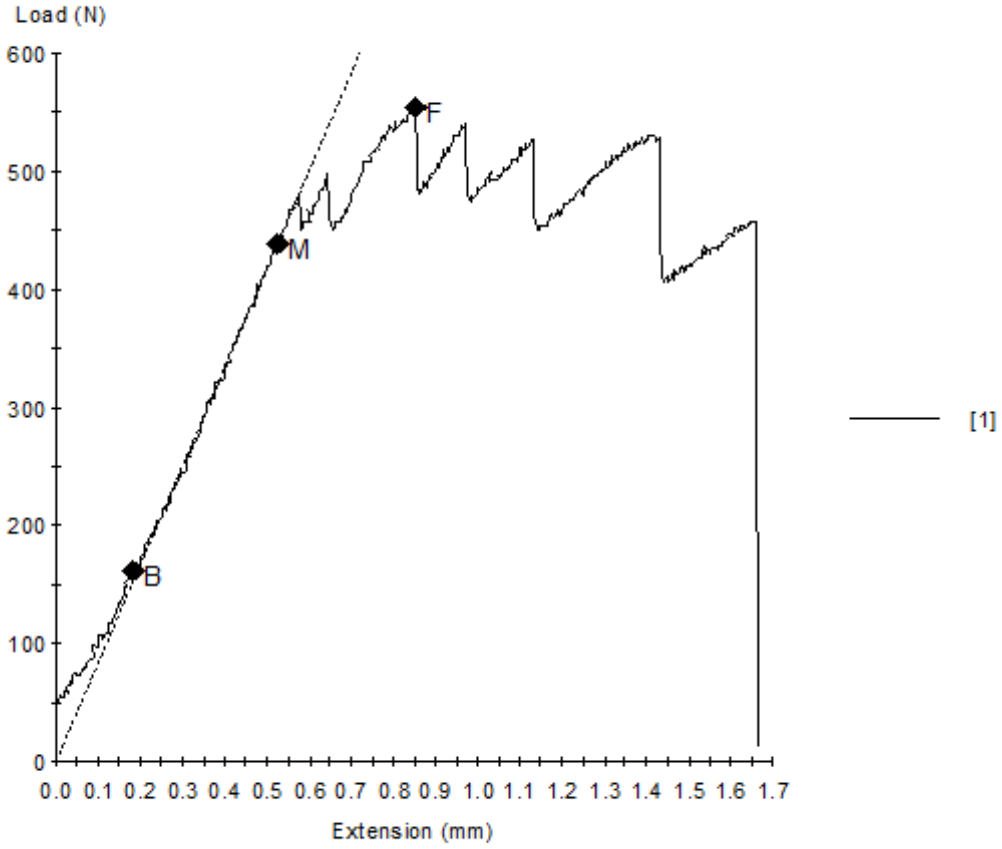

Specimen Results:

Name	Value	Units
Thickness	35.000	mm
Width	50.000	mm
Area	1750	mm^2
Peak Load	557	N
Peak Stress	0.32	MPa
Break Load	554	N
Break Stress	0.32	MPa
Elongation At Break	0.854	mm
Stress At Offset Yield	0.262	MPa
Load At Offset Yield	458.907	N

Sample ID: Geoff-0%G-2.mss
Specimen Number: 2
Tagged: False

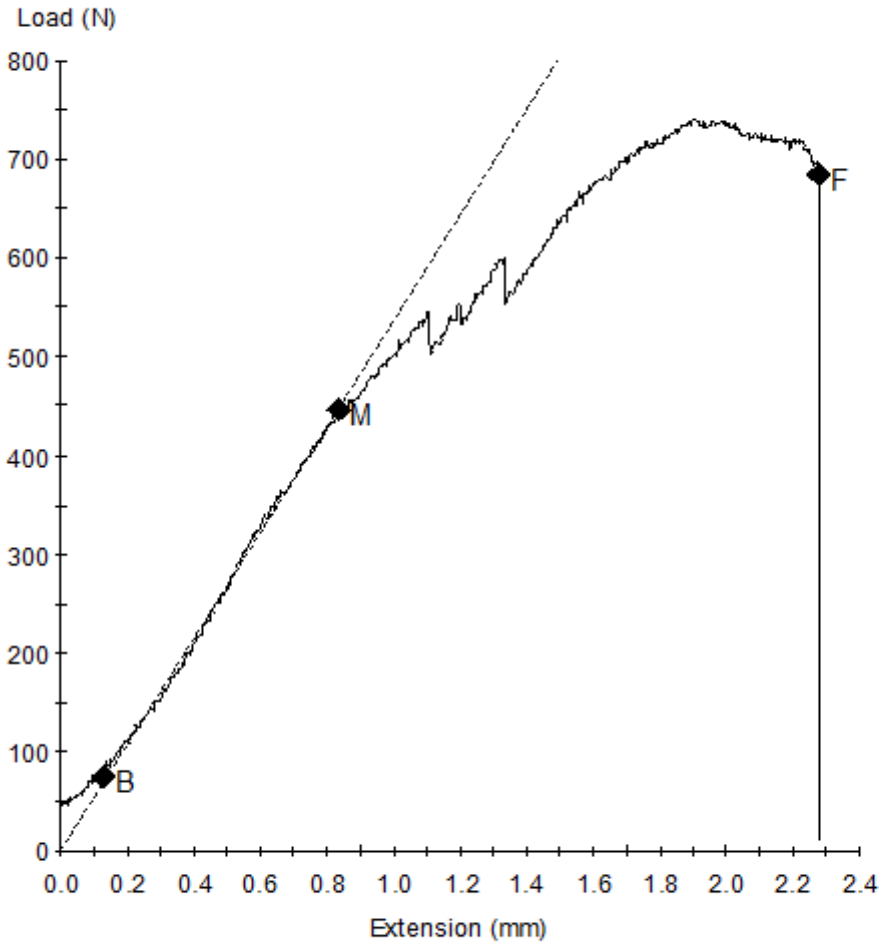

Specimen Results:

Name	Value	Units
Thickness	26.000	mm
Width	50.000	mm
Area	1300	mm^2
Peak Load	741	N
Peak Stress	0.57	MPa
Break Load	683	N
Break Stress	0.53	MPa
Elongation At Break	2.276	mm
Stress At Offset Yield	0.370	MPa
Load At Offset Yield	480.560	N

Sample ID: Geoff -0%G-3.mss
Specimen Number: 3
Tagged: False

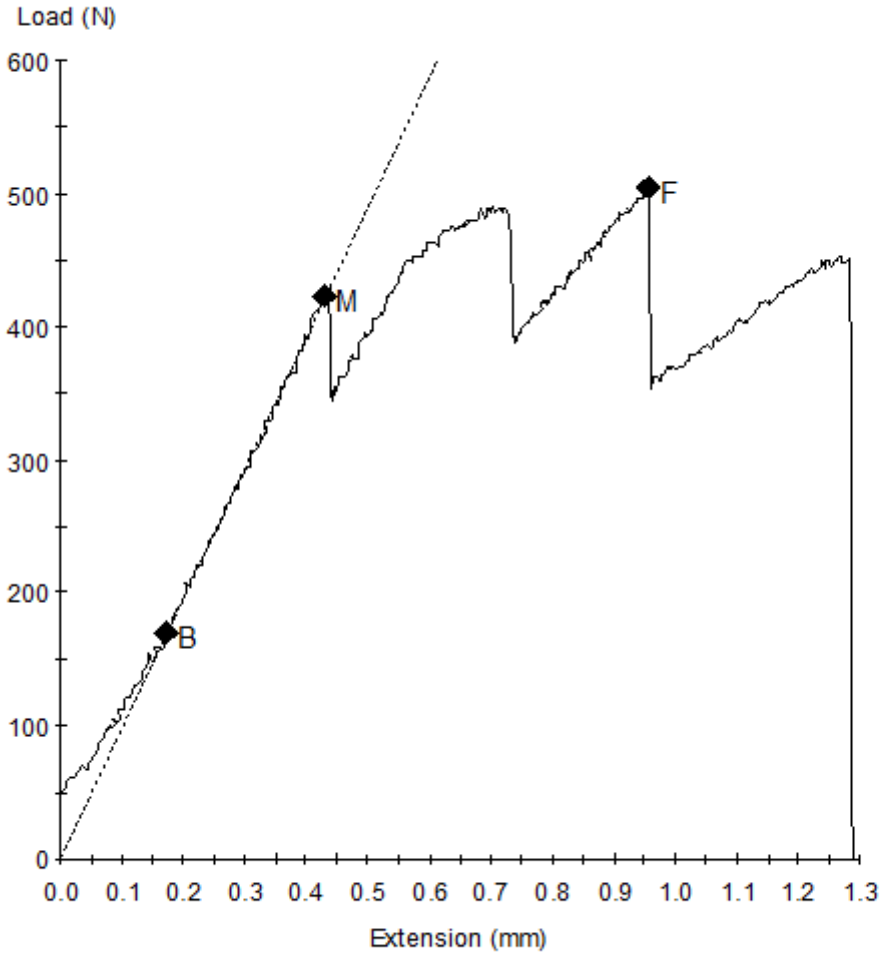

Specimen Results:

Name	Value	Units
Thickness	26.000	mm
Width	50.000	mm
Area	1300	mm^2
Peak Load	505	N
Peak Stress	0.39	MPa
Break Load	505	N
Break Stress	0.39	MPa
Elongation At Break	0.958	mm
Stress At Offset Yield	0.264	MPa
Load At Offset Yield	343.089	N

Sample ID: Geoff-0%G-4.mss
Specimen Number: 4
Tagged: False

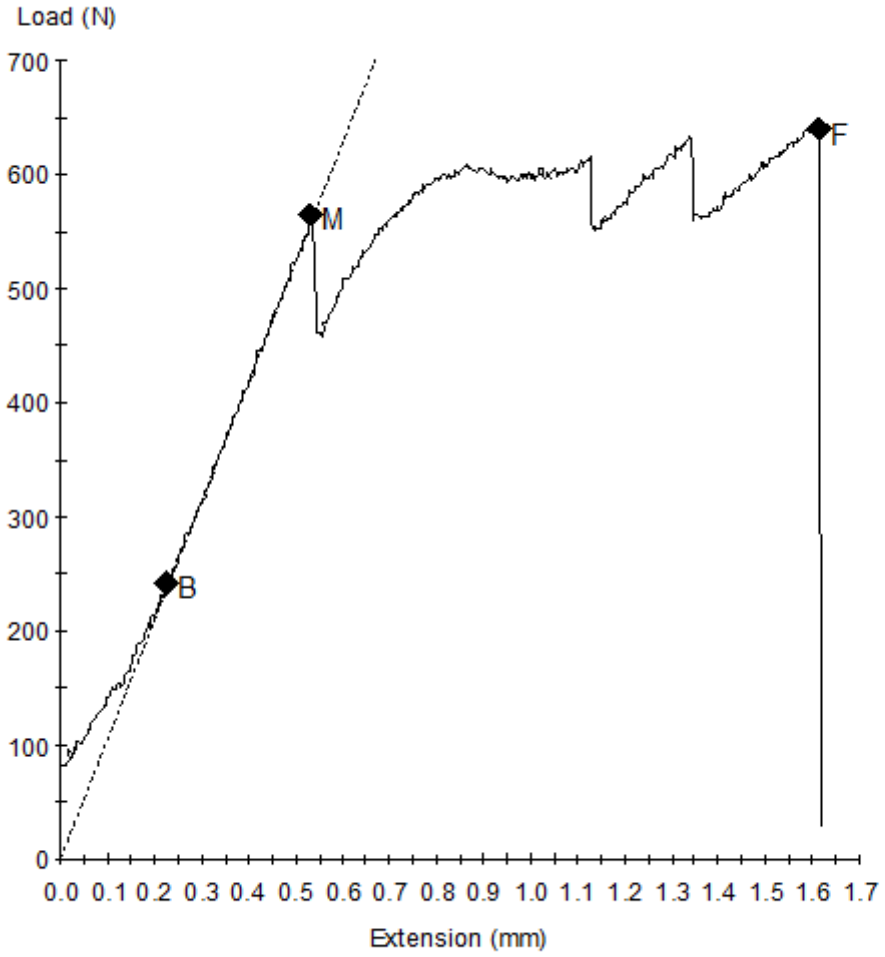

Specimen Results:

Name	Value	Units
Thickness	26.000	mm
Width	50.000	mm
Area	1300	mm^2
Peak Load	645	N
Peak Stress	0.50	MPa
Break Load	641	N
Break Stress	0.49	MPa
Elongation At Break	1.611	mm
Stress At Offset Yield	0.354	MPa
Load At Offset Yield	459.914	N

Sample ID: Geoff-0%G-5.mss
Specimen Number: 5
Tagged: False

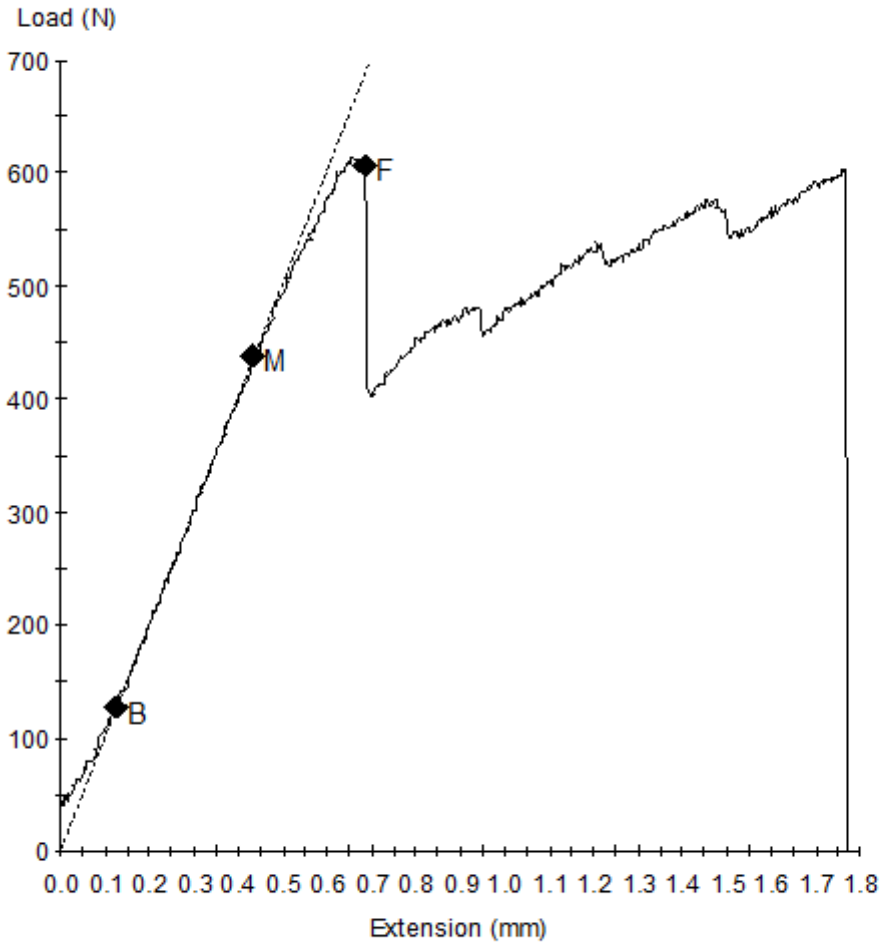

[5]

Specimen Results:

Name	Value	Units
Thickness	26.000	mm
Width	50.000	mm
Area	1300	mm^2
Peak Load	615	N
Peak Stress	0.47	MPa
Break Load	606	N
Break Stress	0.47	MPa
Elongation At Break	0.684	mm
Stress At Offset Yield	0.470	MPa
Load At Offset Yield	610.981	N

Sample ID: Geoff-0%G-6.mss
Specimen Number: 6
Tagged: False

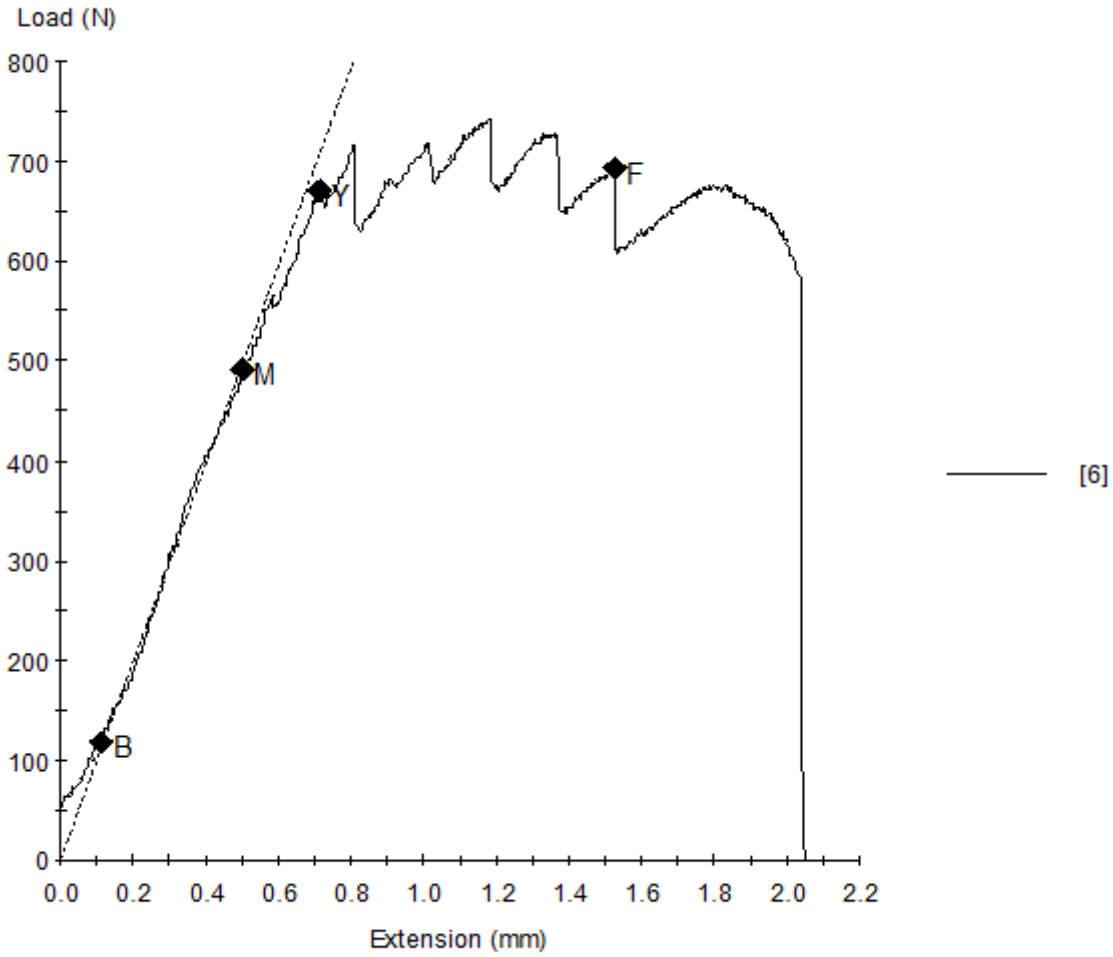

Specimen Results:

Name	Value	Units
Thickness	26.000	mm
Width	50.000	mm
Area	1300	mm^2
Peak Load	743	N
Peak Stress	0.57	MPa
Break Load	694	N
Break Stress	0.53	MPa
Elongation At Break	1.524	mm
Stress At Offset Yield	0.504	MPa

Load At Offset Yield 654.622 N
Geoff-0%G

Report Date: 24/02/2009

Test Date : 24/02/2009
Method : MMT fracture toughness Test .msm

Specimen Results:

Specimen #	Thickness mm	Width mm	Area mm^2	Peak Load N	Peak Stress MPa	Break Load N	Break Stress MPa
1	35.000	50.000	1750	557	0.32	554	0.32
2	26.000	50.000	1300	741	0.57	683	0.53
3	26.000	50.000	1300	505	0.39	505	0.39
4	26.000	50.000	1300	645	0.50	641	0.49
5	26.000	50.000	1300	615	0.47	606	0.47
6	26.000	50.000	1300	743	0.57	694	0.53
Mean	**27.500**	**50.000**	**1375**	**634**	**0.47**	**614**	**0.45**
Std Dev	**3.674**	**0.000**	**184**	**96**	**0.10**	**74**	**0.09**

Specimen #	Elongation At Break mm	Stress At Offset Yield MPa	Load At Offset Yield N				
1	0.854	0.262	458.907				
2	2.276	0.370	480.560				
3	0.958	0.264	343.089				
4	1.611	0.354	459.914				
5	0.684	0.470	610.981				
6	1.524	0.504	654.622				
Mean	**1.318**	**0.371**	**501.345**				
Std Dev	**0.599**	**0.101**	**113.585**				

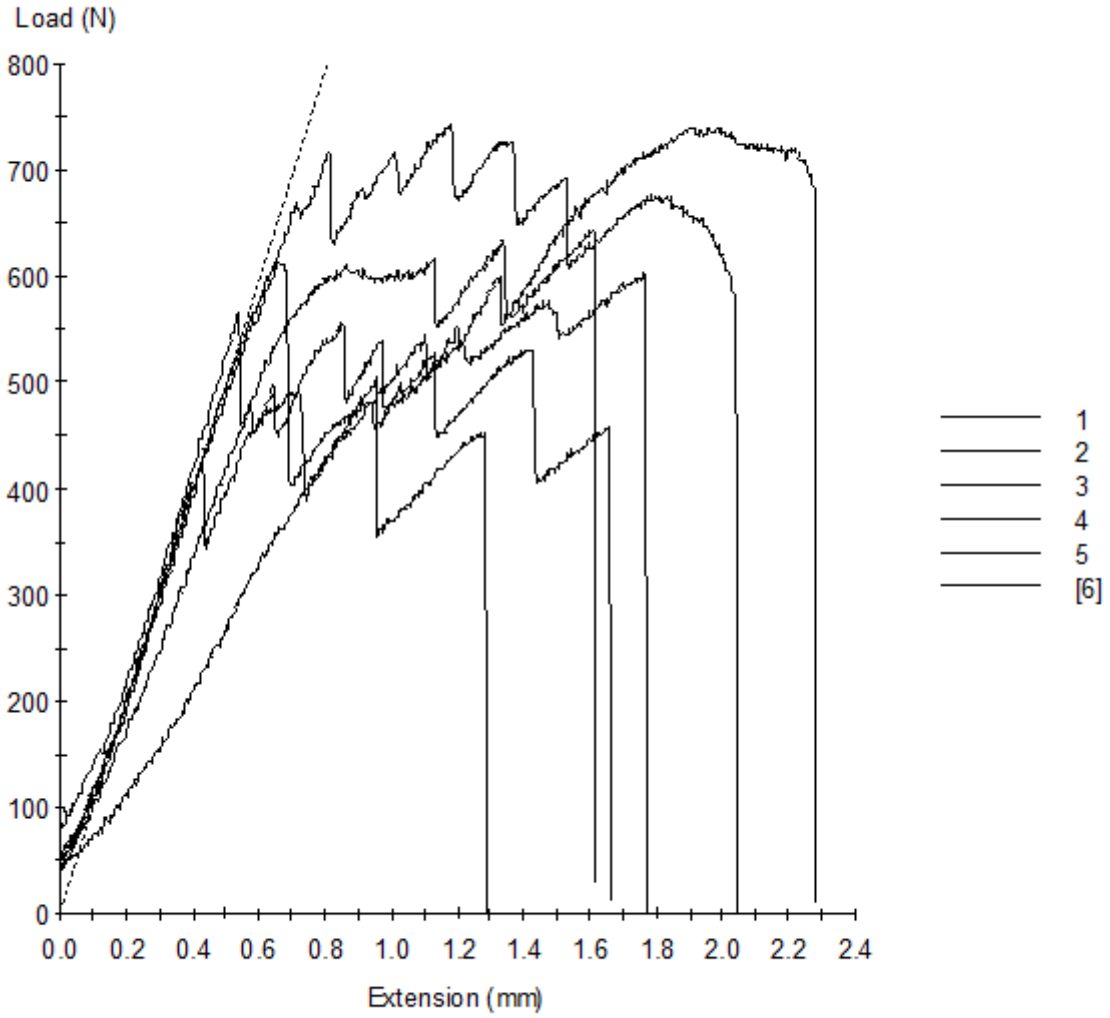
Load (N)
800
700
600
500
400
300
200
100
0
0.0
0.2
0.4
0.6
0.8
1.0
1.2
1.4
1.6
1.8
2.0
2.2
2.4
Extension (mm)
1
2
3
4
5
[6]

Sample ID: Geoff-5%G-1.mss
Specimen Number: 1
Tagged: False

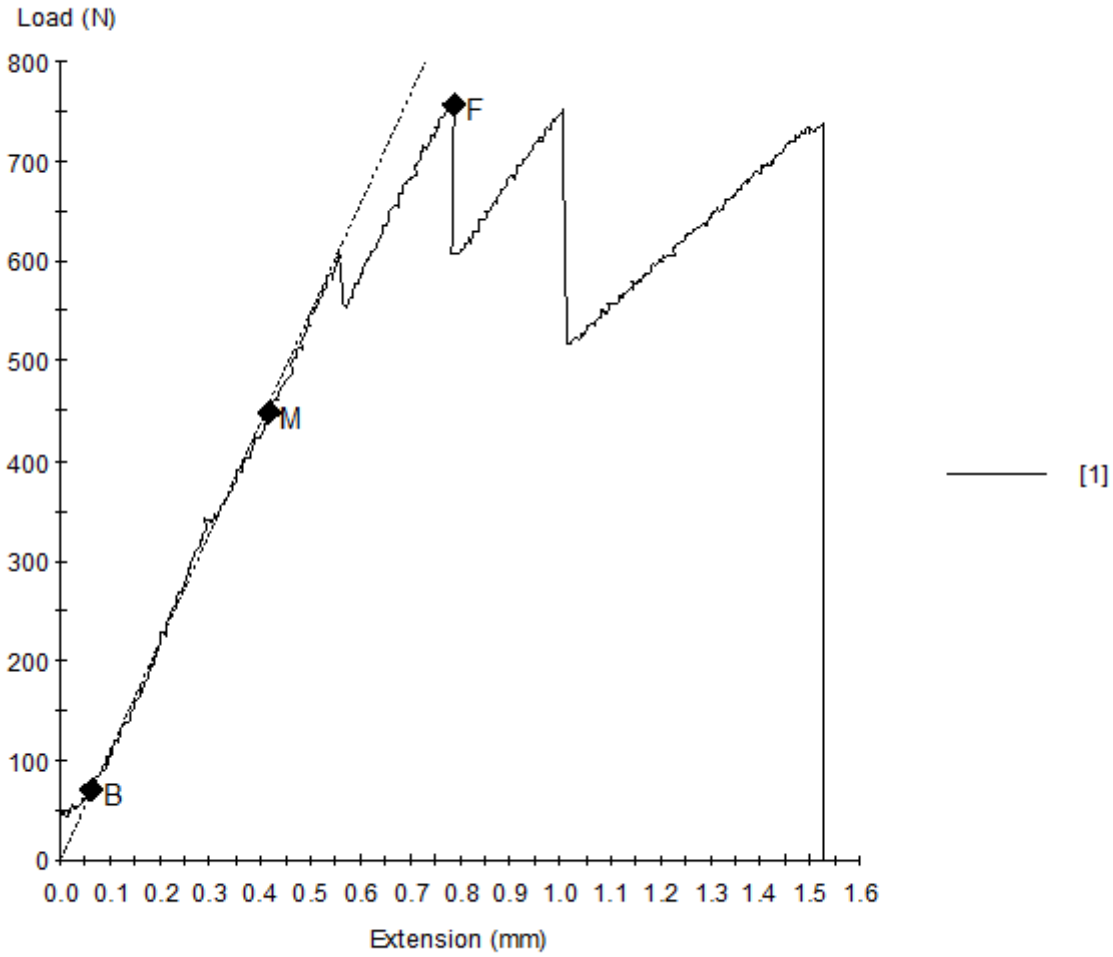

Specimen Results:

Name	Value	Units
Thickness	26.000	mm
Width	50.000	mm
Area	1300	mm^2
Peak Load	757	N
Peak Stress	0.58	MPa
Break Load	757	N
Break Stress	0.58	MPa
Elongation At Break	0.787	mm
Stress At Offset Yield	0.429	MPa
Load At Offset Yield	557.100	N

Sample ID: Geoff-5%G-2.mss
Specimen Number: 2
Tagged: False

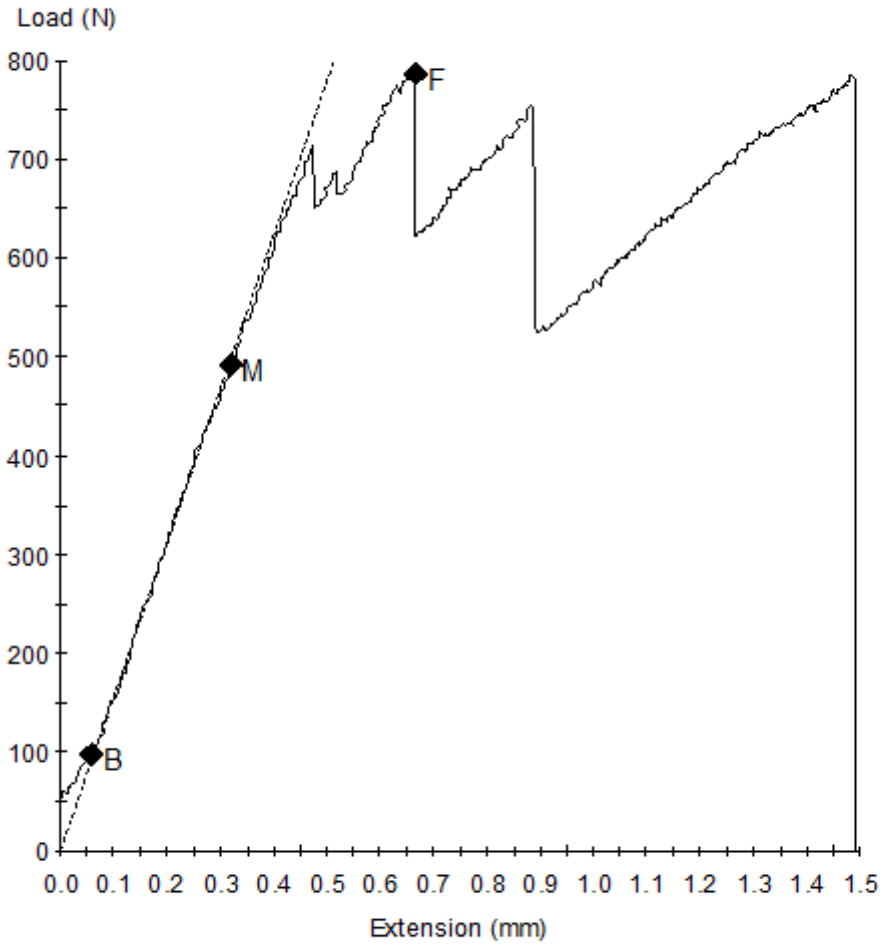

[2]

Specimen Results:

Name	Value	Units
Thickness	26.000	mm
Width	50.000	mm
Area	1300	mm^2
Peak Load	786	N
Peak Stress	0.60	MPa
Break Load	786	N
Break Stress	0.60	MPa
Elongation At Break	0.665	mm
Stress At Offset Yield	0.501	MPa
Load At Offset Yield	651.265	N

Sample ID: Geoff-5%G-3.mss
Specimen Number: 3
Tagged: False

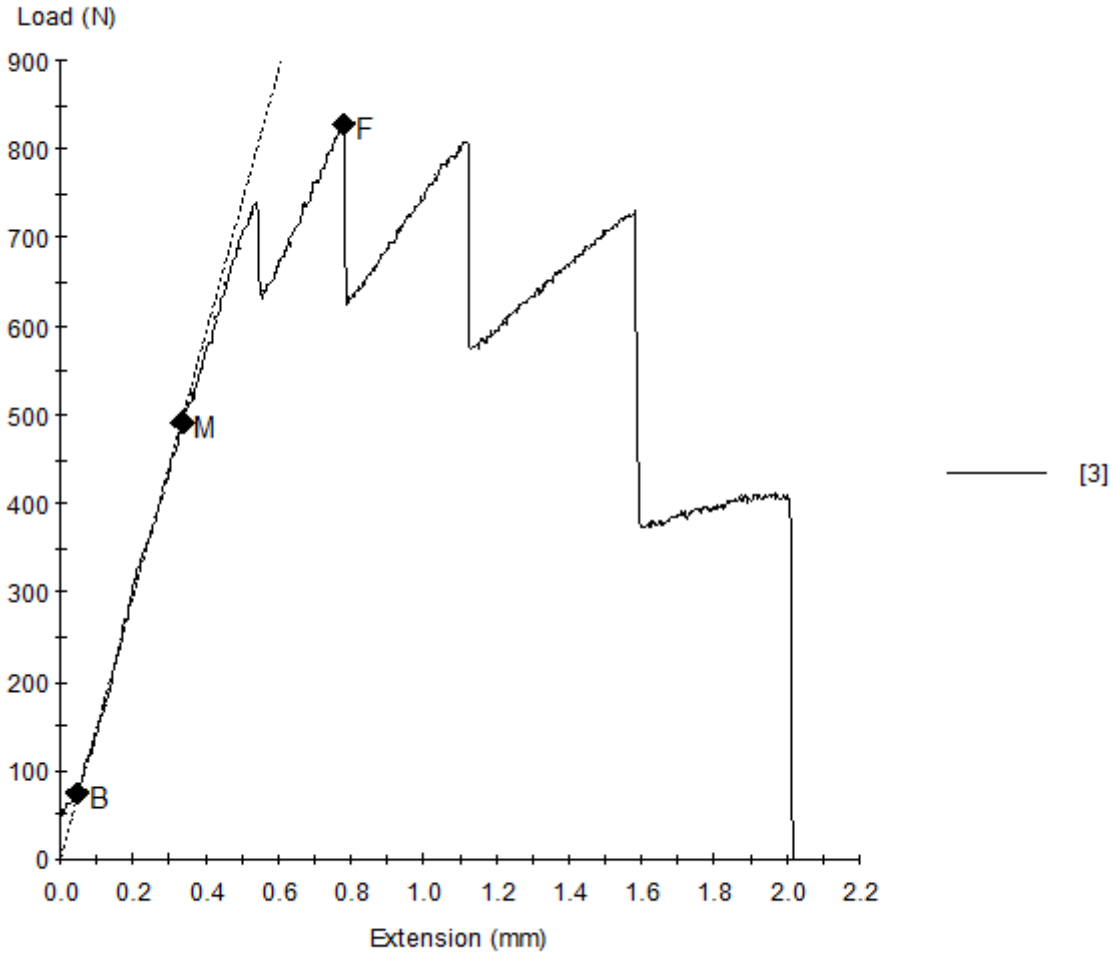

Specimen Results:

Name	Value	Units
Thickness	26.000	mm
Width	50.000	mm
Area	1300	mm^2
Peak Load	829	N
Peak Stress	0.64	MPa
Break Load	829	N
Break Stress	0.64	MPa
Elongation At Break	0.779	mm
Stress At Offset Yield	0.496	MPa
Load At Offset Yield	644.551	N

Sample ID: Geoff-5%G4.mss
Specimen Number: 4
Tagged: False

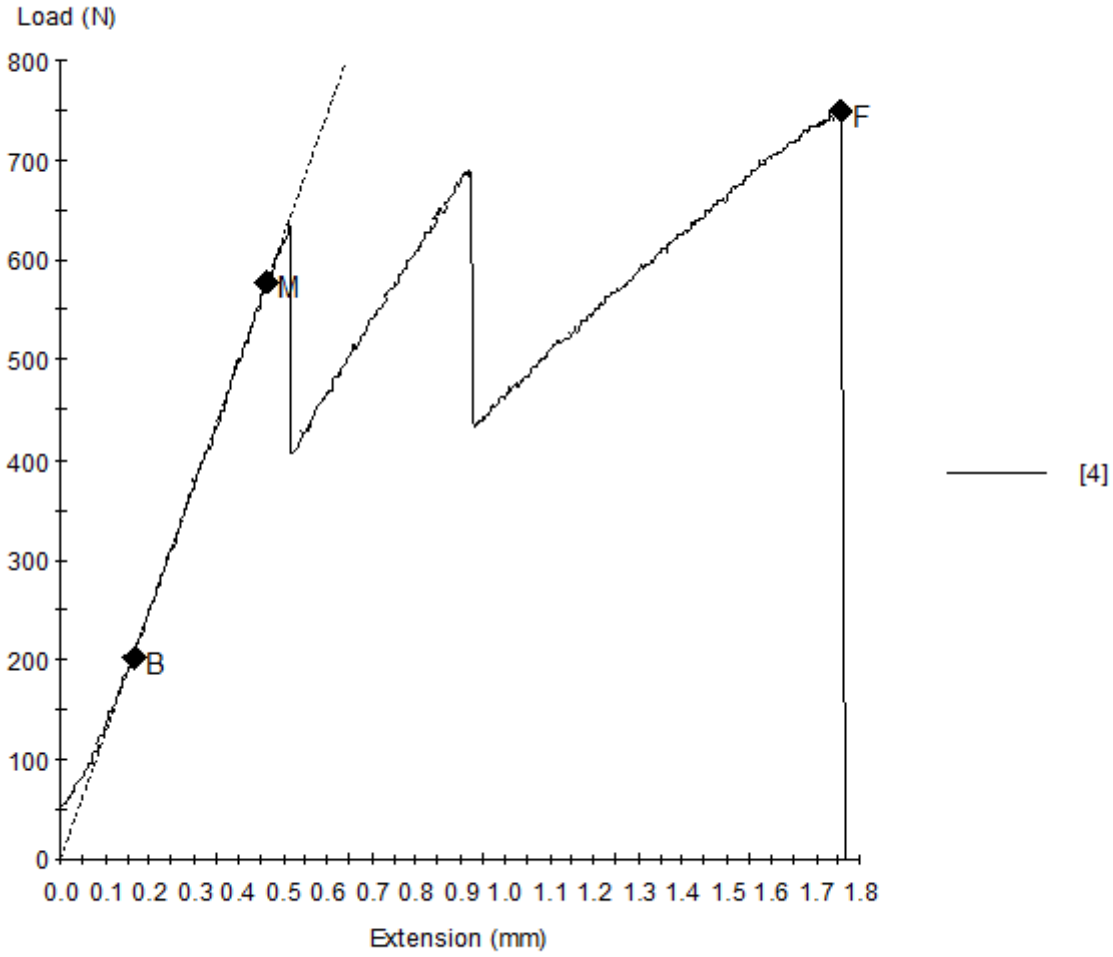

Specimen Results:

Name	Value	Units
Thickness	26.000	mm
Width	50.000	mm
Area	1300	mm^2
Peak Load	750	N
Peak Stress	0.58	MPa
Break Load	750	N
Break Stress	0.58	MPa
Elongation At Break	1.758	mm
Stress At Offset Yield	0.311	MPa
Load At Offset Yield	404.859	N

Sample ID: Geoff-5%G-5.mss
Specimen Number: 5
Tagged: False

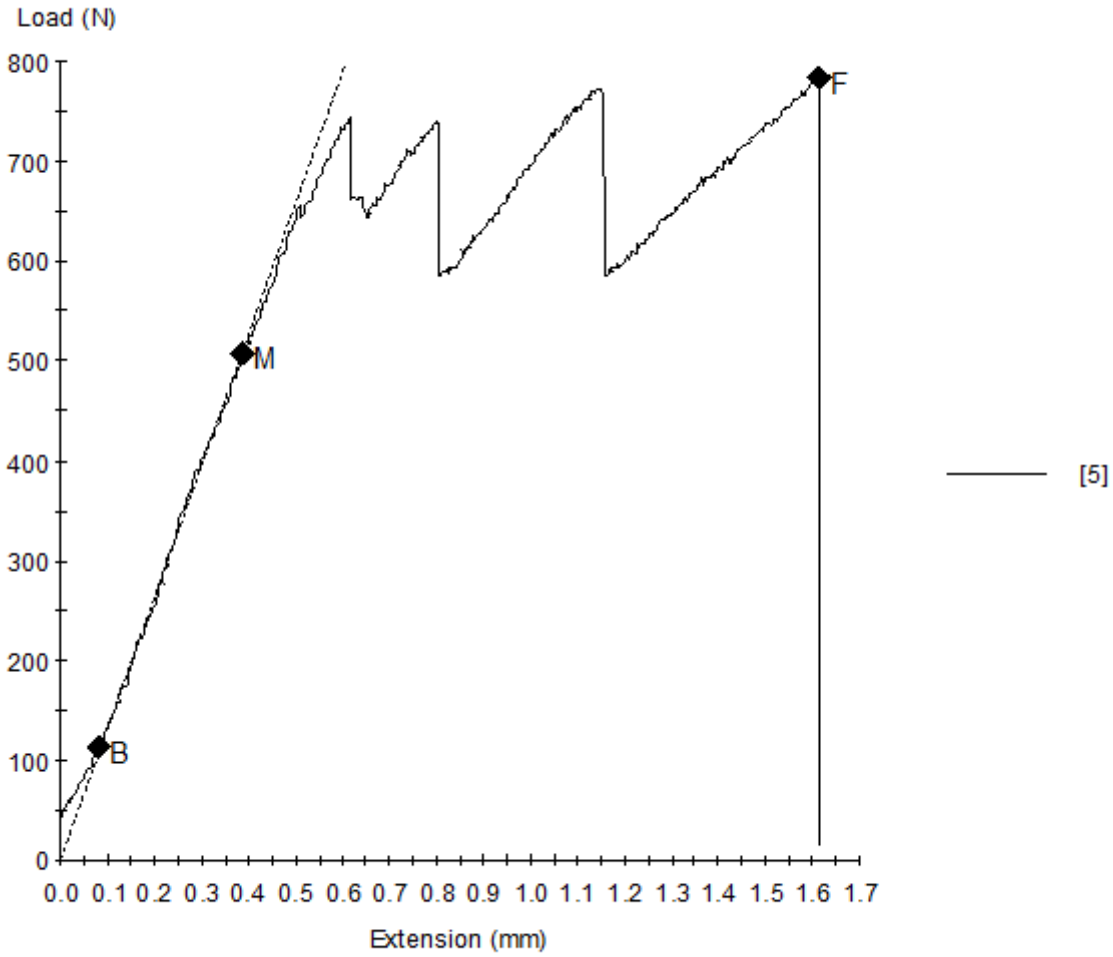

Specimen Results:

Name	Value	Units
Thickness	26.000	mm
Width	50.000	mm
Area	1300	mm^2
Peak Load	783	N
Peak Stress	0.60	MPa
Break Load	783	N
Break Stress	0.60	MPa
Elongation At Break	1.611	mm
Stress At Offset Yield	0.509	MPa
Load At Offset Yield	661.504	N

Sample ID: Geoff-5%G-6.mss
Specimen Number: 6
Tagged: False

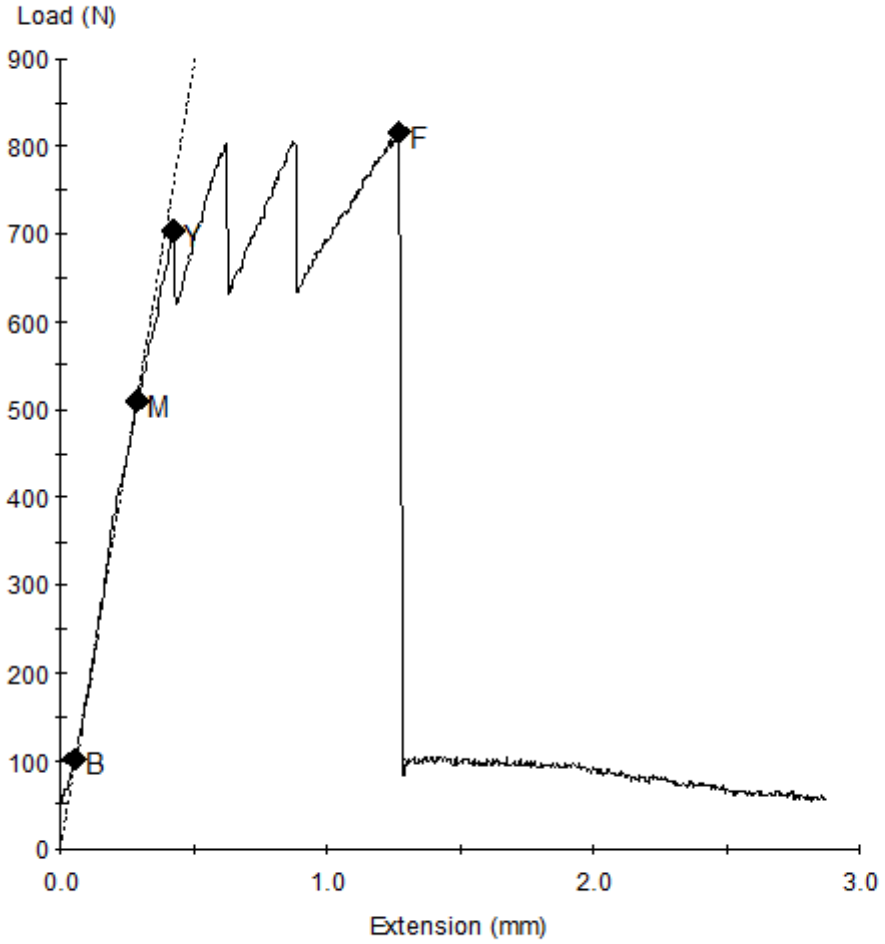

[6]

Specimen Results:

Name	Value	Units
Thickness	26.000	mm
Width	50.000	mm
Area	1300	mm^2
Peak Load	815	N
Peak Stress	0.63	MPa
Break Load	815	N
Break Stress	0.63	MPa
Elongation At Break	1.272	mm
Stress At Offset Yield	0.476	MPa
Load At Offset Yield	619.037	N

Report Date: 24/02/2009

Test Date : 24/02/2009
Method : MMT fracture toughness Test .msm

Specimen Results:

Specimen #	Thickness mm	Width mm	Area mm^2	Peak Load N	Peak Stress MPa	Break Load N	Break Stress MPa
1	26.000	50.000	1300	757	0.58	757	0.58
2	26.000	50.000	1300	786	0.60	786	0.60
3	26.000	50.000	1300	829	0.64	829	0.64
4	26.000	50.000	1300	750	0.58	750	0.58
5	26.000	50.000	1300	783	0.60	783	0.60
6	26.000	50.000	1300	815	0.63	815	0.63
Mean	**26.000**	**50.000**	**1300**	**787**	**0.61**	**787**	**0.61**
Std Dev	**0.000**	**0.000**	**0**	**31**	**0.02**	**31**	**0.02**

Specimen #	Elongation At Break mm	Stress At Offset Yield MPa	Load At Offset Yield N				
1	0.787	0.429	557.100				
2	0.665	0.501	651.265				
3	0.779	0.496	644.551				
4	1.758	0.311	404.859				
5	1.611	0.509	661.504				
6	1.272	0.476	619.037				
Mean	**1.146**	**0.454**	**589.719**				
Std Dev	**0.470**	**0.075**	**98.025**				

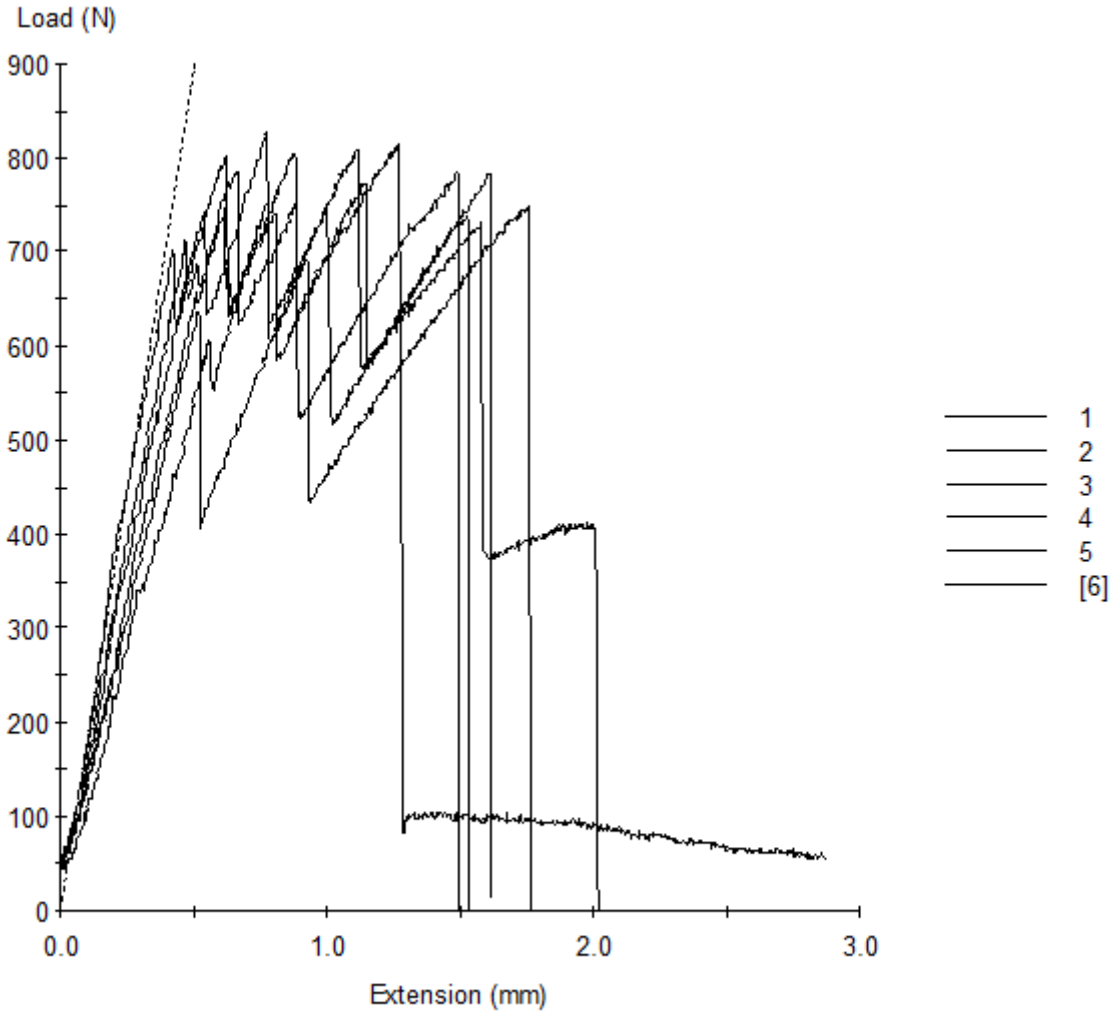
Load (N)
900
800
700
600
500
400
300
200
100
0
0.0
1.0
2.0
3.0
Extension (mm)
1
2
3
4
5
[6]

Sample ID: Geoff-10%G-1.mss
Specimen Number: 1
Tagged: False

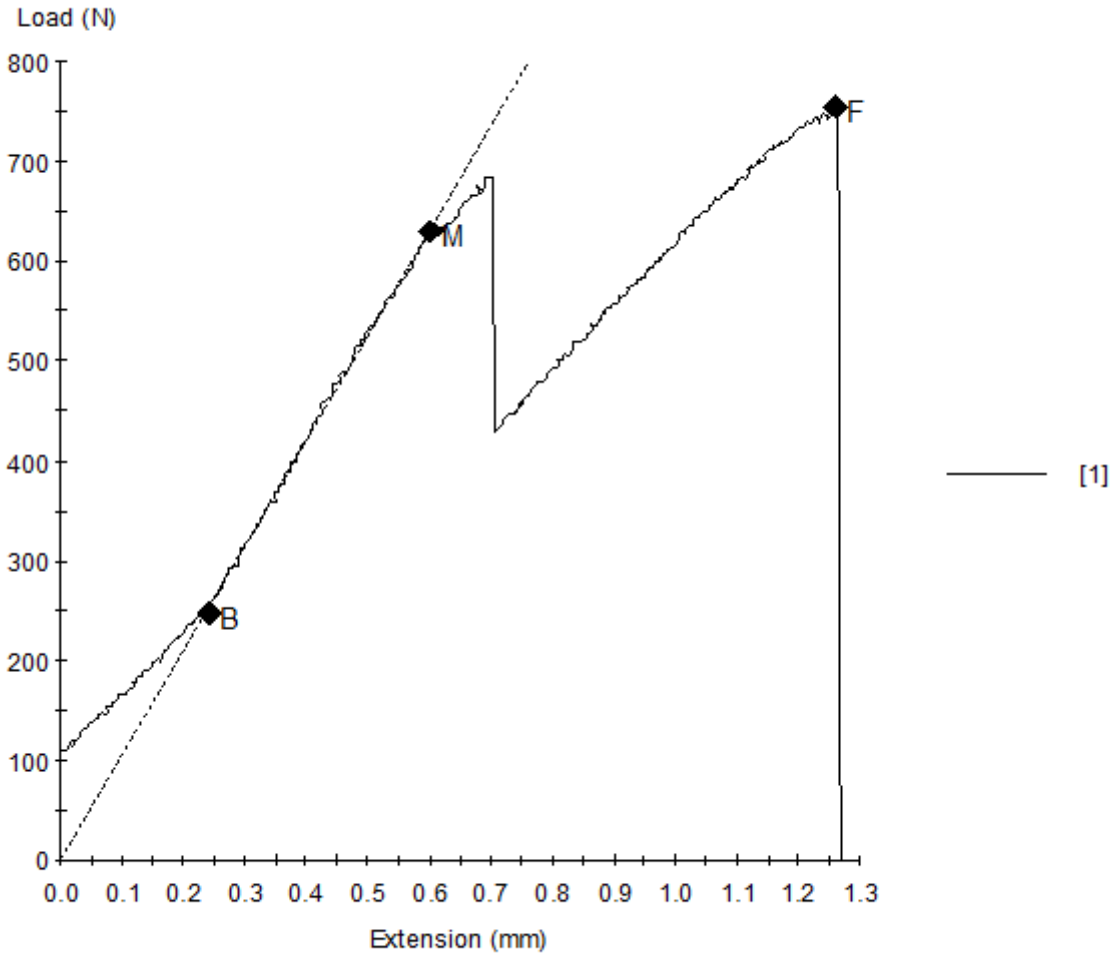

Specimen Results:

Name	Value	Units
Thickness	26.000	mm
Width	50.000	mm
Area	1300	mm^2
Peak Load	755	N
Peak Stress	0.58	MPa
Break Load	755	N
Break Stress	0.58	MPa
Elongation At Break	1.263	mm
Stress At Offset Yield	0.527	MPa
Load At Offset Yield	684.835	N

Sample ID: Geoff-10%G-2.mss
Specimen Number: 2
Tagged: False

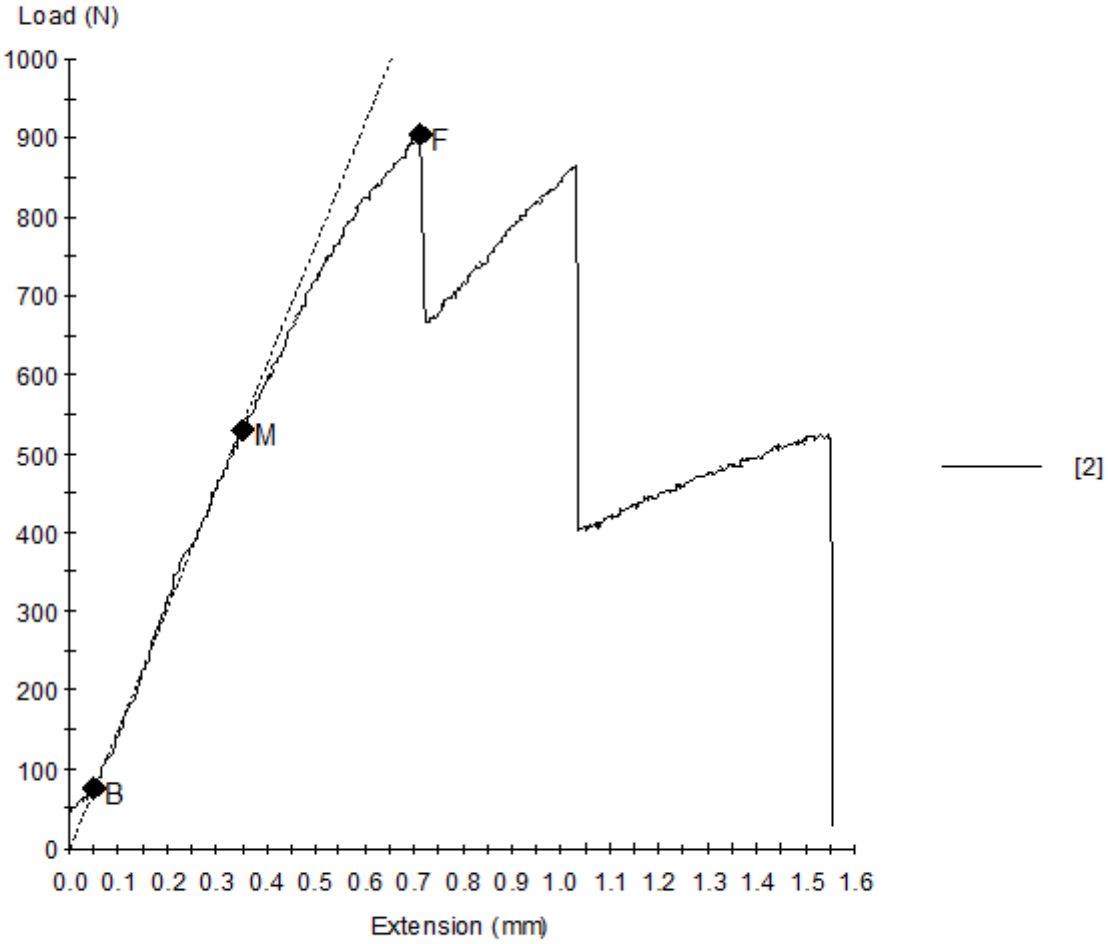

Specimen Results:

Name	Value	Units
Thickness	26.000	mm
Width	50.000	mm
Area	1300	mm^2
Peak Load	903	N
Peak Stress	0.69	MPa
Break Load	903	N
Break Stress	0.69	MPa
Elongation At Break	0.716	mm
Stress At Offset Yield	0.612	MPa
Load At Offset Yield	795.618	N

Sample ID: Geoff-10%G-3.mss
Specimen Number: 3
Tagged: False

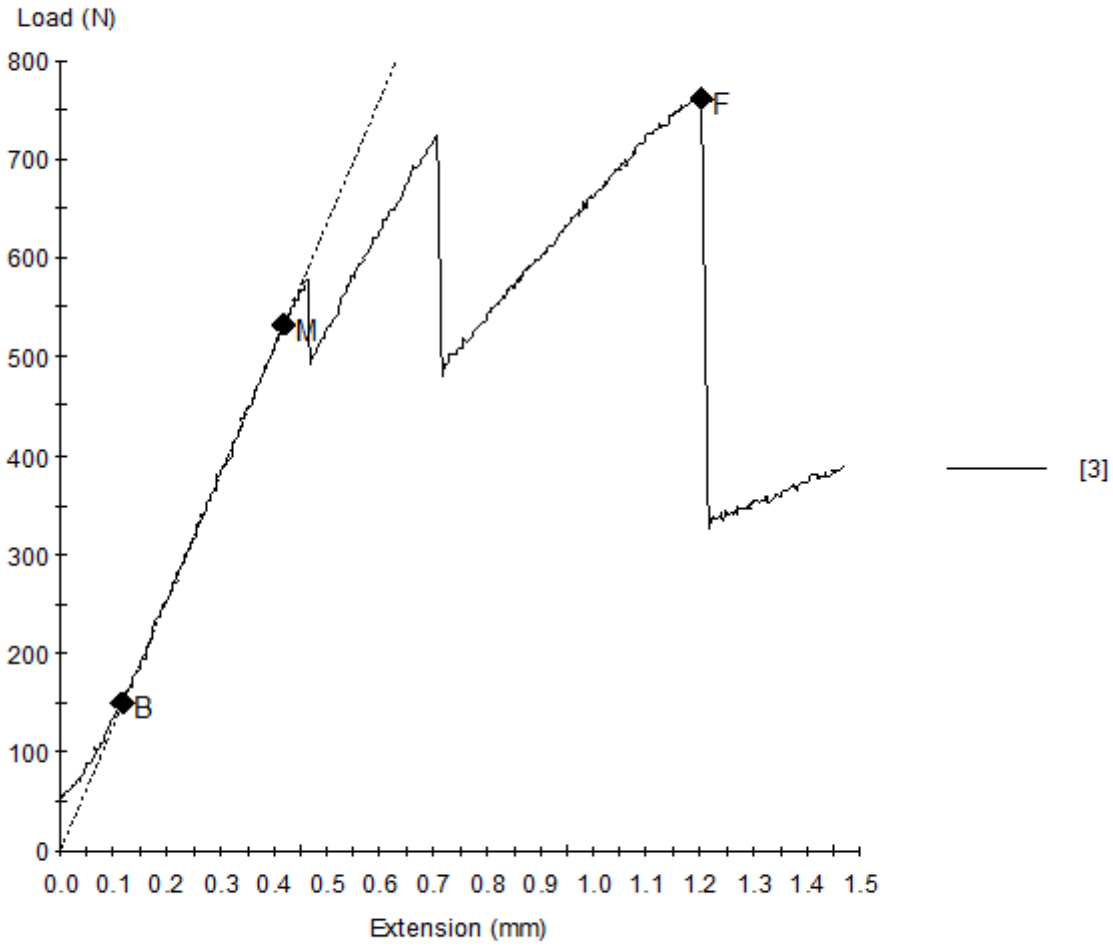

Specimen Results:

Name	Value	Units
Thickness	26.000	mm
Width	50.000	mm
Area	1300	mm^2
Peak Load	765	N
Peak Stress	0.59	MPa
Break Load	762	N
Break Stress	0.59	MPa
Elongation At Break	1.205	mm
Stress At Offset Yield	0.379	MPa
Load At Offset Yield	492.813	N

Sample ID: Geoff-10%G-4.mss
Specimen Number: 4
Tagged: False

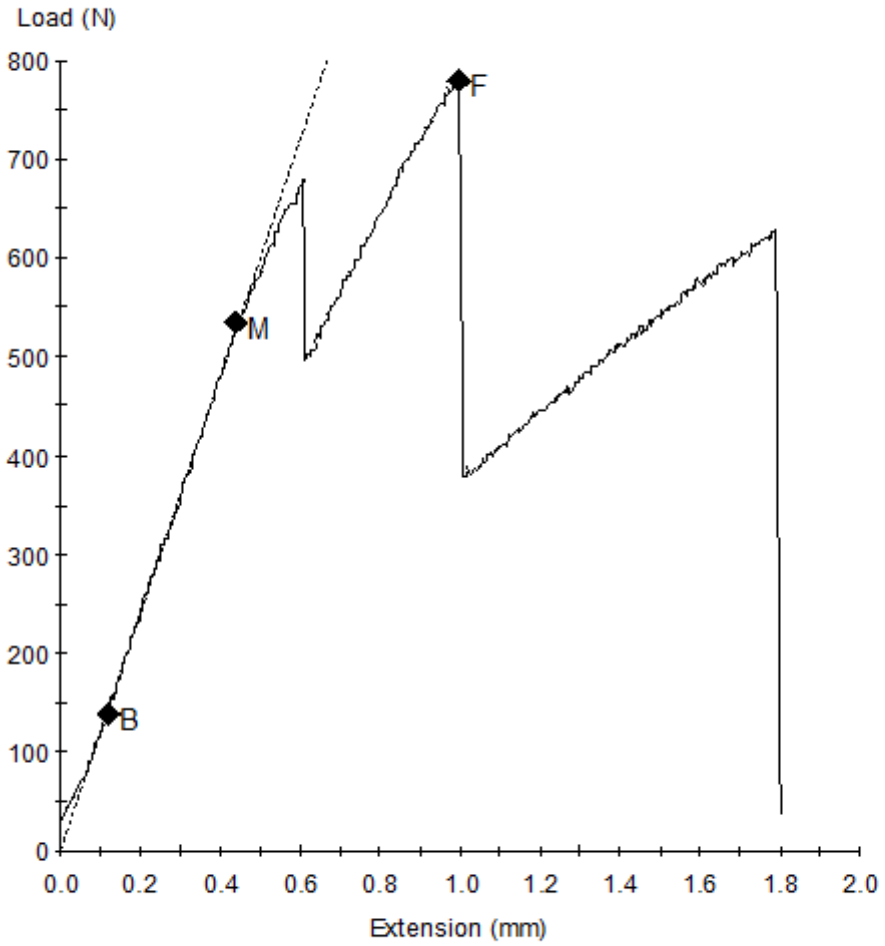

[4]

Specimen Results:

Name	Value	Units
Thickness	26.000	mm
Width	50.000	mm
Area	1300	mm^2
Peak Load	779	N
Peak Stress	0.60	MPa
Break Load	779	N
Break Stress	0.60	MPa
Elongation At Break	0.996	mm
Stress At Offset Yield	0.382	MPa
Load At Offset Yield	496.841	N

Sample ID: Geoff-10%G-5.mss
Specimen Number: 5
Tagged: False

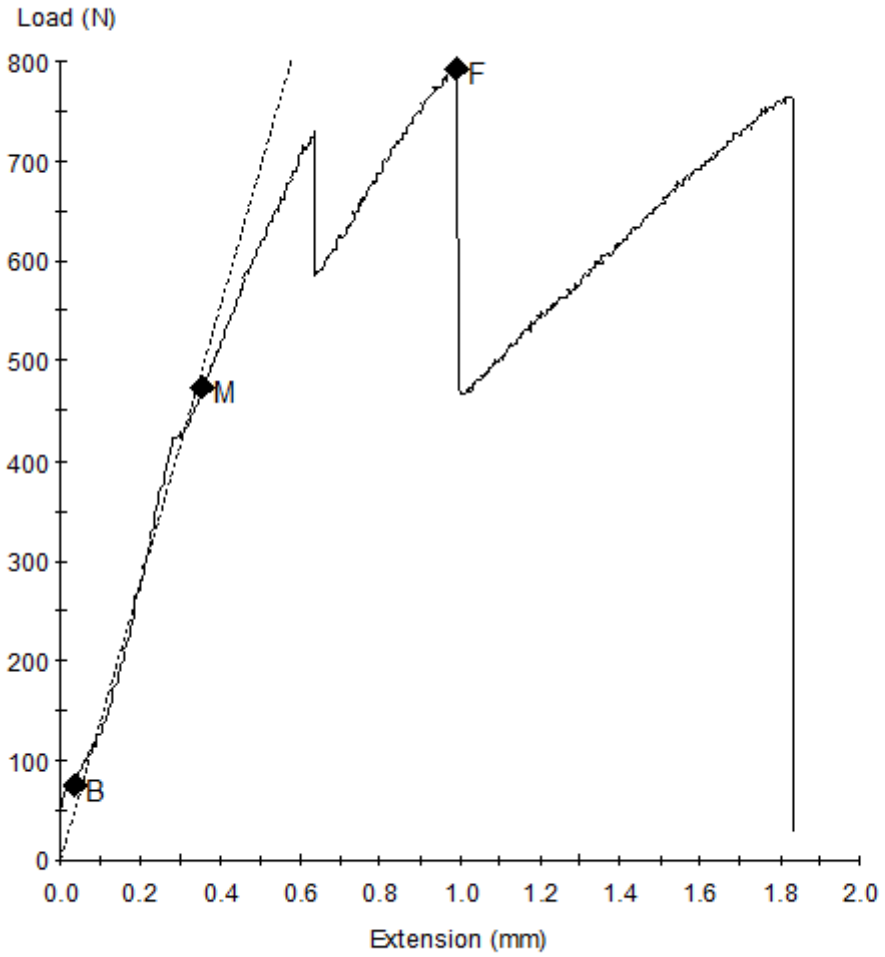

Specimen Results:

Name	Value	Units
Thickness	26.000	mm
Width	50.000	mm
Area	1300	mm^2
Peak Load	792	N
Peak Stress	0.61	MPa
Break Load	792	N
Break Stress	0.61	MPa
Elongation At Break	0.990	mm
Stress At Offset Yield	0.465	MPa
Load At Offset Yield	604.266	N

Sample ID: Geoff-10%G-6.mss
Specimen Number: 6
Tagged: False

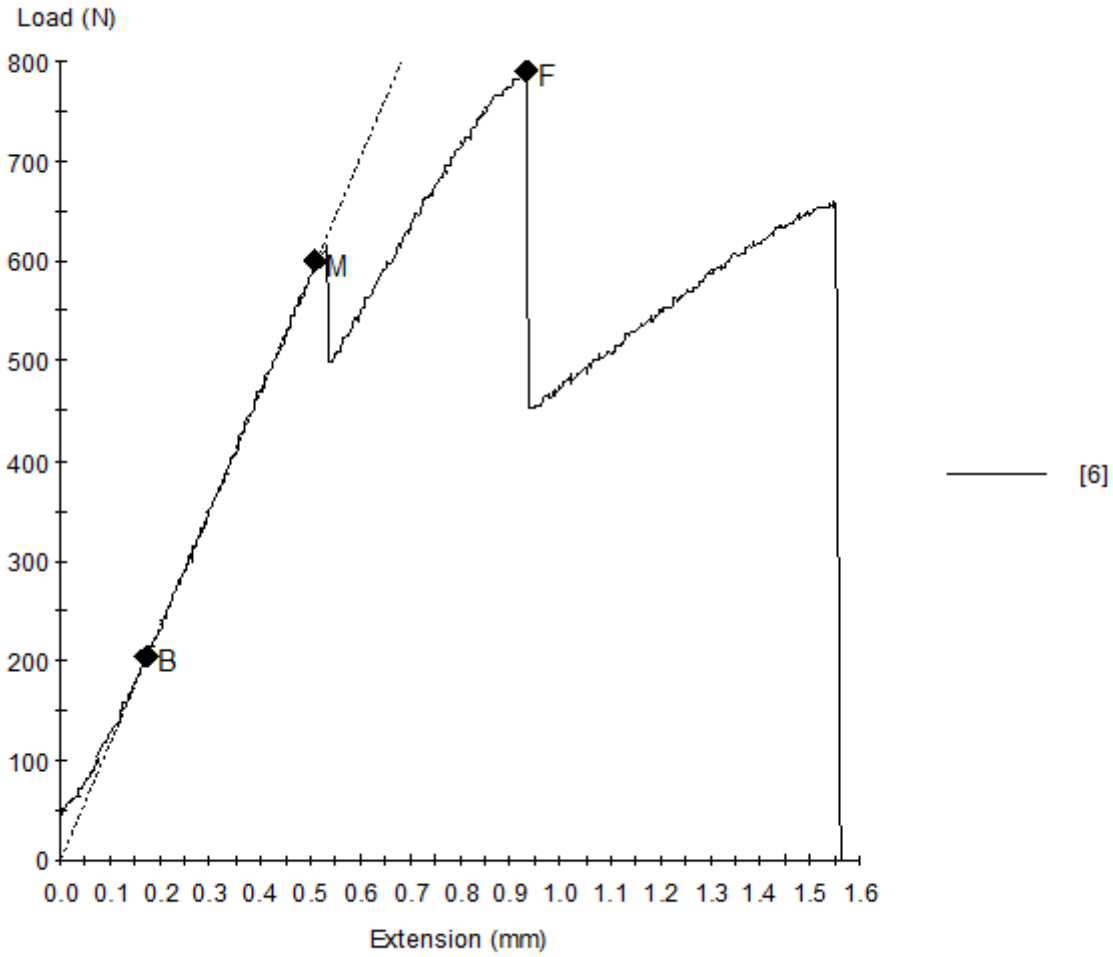

Specimen Results:

Name	Value	Units
Thickness	26.000	mm
Width	50.000	mm
Area	1300	mm^2
Peak Load	791	N
Peak Stress	0.61	MPa
Break Load	791	N
Break Stress	0.61	MPa
Elongation At Break	0.931	mm
Stress At Offset Yield	0.383	MPa

Load At Offset Yield 498.016 N

Geoff-10%G

Report Date: 24/02/2009

Test Date : 24/02/2009
Method : MMT fracture toughness Test .msm

Specimen Results:

Specimen #	Thickness mm	Width mm	Area mm^2	Peak Load N	Peak Stress MPa	Break Load N	Break Stress MPa
1	26.000	50.000	1300	755	0.58	755	0.58
2	26.000	50.000	1300	903	0.69	903	0.69
3	26.000	50.000	1300	765	0.59	762	0.59
4	26.000	50.000	1300	779	0.60	779	0.60
5	26.000	50.000	1300	792	0.61	792	0.61
6	26.000	50.000	1300	791	0.61	791	0.61
Mean	**26.000**	**50.000**	**1300**	**798**	**0.61**	**797**	**0.61**
Std Dev	**0.000**	**0.000**	**0**	**54**	**0.04**	**54**	**0.04**

Specimen #	Elongation At Break mm	Stress At Offset Yield MPa	Load At Offset Yield N				
1	1.263	0.527	684.835				
2	0.716	0.612	795.618				
3	1.205	0.379	492.813				
4	0.996	0.382	496.841				
5	0.954	0.380	493.484				
6	0.931	0.383	498.016				
Mean	**1.011**	**0.444**	**576.935**				
Std Dev	**0.199**	**0.101**	**131.262**				

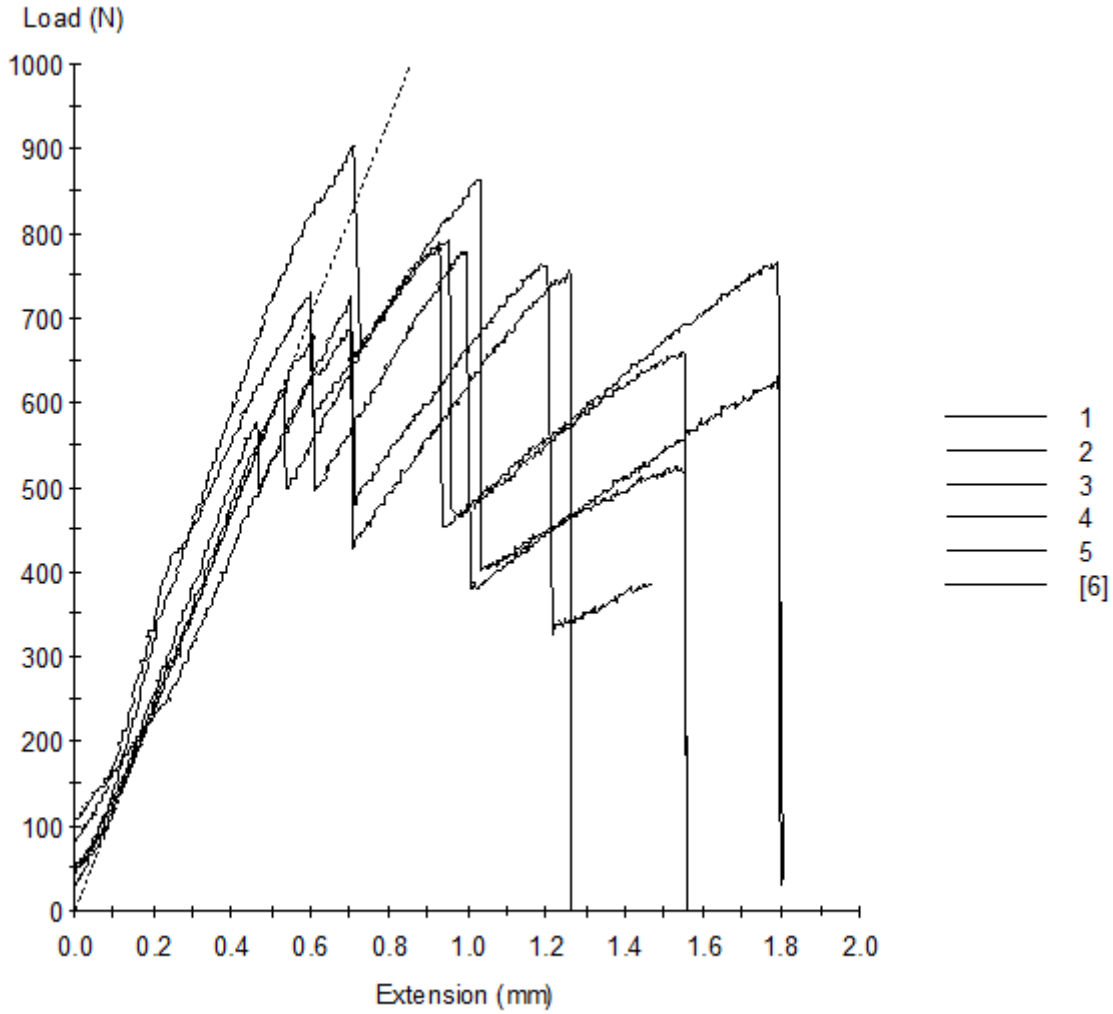
Load (N)
1000
900
800
700
600
500
400
300
200
100
0
0.0
0.2
0.4
0.6
0.8
1.0
1.2
1.4
1.6
1.8
2.0
Extension (mm)
1
2
3
4
5
[6]

Sample ID: Geoff-15%G-1.mss
Specimen Number: 1
Tagged: False

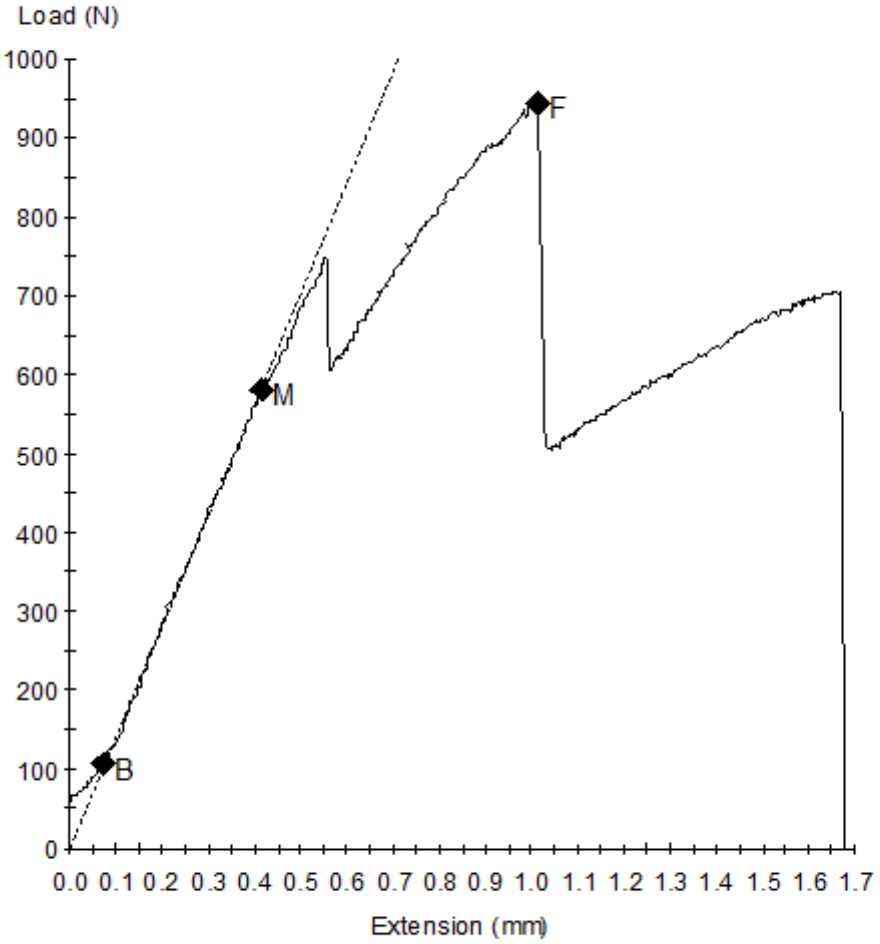

Specimen Results:

Name	Value	Units
Thickness	26.000	mm
Width	50.000	mm
Area	1300	mm^2
Peak Load	943	N
Peak Stress	0.73	MPa
Break Load	943	N
Break Stress	0.73	MPa
Elongation At Break	1.012	mm
Stress At Offset Yield	0.467	MPa
Load At Offset Yield	606.952	N

Sample ID: Geoff-15%G-2.mss
Specimen Number: 2
Tagged: False

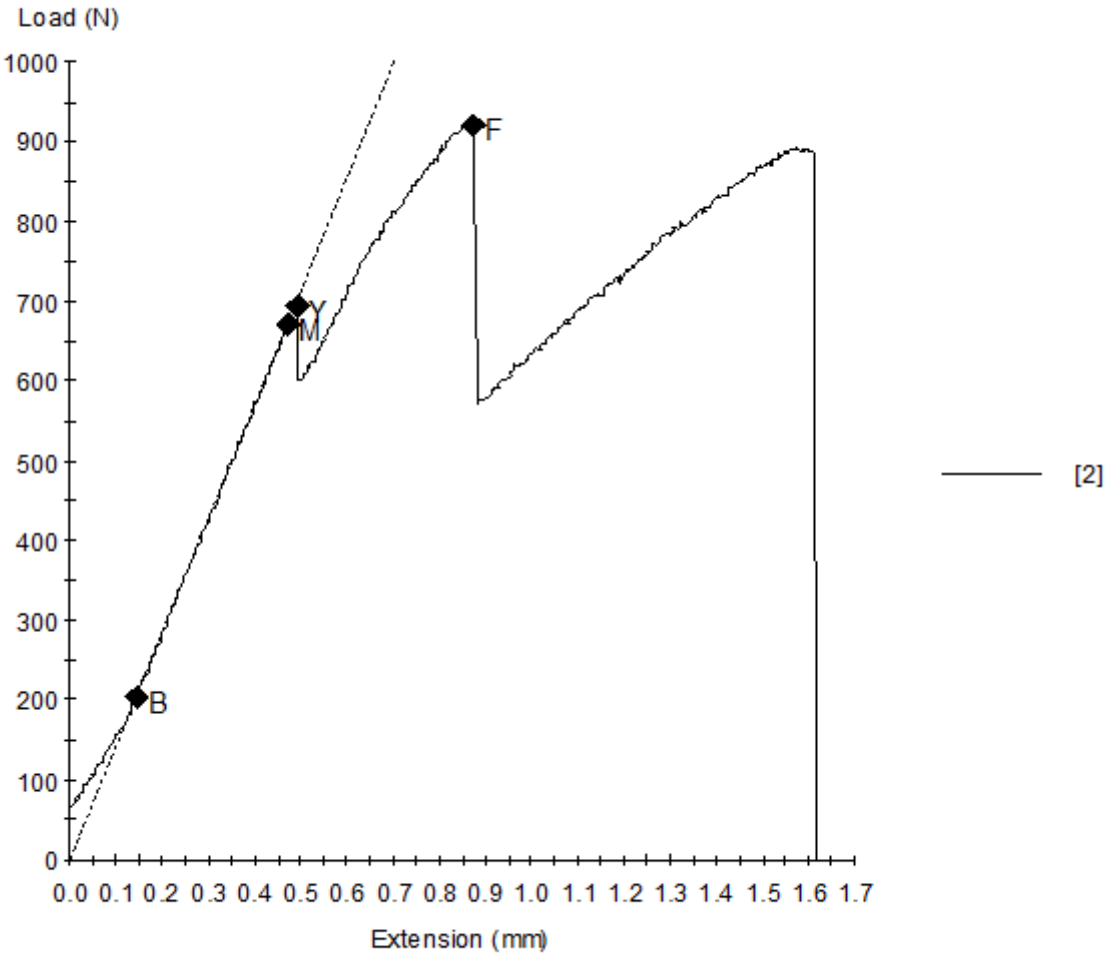

Specimen Results:

Name	Value	Units
Thickness	26.000	mm
Width	50.000	mm
Area	1300	mm^2
Peak Load	927	N
Peak Stress	0.71	MPa
Break Load	921	N
Break Stress	0.71	MPa
Elongation At Break	0.875	mm
Stress At Offset Yield	0.461	MPa
Load At Offset Yield	599.567	N

Sample ID: Geoff-15%G-3.mss
Specimen Number: 3
Tagged: False

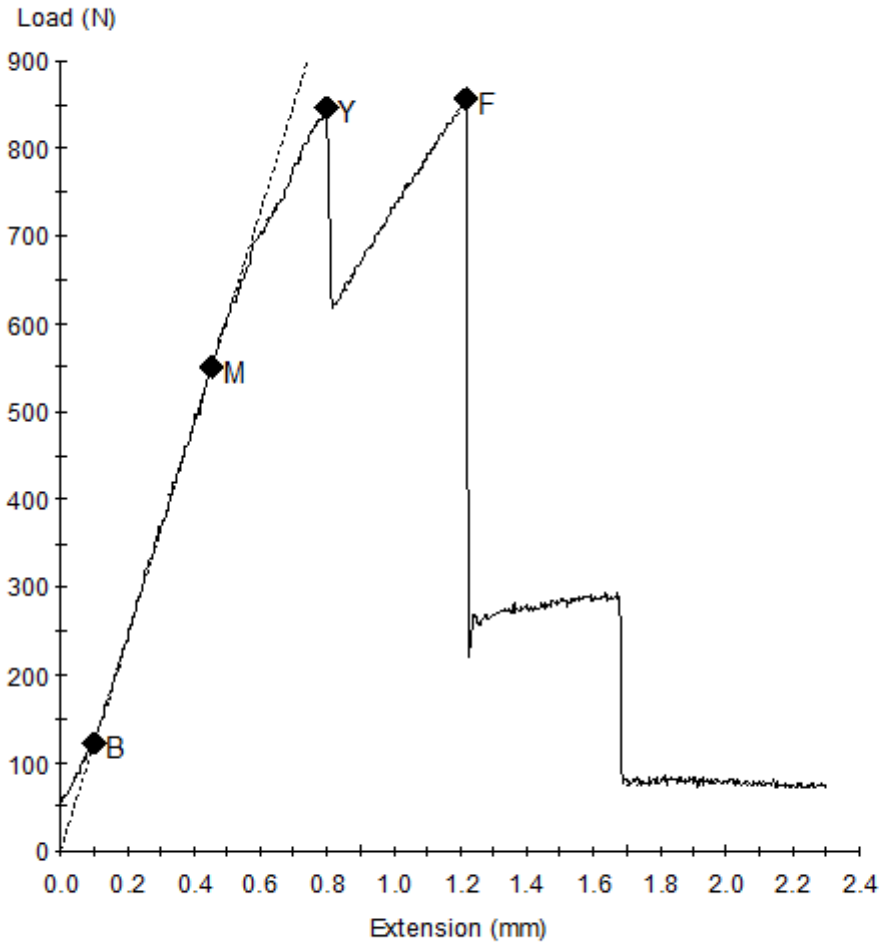

[3]

Specimen Results:

Name	Value	Units
Thickness	26.000	mm
Width	50.000	mm
Area	1300	mm^2
Peak Load	856	N
Peak Stress	0.66	MPa
Break Load	856	N
Break Stress	0.66	MPa
Elongation At Break	1.219	mm
Stress At Offset Yield	0.571	MPa
Load At Offset Yield	741.905	N

Sample ID: Geoff-15%G-4.mss
Specimen Number: 4
Tagged: False

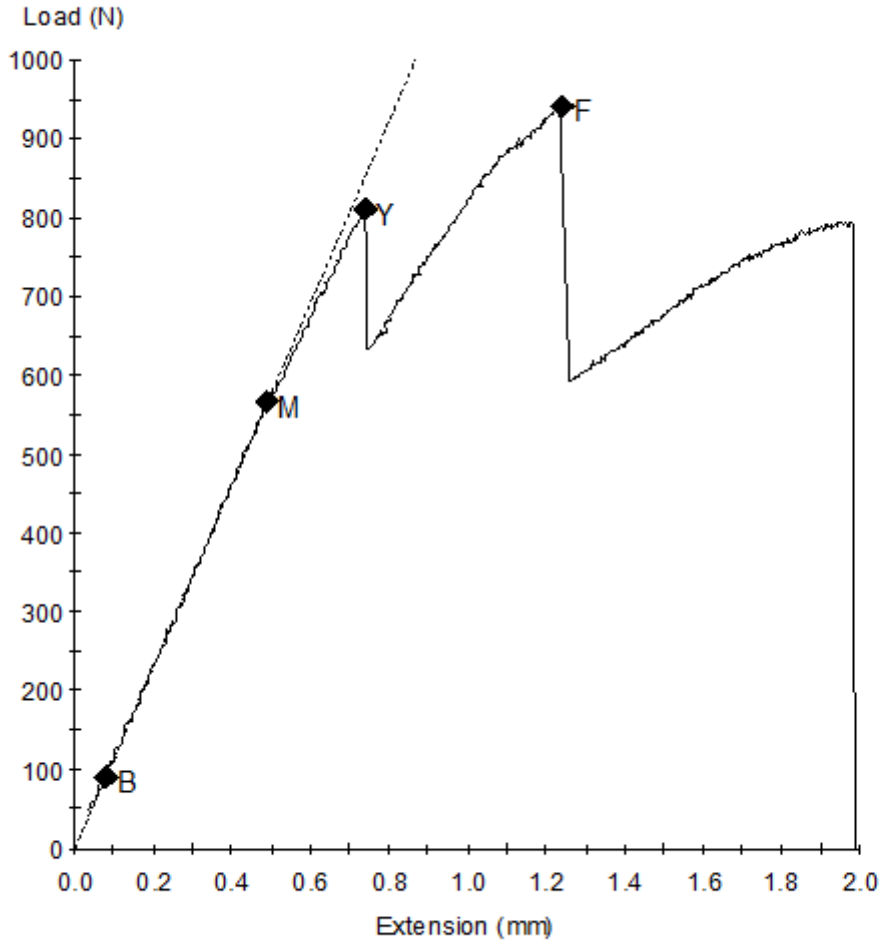

Specimen Results:

Name	Value	Units
Thickness	26.000	mm
Width	50.000	mm
Area	1300	mm^2
Peak Load	940	N
Peak Stress	0.72	MPa
Break Load	940	N
Break Stress	0.72	MPa
Elongation At Break	1.242	mm
Stress At Offset Yield	0.487	MPa
Load At Offset Yield	632.466	N

Sample ID: Geoff-15%G-5.mss
Specimen Number: 5
Tagged: False

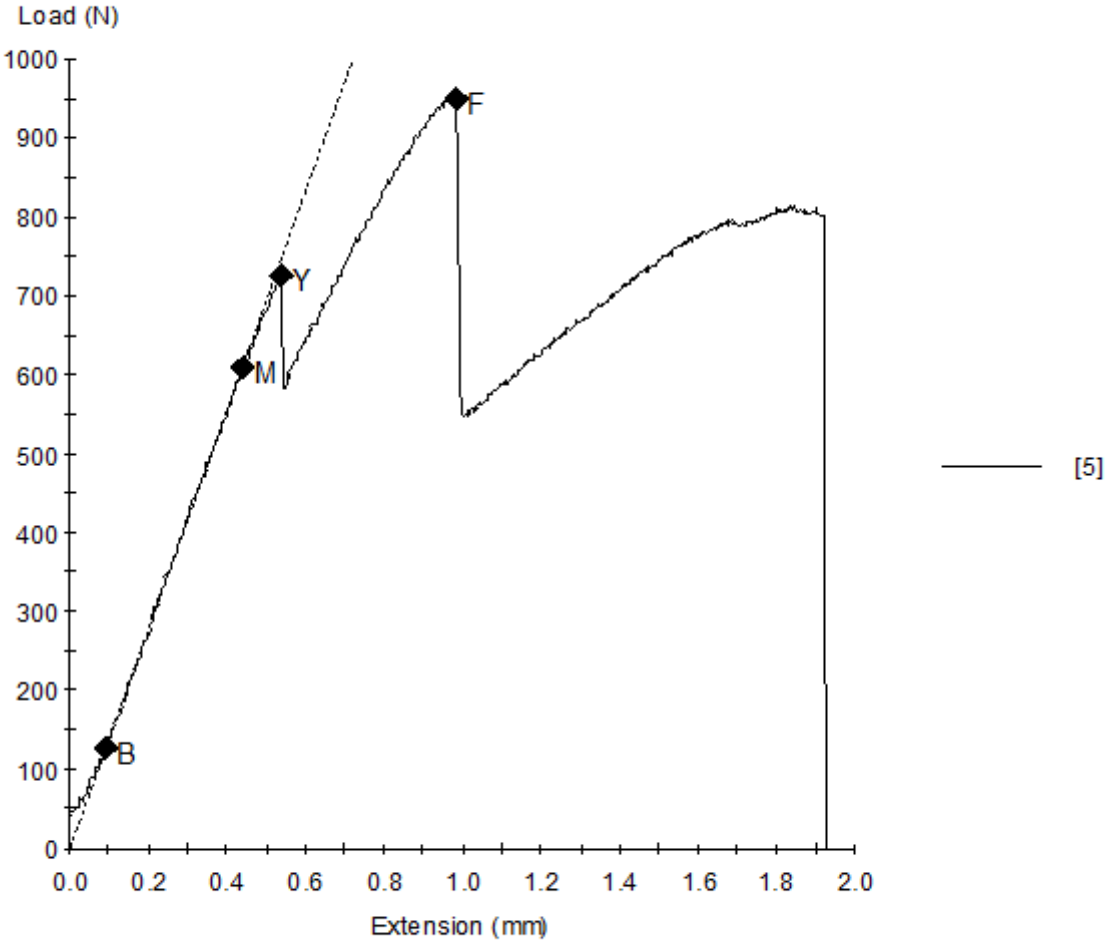

Specimen Results:

Name	Value	Units
Thickness	26.000	mm
Width	50.000	mm
Area	1300	mm^2
Peak Load	953	N
Peak Stress	0.73	MPa
Break Load	950	N
Break Stress	0.73	MPa
Elongation At Break	0.986	mm
Stress At Offset Yield	0.449	MPa
Load At Offset Yield	583.453	N

Sample ID: Geoff-15%G-6.mss
Specimen Number: 6
Tagged: False

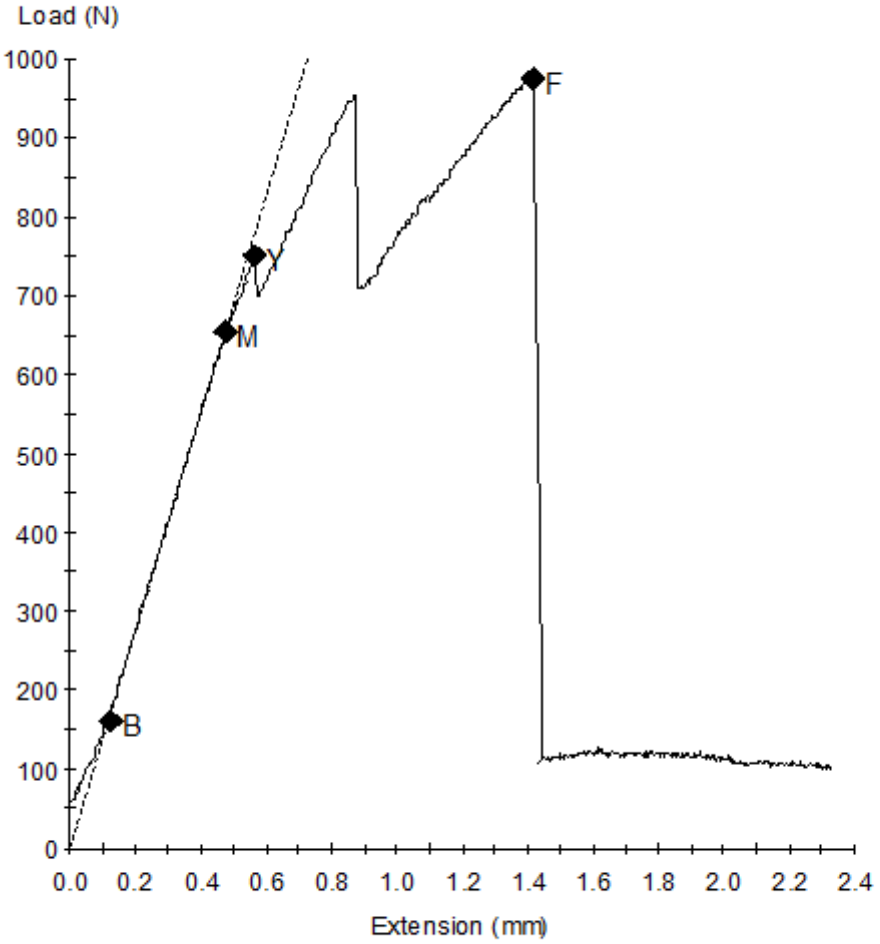

Specimen Results:

Name	Value	Units
Thickness	26.000	mm
Width	50.000	mm
Area	1300	mm^2
Peak Load	977	N
Peak Stress	0.75	MPa
Break Load	974	N
Break Stress	0.75	MPa
Elongation At Break	1.420	mm
Stress At Offset Yield	0.538	MPa
Load At Offset Yield	698.935	N

Geoff
15%G

Report Date: 24/02/2009

Test Date : 24/02/2009
Method : MMT fracture toughness Test .msm

Specimen Results:

Specimen #	Thickness mm	Width mm	Area mm^2	Peak Load N	Peak Stress MPa	Break Load N	Break Stress MPa
1	26.000	50.000	1300	943	0.73	943	0.73
2	26.000	50.000	1300	927	0.71	921	0.71
3	26.000	50.000	1300	856	0.66	856	0.66
4	26.000	50.000	1300	940	0.72	940	0.72
5	26.000	50.000	1300	953	0.73	950	0.73
6	26.000	50.000	1300	977	0.75	974	0.75
Mean	**26.000**	**50.000**	**1300**	**933**	**0.72**	**931**	**0.72**
Std Dev	**0.000**	**0.000**	**0**	**41**	**0.03**	**40**	**0.03**

Specimen #	Elongation At Break mm	Stress At Offset Yield MPa	Load At Offset Yield N				
1	1.012	0.467	606.952				
2	0.875	0.461	599.567				
3	1.219	0.571	741.905				
4	1.242	0.487	632.466				
5	0.986	0.449	583.453				
6	1.420	0.538	698.935				
Mean	**1.125**	**0.495**	**643.879**				
Std Dev	**0.202**	**0.048**	**62.847**				

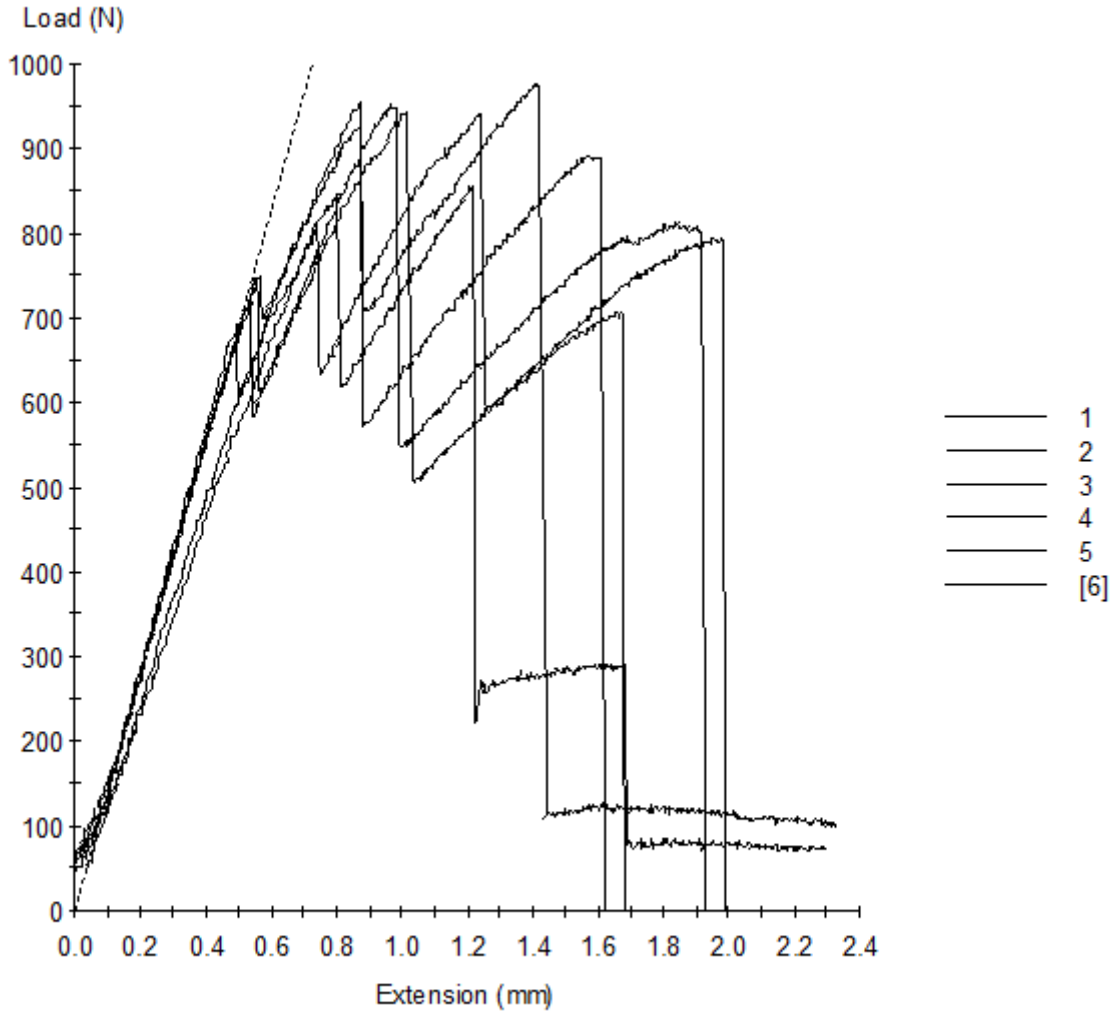
Load (N)
1000
900
800
700
600
500
400
300
200
100
0
0.0
0.2
0.4
0.6
0.8
1.0
1.2
1.4
1.6
1.8
2.0
2.2
2.4
Extension (mm)
1
2
3
4
5
[6]

Sample ID: Geoff-20%G-1.mss
Specimen Number: 1
Tagged: False

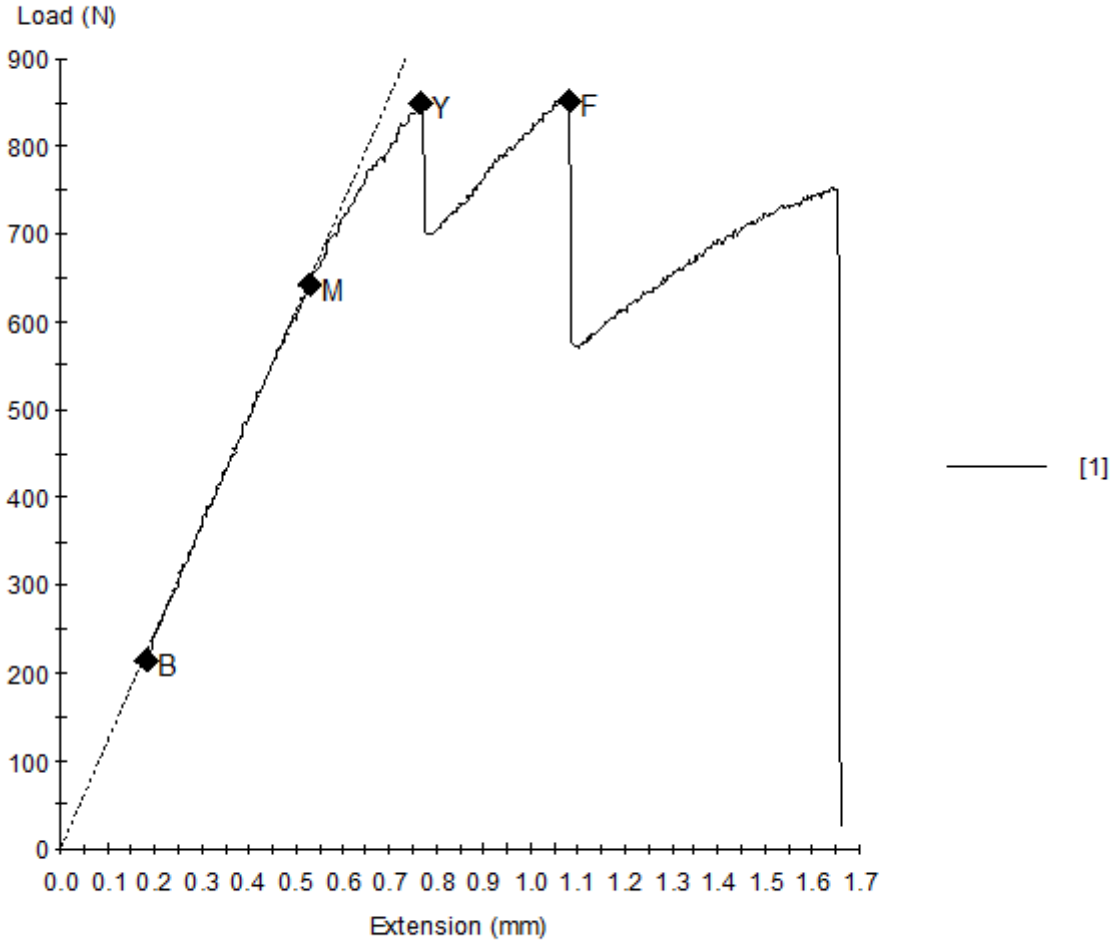

Specimen Results:

Name	Value	Units
Thickness	26.000	mm
Width	50.000	mm
Area	1300	mm^2
Peak Load	853	N
Peak Stress	0.66	MPa
Break Load	853	N
Break Stress	0.66	MPa
Elongation At Break	1.083	mm
Stress At Offset Yield	0.622	MPa
Load At Offset Yield	808.039	N

Sample ID: Geoff-20%G-2.mss
Specimen Number: 2
Tagged: False

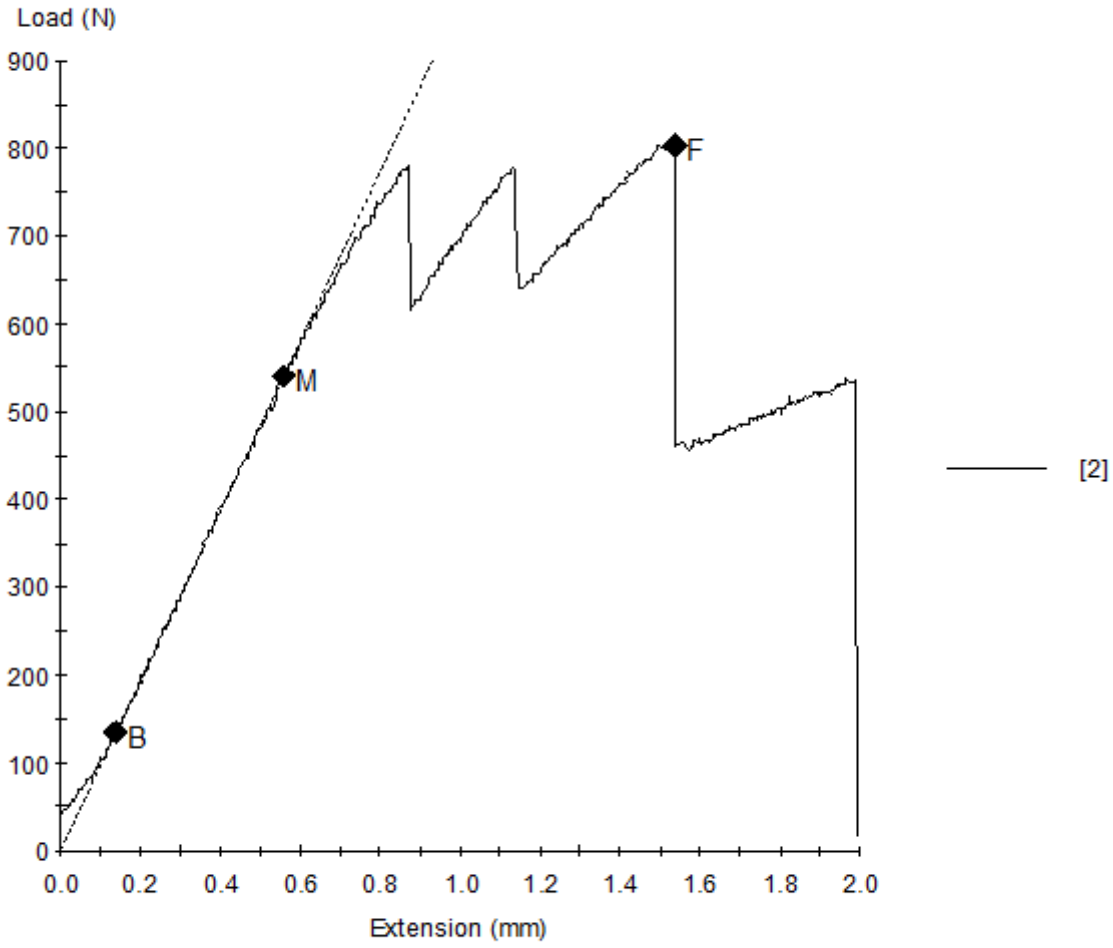

Specimen Results:

Name	Value	Units
Thickness	26.000	mm
Width	50.000	mm
Area	1300	mm^2
Peak Load	809	N
Peak Stress	0.62	MPa
Break Load	803	N
Break Stress	0.62	MPa
Elongation At Break	1.540	mm
Stress At Offset Yield	0.597	MPa
Load At Offset Yield	775.475	N

Sample ID: Geoff-20%G-3.mss
Specimen Number: 3
Tagged: False

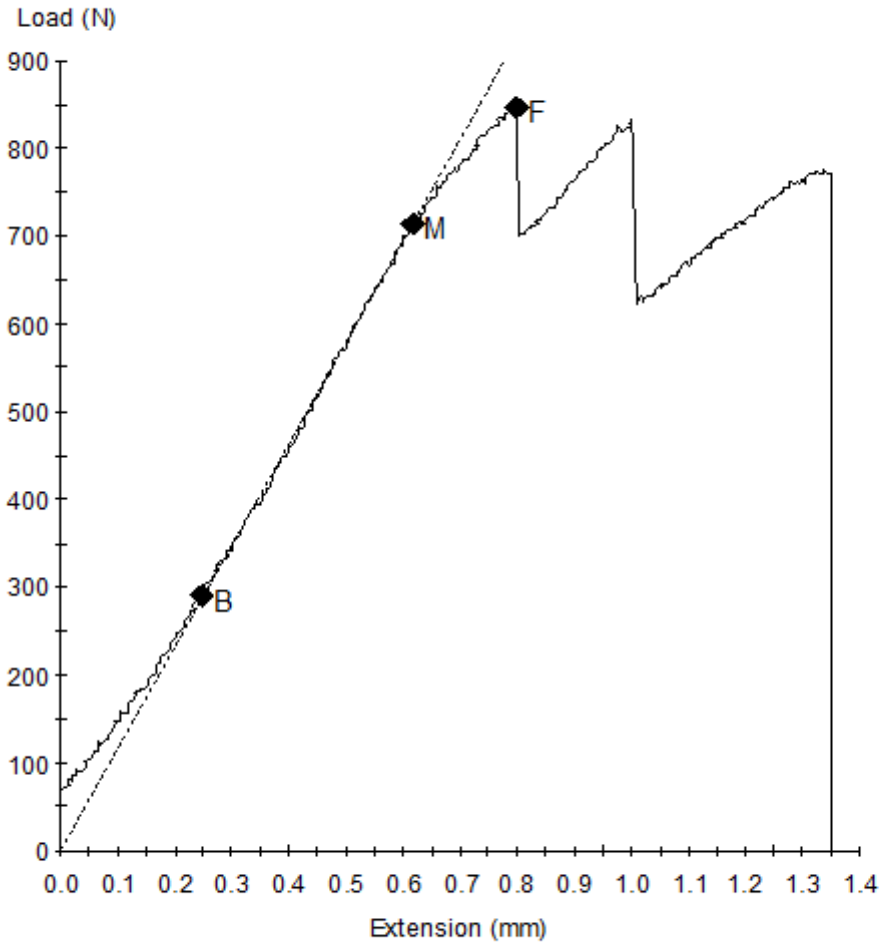

[3]

Specimen Results:

Name	Value	Units
Thickness	26.000	mm
Width	50.000	mm
Area	1300	mm^2
Peak Load	846	N
Peak Stress	0.65	MPa
Break Load	846	N
Break Stress	0.65	MPa
Elongation At Break	0.798	mm
Stress At Offset Yield	0.635	MPa
Load At Offset Yield	825.999	N

Sample ID: Geoff-20%G-4.mss
Specimen Number: 4
Tagged: False

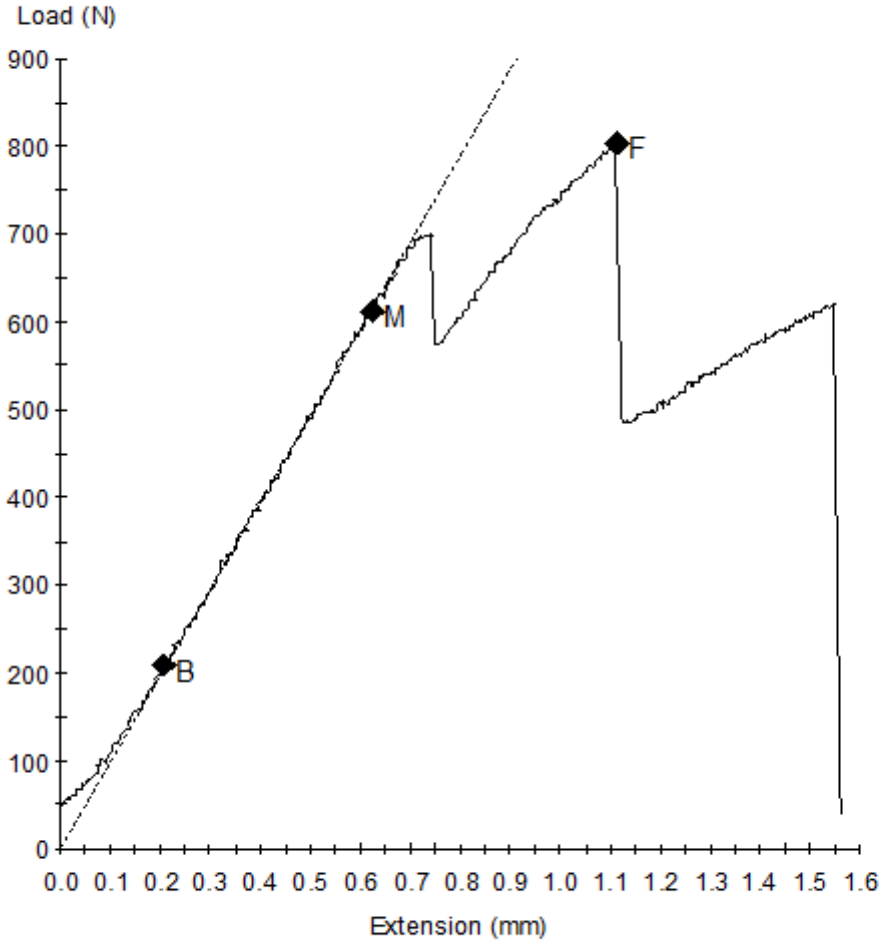

Specimen Results:

Name	Value	Units
Thickness	26.000	mm
Width	50.000	mm
Area	1300	mm^2
Peak Load	804	N
Peak Stress	0.62	MPa
Break Load	804	N
Break Stress	0.62	MPa
Elongation At Break	1.115	mm
Stress At Offset Yield	0.442	MPa
Load At Offset Yield	574.053	N

Sample ID: Geoff-20%G-5.mss
Specimen Number: 5
Tagged: False

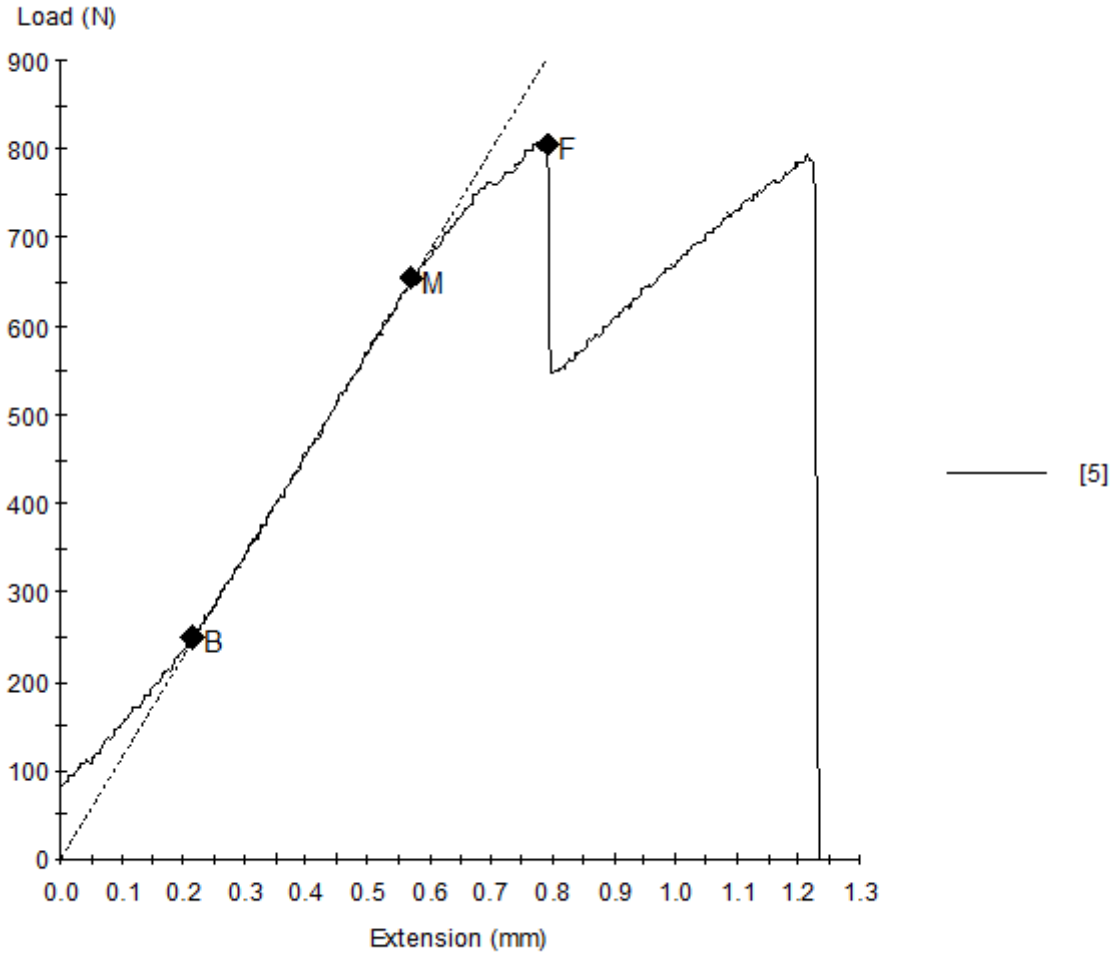

Specimen Results:

Name	Value	Units
Thickness	26.000	mm
Width	50.000	mm
Area	1300	mm^2
Peak Load	809	N
Peak Stress	0.62	MPa
Break Load	806	N
Break Stress	0.62	MPa
Elongation At Break	0.794	mm
Stress At Offset Yield	0.597	MPa
Load At Offset Yield	775.475	N

Sample ID: Geoff-20%G-6.mss
Specimen Number: 6
Tagged: False

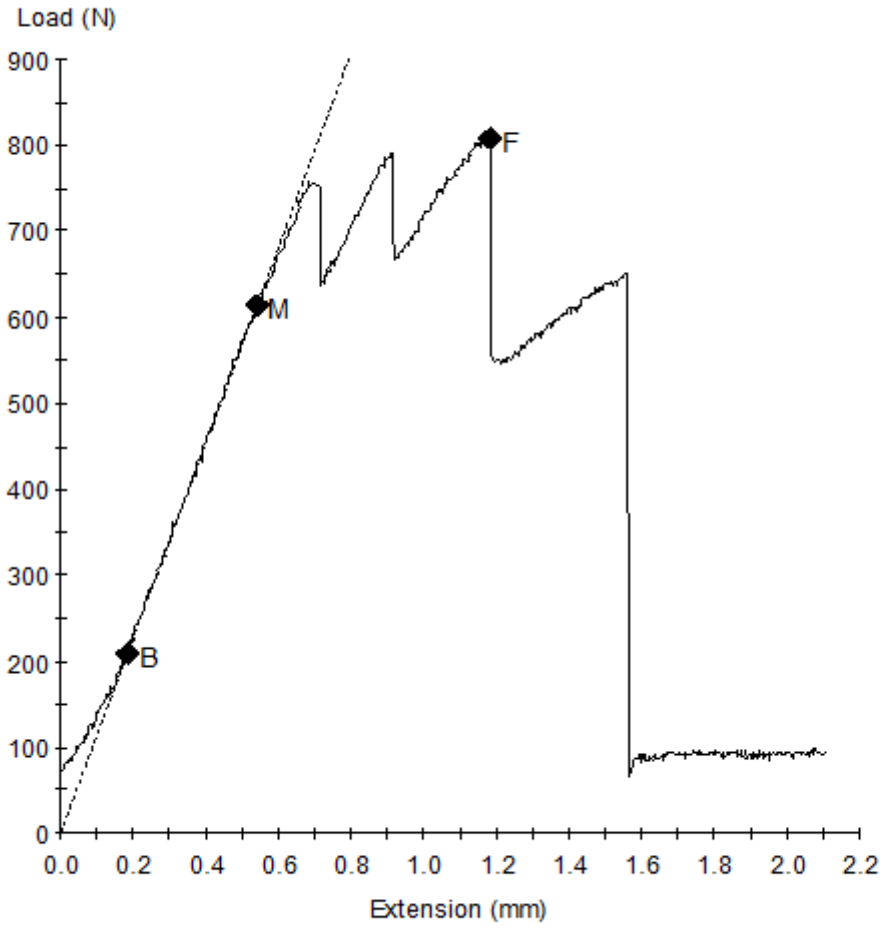

Specimen Results:

Name	Value	Units
Thickness	26.000	mm
Width	50.000	mm
Area	1300	mm^2
Peak Load	811	N
Peak Stress	0.62	MPa
Break Load	809	N
Break Stress	0.62	MPa
Elongation At Break	1.183	mm
Stress At Offset Yield	0.489	MPa
Load At Offset Yield	635.655	N

Geoff-20%G

Report Date: 24/02/2009

Test Date : 24/02/2009
Method : MMT fracture toughness Test .msm

Specimen Results:

Specimen #	Thickness mm	Width mm	Area mm^2	Peak Load N	Peak Stress MPa	Break Load N	Break Stress MPa
1	26.000	50.000	1300	853	0.66	853	0.66
2	26.000	50.000	1300	809	0.62	803	0.62
3	26.000	50.000	1300	846	0.65	846	0.65
4	26.000	50.000	1300	804	0.62	804	0.62
5	26.000	50.000	1300	809	0.62	806	0.62
6	26.000	50.000	1300	811	0.62	809	0.62
Mean	**26.000**	**50.000**	**1300**	**822**	**0.63**	**820**	**0.63**
Std Dev	**0.000**	**0.000**	**0**	**22**	**0.02**	**23**	**0.02**

Specimen #	Elongation At Break mm	Stress At Offset Yield MPa	Load At Offset Yield N				
1	1.083	0.622	808.039				
2	1.540	0.597	775.475				
3	0.798	0.635	825.999				
4	1.115	0.442	574.053				
5	0.794	0.597	775.475				
6	1.183	0.489	635.655				
Mean	**1.085**	**0.563**	**732.449**				
Std Dev	**0.277**	**0.079**	**102.593**				

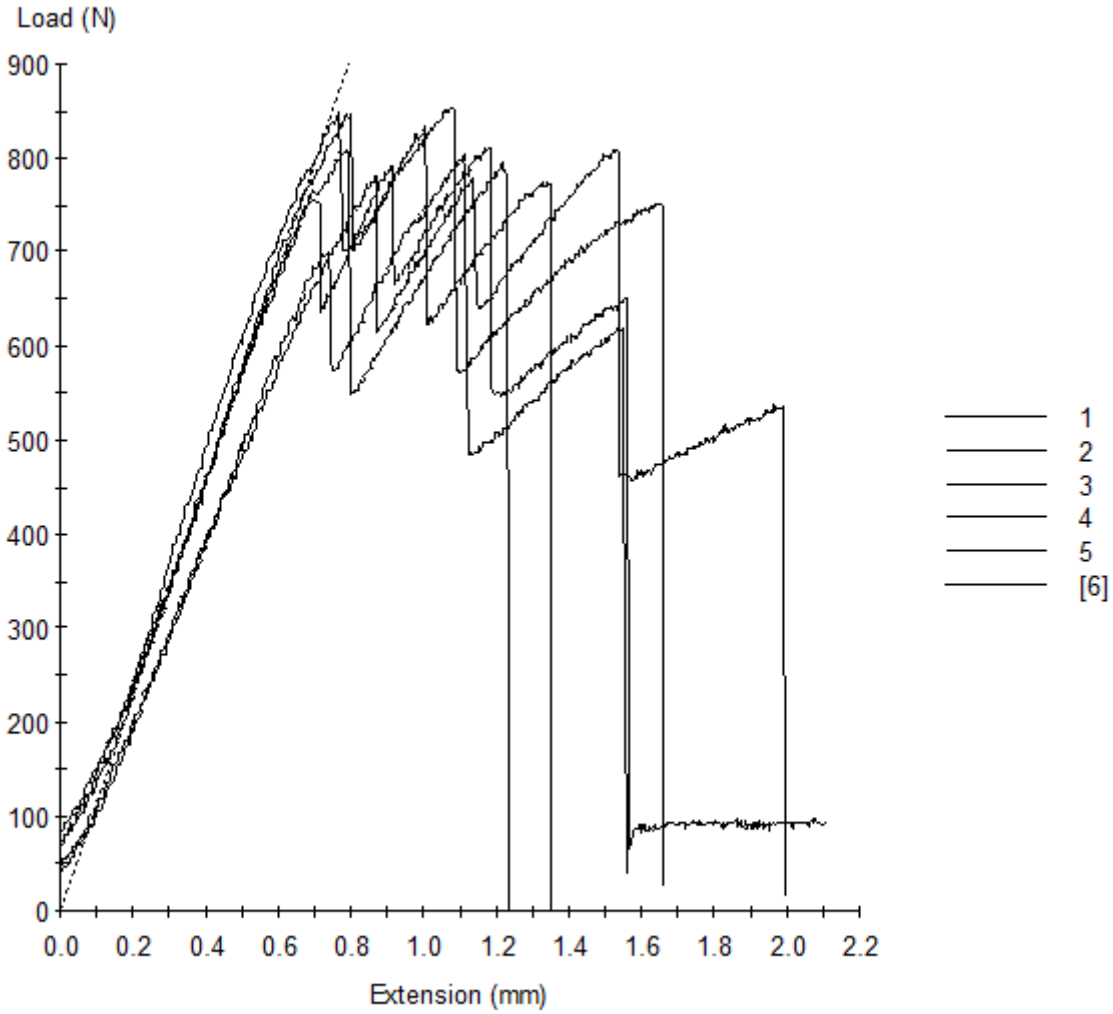
Load (N)
900
800
700
600
500
400
300
200
100
0
0.0
0.2
0.4
0.6
0.8
1.0
1.2
1.4
1.6
1.8
2.0
2.2
Extension (mm)
1
2
3
4
5
[6]

Sample ID: Geoff-25%G-1.mss
Specimen Number: 1
Tagged: False

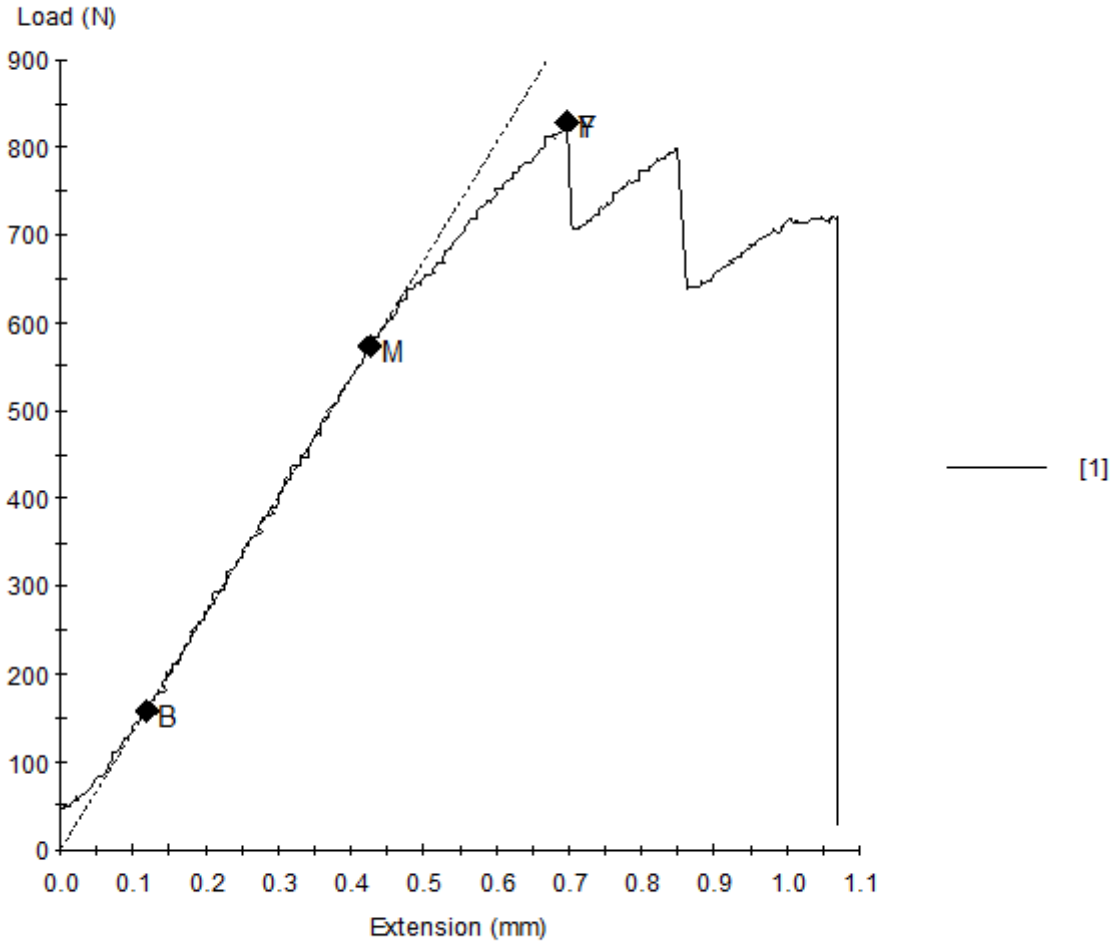

Specimen Results:

Name	Value	Units
Thickness	26.000	mm
Width	50.000	mm
Area	1300	mm^2
Peak Load	829	N
Peak Stress	0.64	MPa
Break Load	829	N
Break Stress	0.64	MPa
Elongation At Break	0.696	mm
Stress At Offset Yield	0.588	MPa
Load At Offset Yield	764.733	N

Sample ID: Geoff-25%G-2.mss
Specimen Number: 2
Tagged: False

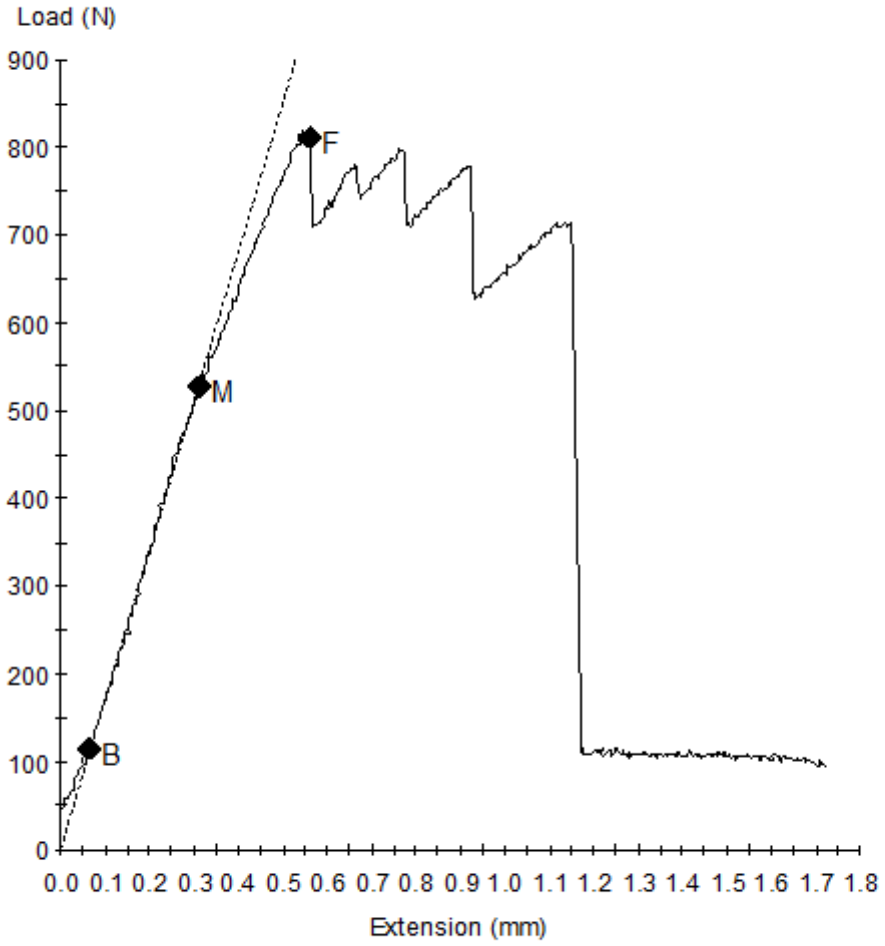

[2]

Specimen Results:

Name	Value	Units
Thickness	26.000	mm
Width	50.000	mm
Area	1300	mm^2
Peak Load	819	N
Peak Stress	0.63	MPa
Break Load	810	N
Break Stress	0.62	MPa
Elongation At Break	0.562	mm
Stress At Offset Yield	0.599	MPa
Load At Offset Yield	778.832	N

Sample ID: Geoff-25%G-3.mss
Specimen Number: 3
Tagged: False

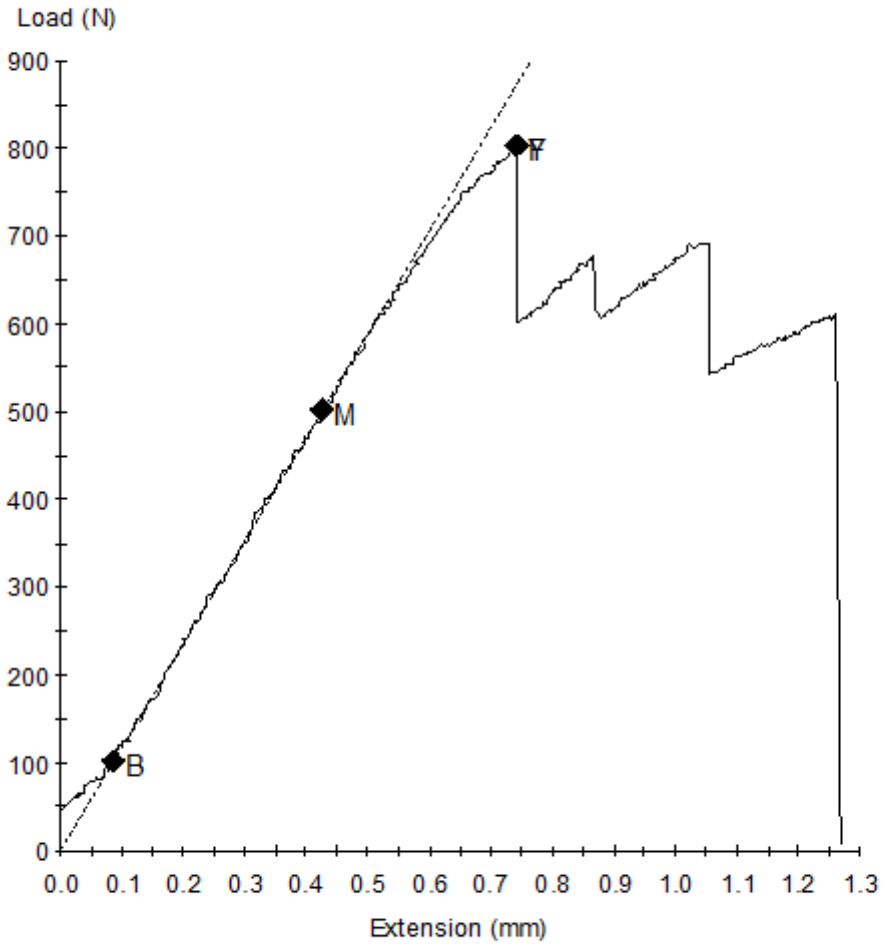

Specimen Results:

Name	Value	Units
Thickness	26.000	mm
Width	50.000	mm
Area	1300	mm^2
Peak Load	802	N
Peak Stress	0.62	MPa
Break Load	802	N
Break Stress	0.62	MPa
Elongation At Break	0.740	mm
Stress At Offset Yield	0.607	MPa
Load At Offset Yield	788.903	N

Sample ID: Geoff-25%G-4.mss
Specimen Number: 4
Tagged: False

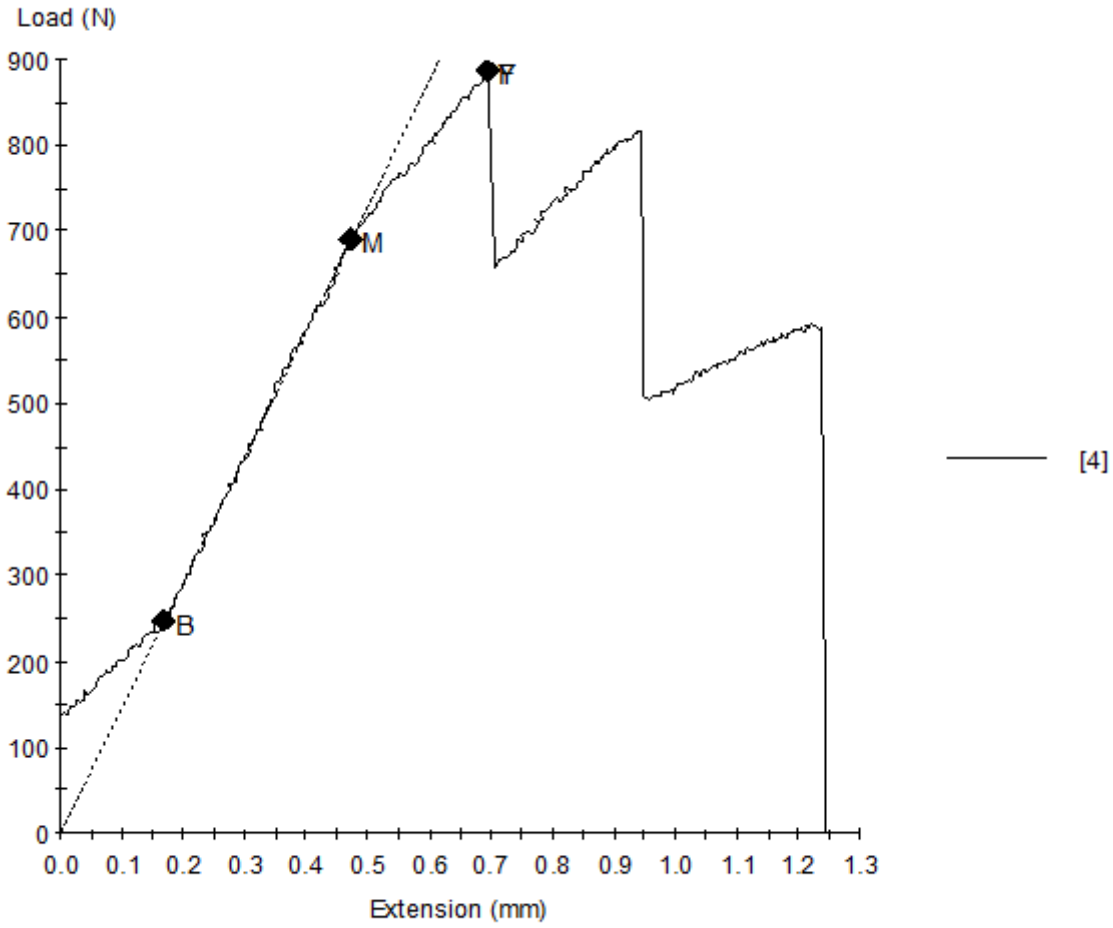

Specimen Results:

Name	Value	Units
Thickness	26.000	mm
Width	50.000	mm
Area	1300	mm^2
Peak Load	887	N
Peak Stress	0.68	MPa
Break Load	887	N
Break Stress	0.68	MPa
Elongation At Break	0.695	mm
Stress At Offset Yield	0.618	MPa
Load At Offset Yield	803.003	N

Sample ID: Geoff-25%G-5.mss
Specimen Number: 5
Tagged: False

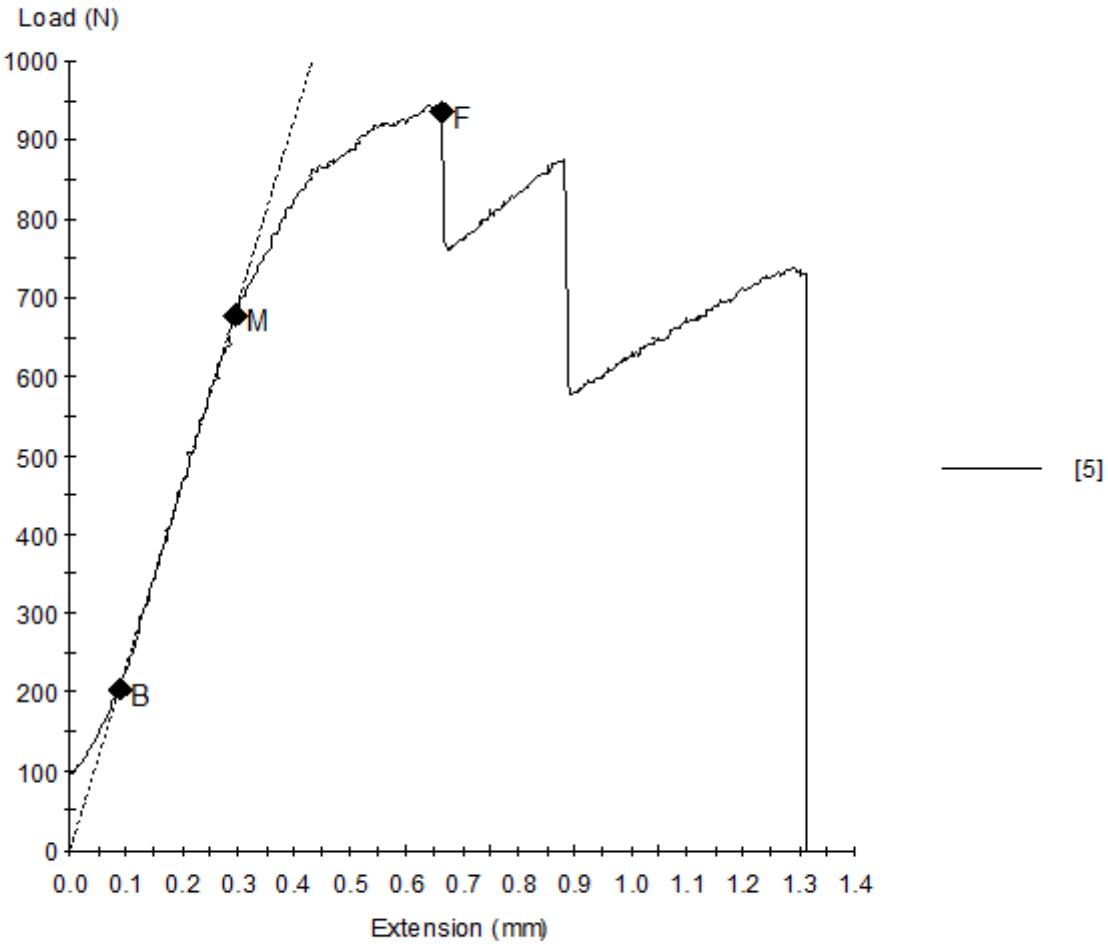

Specimen Results:

Name	Value	Units
Thickness	26.000	mm
Width	50.000	mm
Area	1300	mm^2
Peak Load	943	N
Peak Stress	0.73	MPa
Break Load	935	N
Break Stress	0.72	MPa
Elongation At Break	0.665	mm
Stress At Offset Yield	0.645	MPa
Load At Offset Yield	838.588	N

Sample ID: Geoff-25%G-6.mss
Specimen Number: 6
Tagged: False

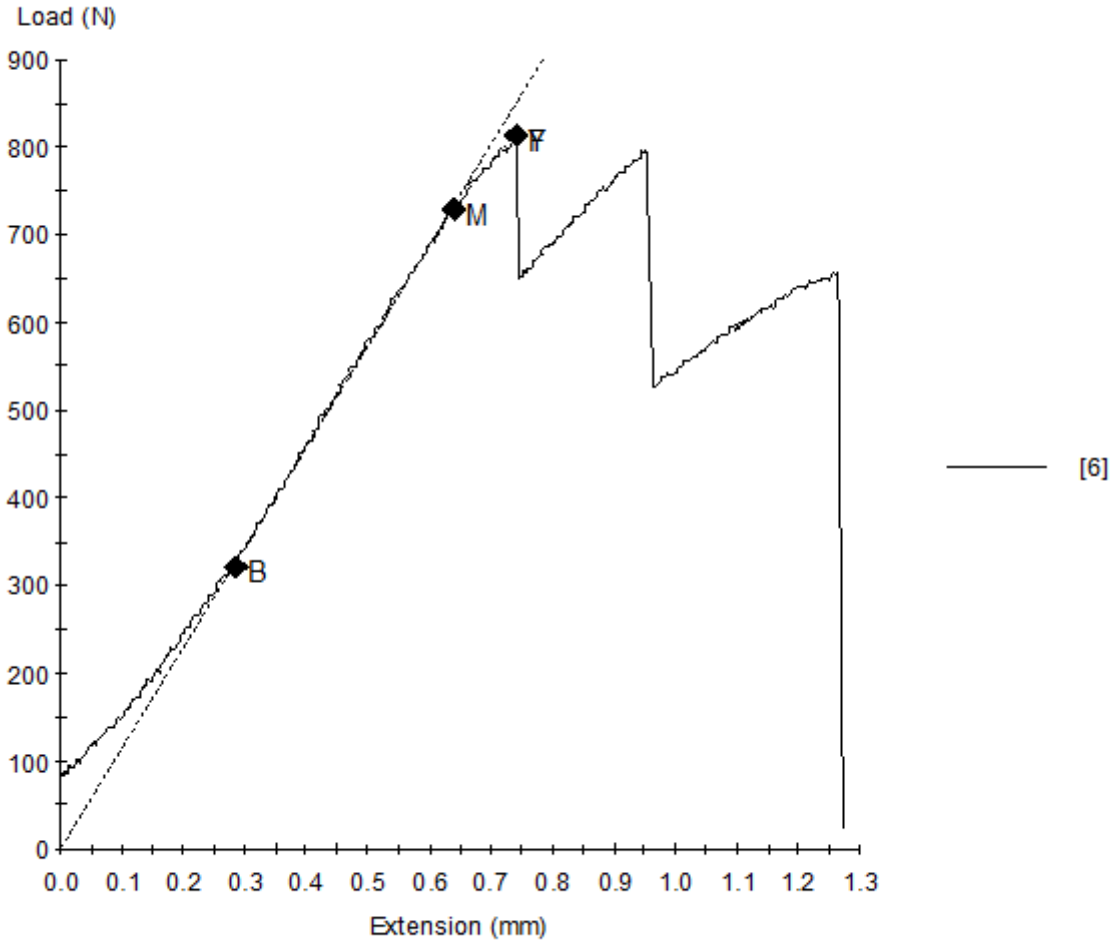

Specimen Results:

Name	Value	Units
Thickness	26.000	mm
Width	50.000	mm
Area	1300	mm^2
Peak Load	812	N
Peak Stress	0.62	MPa
Break Load	812	N
Break Stress	0.62	MPa
Elongation At Break	0.742	mm
Stress At Offset Yield	0.501	MPa
Load At Offset Yield	651.265	N

Geoff-25%G

Report Date: 26/02/2009

Test Date : 26/02/2009
Method : MMT fracture toughness Test .msm

Specimen Results:

Specimen #	Thickness mm	Width mm	Area mm^2	Peak Load N	Peak Stress MPa	Break Load N	Break Stress MPa
1	26.000	50.000	1300	829	0.64	829	0.64
2	26.000	50.000	1300	819	0.63	810	0.62
3	26.000	50.000	1300	802	0.62	802	0.62
4	26.000	50.000	1300	887	0.68	887	0.68
5	26.000	50.000	1300	943	0.73	935	0.72
6	26.000	50.000	1300	812	0.62	812	0.62
Mean	**26.000**	**50.000**	**1300**	**849**	**0.65**	**846**	**0.65**
Std Dev	**0.000**	**0.000**	**0**	**55**	**0.04**	**53**	**0.04**

Specimen #	Elongation At Break mm	Stress At Offset Yield MPa	Load At Offset Yield N				
1	0.696	0.588	764.733				
2	0.562	0.599	778.832				
3	0.740	0.607	788.903				
4	0.695	0.618	803.003				
5	0.665	0.645	838.588				
6	0.742	0.501	651.265				
Mean	**0.684**	**0.593**	**770.887**				
Std Dev	**0.066**	**0.049**	**63.796**				

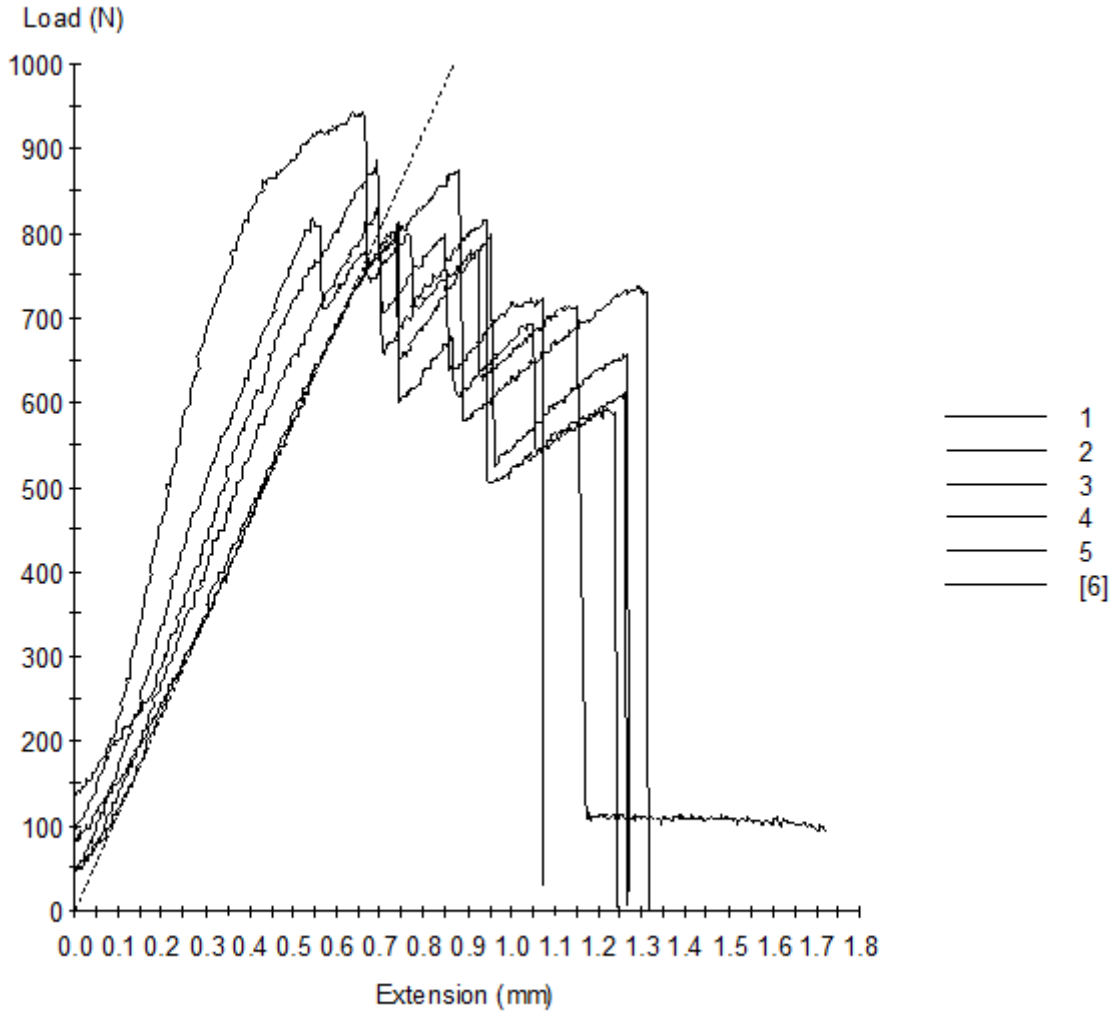
Load (N)
1000
900
800
700
600
500
400
300
200
100
0
0.0 0.1 0.2 0.3 0.4 0.5 0.6 0.7 0.8 0.9 1.0 1.1 1.2 1.3 1.4 1.5 1.6 1.7 1.8
Extension (mm)
1
2
3
4
5
[6]

Sample ID: Geoff-30%G-1.mss
Specimen Number: 1
Tagged: False

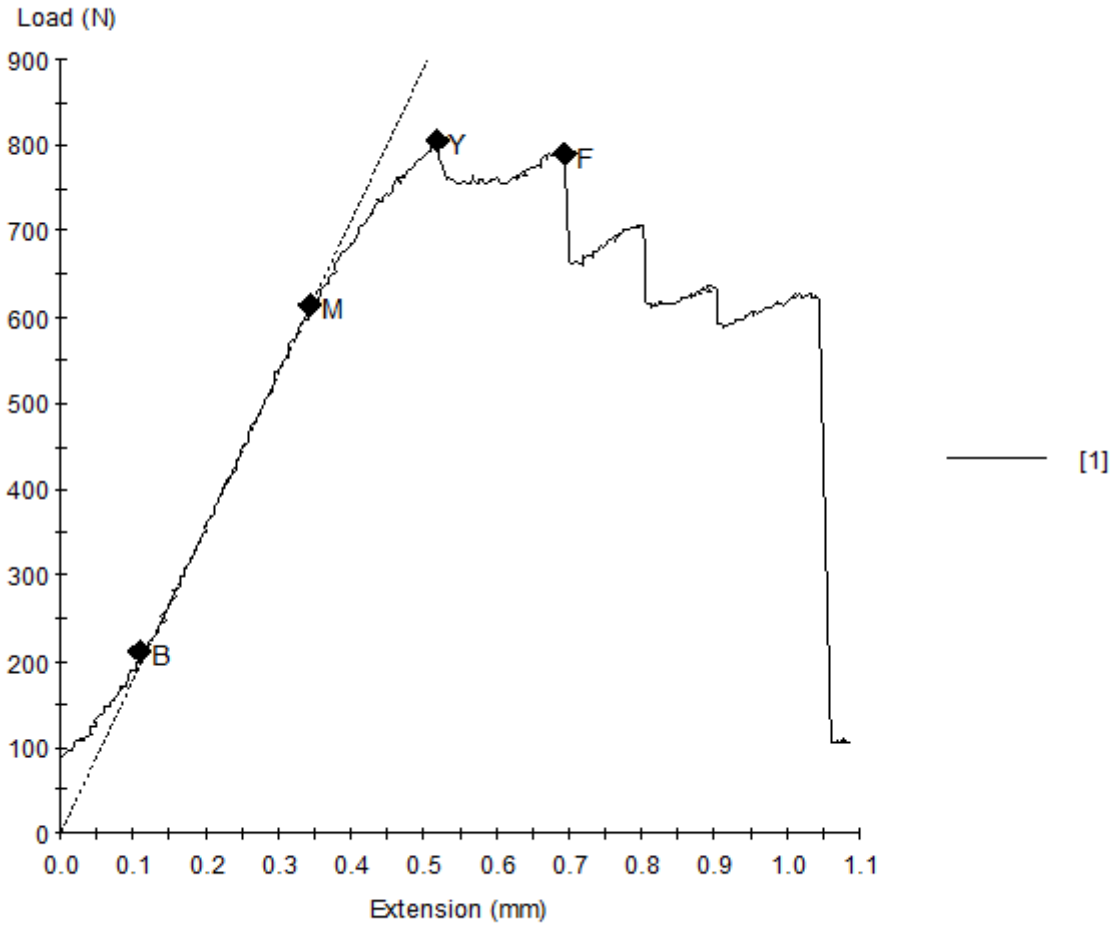

Specimen Results:

Name	Value	Units
Thickness	26.000	mm
Width	50.000	mm
Area	1300	mm^2
Peak Load	806	N
Peak Stress	0.62	MPa
Break Load	790	N
Break Stress	0.61	MPa
Elongation At Break	0.694	mm
Stress At Offset Yield	0.602	MPa
Load At Offset Yield	782.861	N

Sample ID: Geoff-30%G-2.mss
Specimen Number: 2
Tagged: False

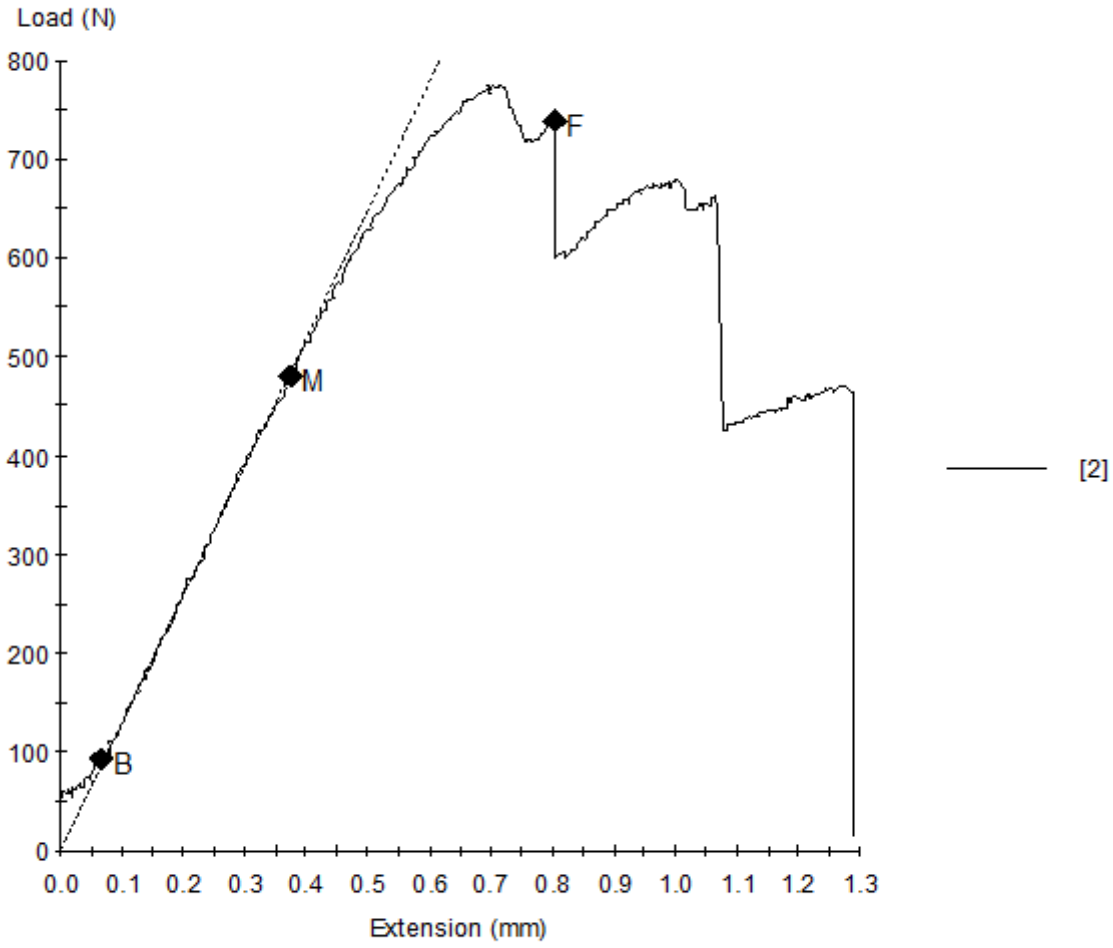

Specimen Results:

Name	Value	Units
Thickness	26.000	mm
Width	50.000	mm
Area	1300	mm^2
Peak Load	775	N
Peak Stress	0.60	MPa
Break Load	739	N
Break Stress	0.57	MPa
Elongation At Break	0.805	mm
Stress At Offset Yield	0.558	MPa
Load At Offset Yield	725.120	N

Sample ID: Geoff-30%G-3.mss
Specimen Number: 3
Tagged: False

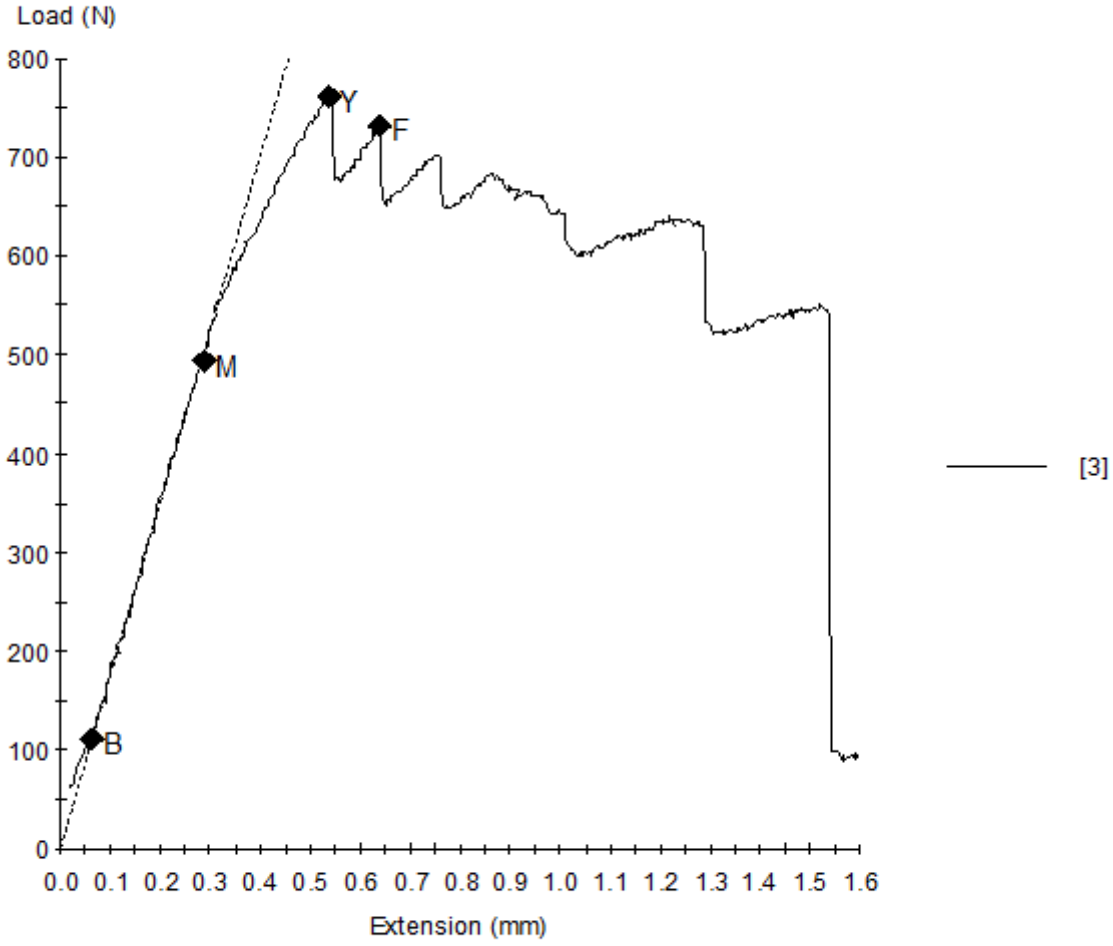

Specimen Results:

Name	Value	Units
Thickness	26.000	mm
Width	50.000	mm
Area	1300	mm^2
Peak Load	762	N
Peak Stress	0.59	MPa
Break Load	732	N
Break Stress	0.56	MPa
Elongation At Break	0.640	mm
Stress At Offset Yield	0.519	MPa
Load At Offset Yield	674.764	N

Sample ID: Geoff-30%G-4.mss
Specimen Number: 4
Tagged: False

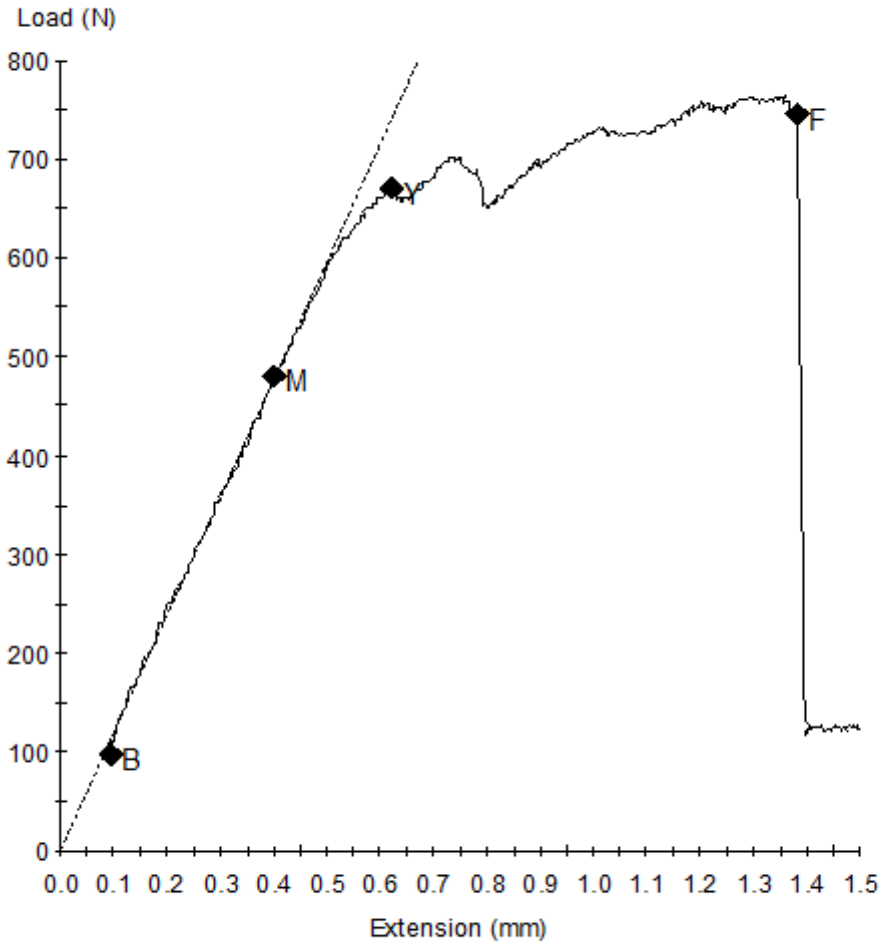

Specimen Results:

Name	Value	Units
Thickness	26.000	mm
Width	50.000	mm
Area	1300	mm^2
Peak Load	765	N
Peak Stress	0.59	MPa
Break Load	745	N
Break Stress	0.57	MPa
Elongation At Break	1.381	mm
Stress At Offset Yield	0.512	MPa
Load At Offset Yield	665.365	N

Sample ID: Geoff-30%G-5.mss
Specimen Number: 5
Tagged: False

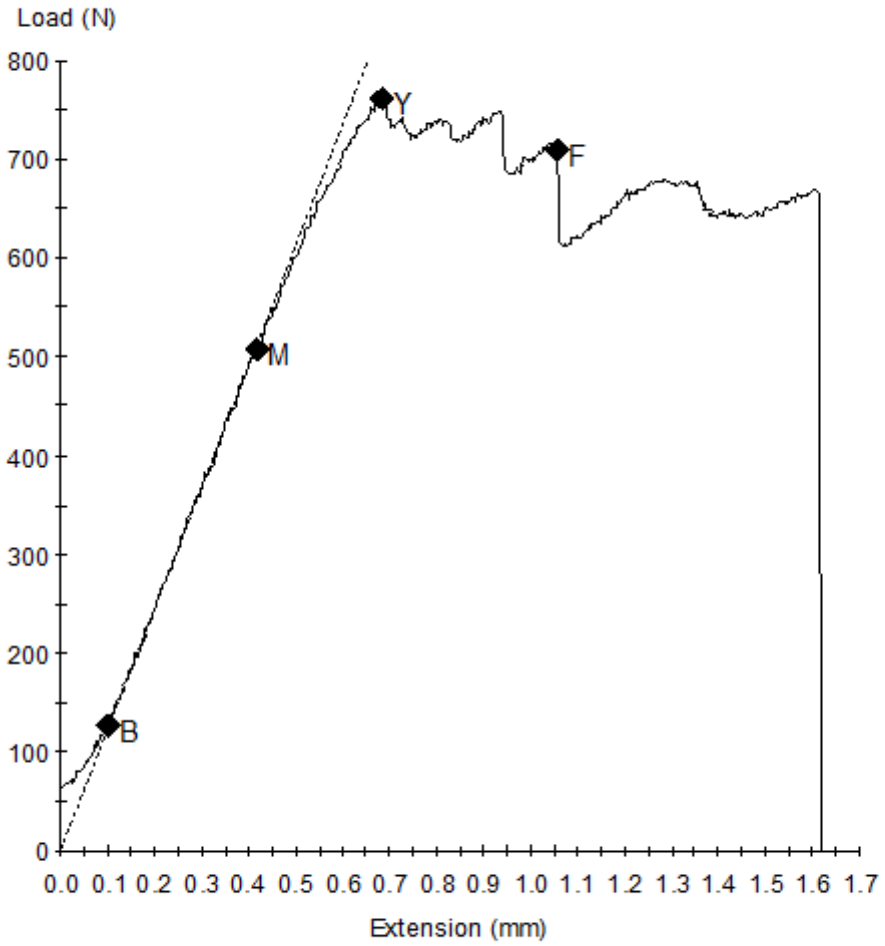

Specimen Results:

Name	Value	Units
Thickness	26.000	mm
Width	50.000	mm
Area	1300	mm^2
Peak Load	761	N
Peak Stress	0.59	MPa
Break Load	709	N
Break Stress	0.55	MPa
Elongation At Break	1.059	mm
Stress At Offset Yield	0.574	MPa
Load At Offset Yield	746.773	N

Sample ID: Geoff-30%G-6.mss
Specimen Number: 6
Tagged: False

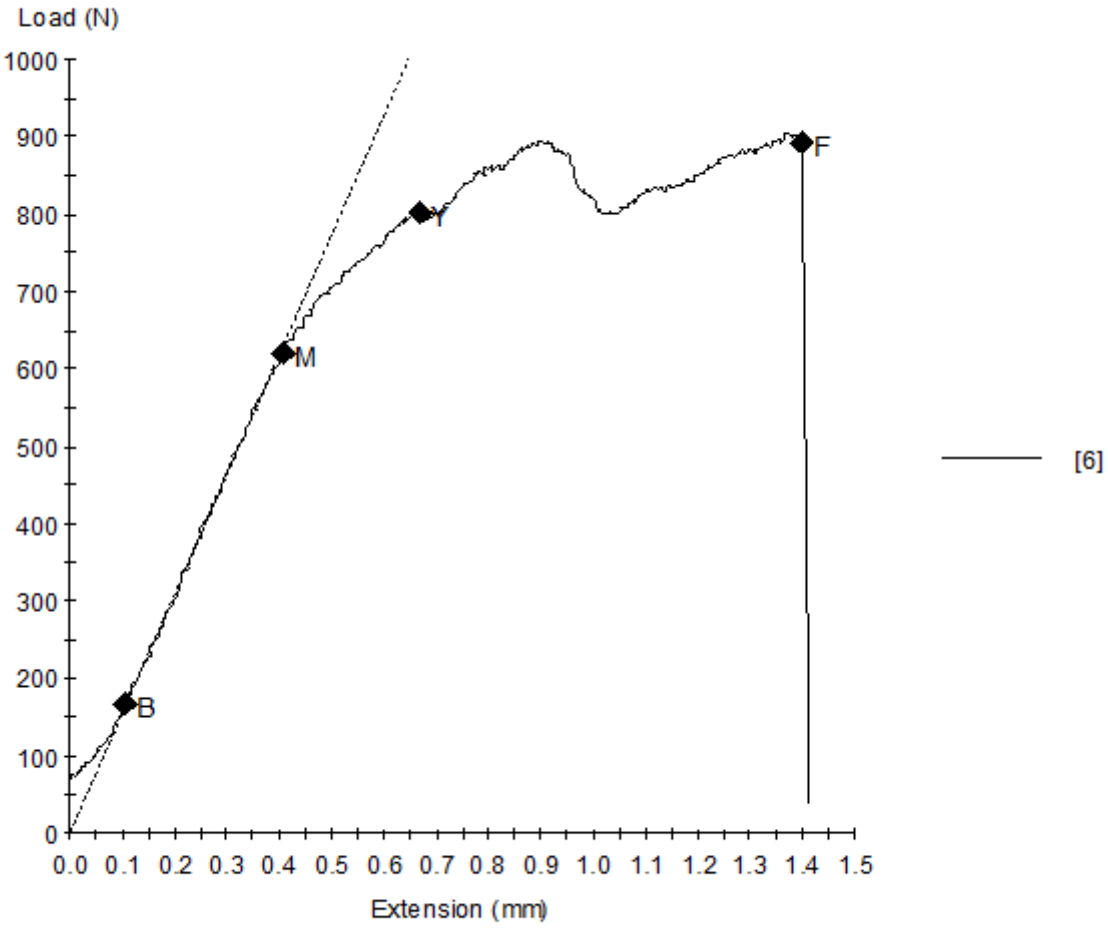

Specimen Results:

Name	Value	Units
Thickness	26.000	mm
Width	50.000	mm
Area	1300	mm^2
Peak Load	903	N
Peak Stress	0.69	MPa
Break Load	894	N
Break Stress	0.69	MPa
Elongation At Break	1.401	mm
Stress At Offset Yield	0.546	MPa
Load At Offset Yield	710.349	N

Geoff-30%G

Report Date: 26/02/2009

Test Date : 26/02/2009
Method : MMT fracture toughness Test .msm

Specimen Results:

Specimen #	Thickness mm	Width mm	Area mm^2	Peak Load N	Peak Stress MPa	Break Load N	Break Stress MPa
1	26.000	50.000	1300	806	0.62	790	0.61
2	26.000	50.000	1300	775	0.60	739	0.57
3	26.000	50.000	1300	762	0.59	732	0.56
4	26.000	50.000	1300	765	0.59	745	0.57
5	26.000	50.000	1300	761	0.59	709	0.55
6	26.000	50.000	1300	903	0.69	894	0.69
Mean	**26.000**	**50.000**	**1300**	**795**	**0.61**	**768**	**0.59**
Std Dev	**0.000**	**0.000**	**0**	**55**	**0.04**	**67**	**0.05**

Specimen #	Elongation At Break mm	Stress At Offset Yield MPa	Load At Offset Yield N				
1	0.694	0.602	782.861				
2	0.805	0.558	725.120				
3	0.640	0.519	674.764				
4	1.381	0.512	665.365				
5	1.059	0.574	746.773				
6	1.401	0.546	710.349				
Mean	**0.997**	**0.552**	**717.538**				
Std Dev	**0.338**	**0.034**	**44.232**				

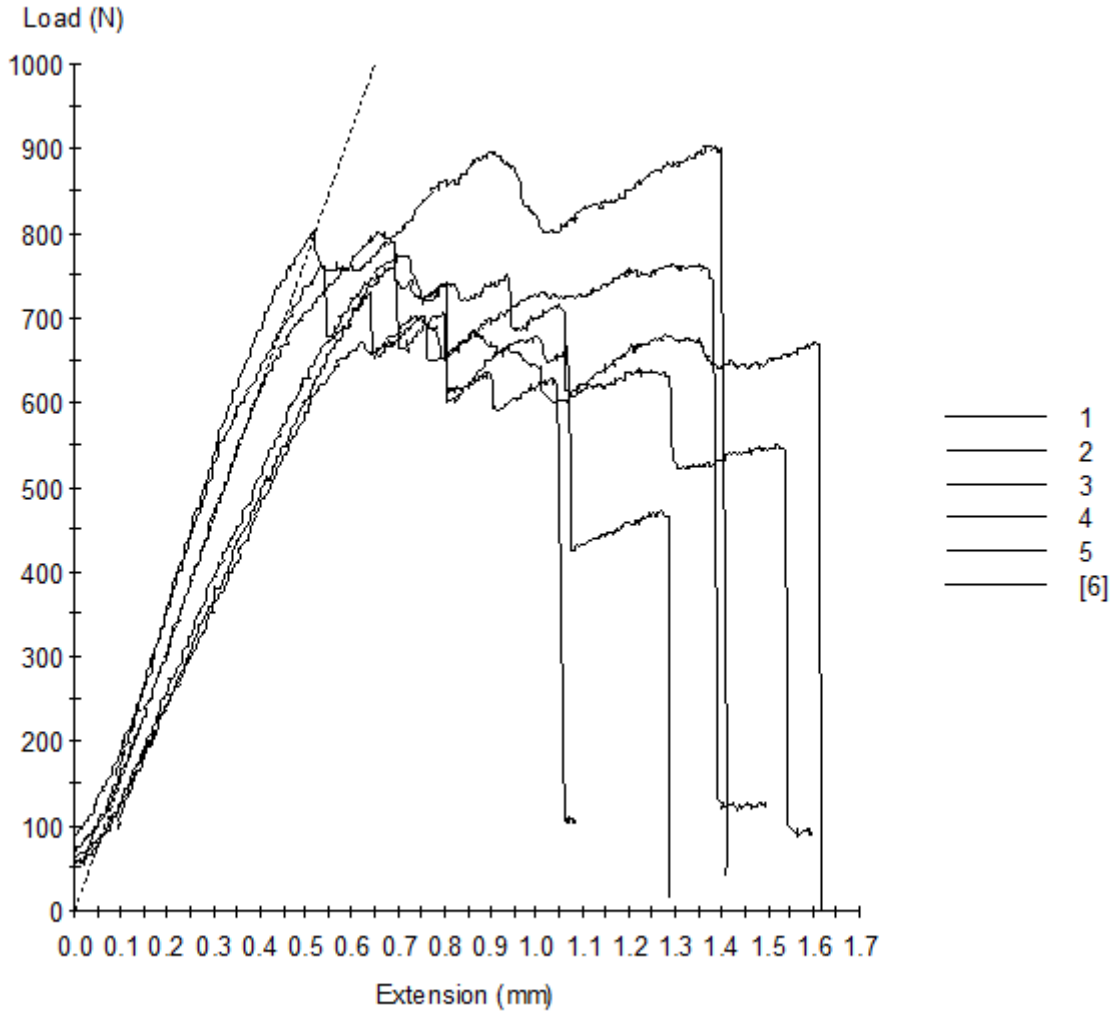
Load (N)
1000
900
800
700
600
500
400
300
200
100
0
0.0 0.1 0.2 0.3 0.4 0.5 0.6 0.7 0.8 0.9 1.0 1.1 1.2 1.3 1.4 1.5 1.6 1.7
Extension (mm)
1
2
3
4
5
[6]

Sample ID: Geoff-35%G-1.mss
Specimen Number: 1
Tagged: False

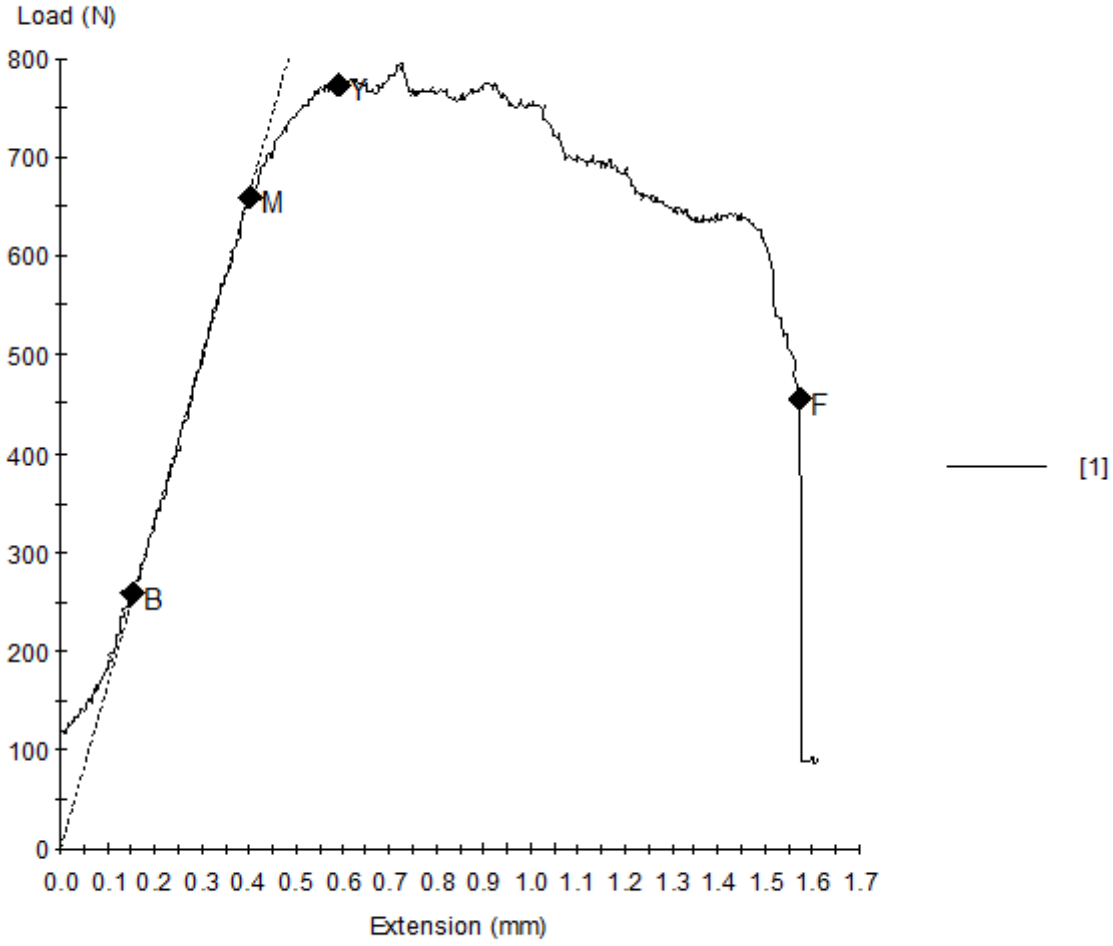

Specimen Results:

Name	Value	Units
Thickness	26.000	mm
Width	50.000	mm
Area	1300	mm^2
Peak Load	796	N
Peak Stress	0.61	MPa
Break Load	457	N
Break Stress	0.35	MPa
Elongation At Break	1.574	mm
Stress At Offset Yield	0.573	MPa
Load At Offset Yield	745.262	N

Sample ID: Geoff-35%G-2.mss
Specimen Number: 2
Tagged: False

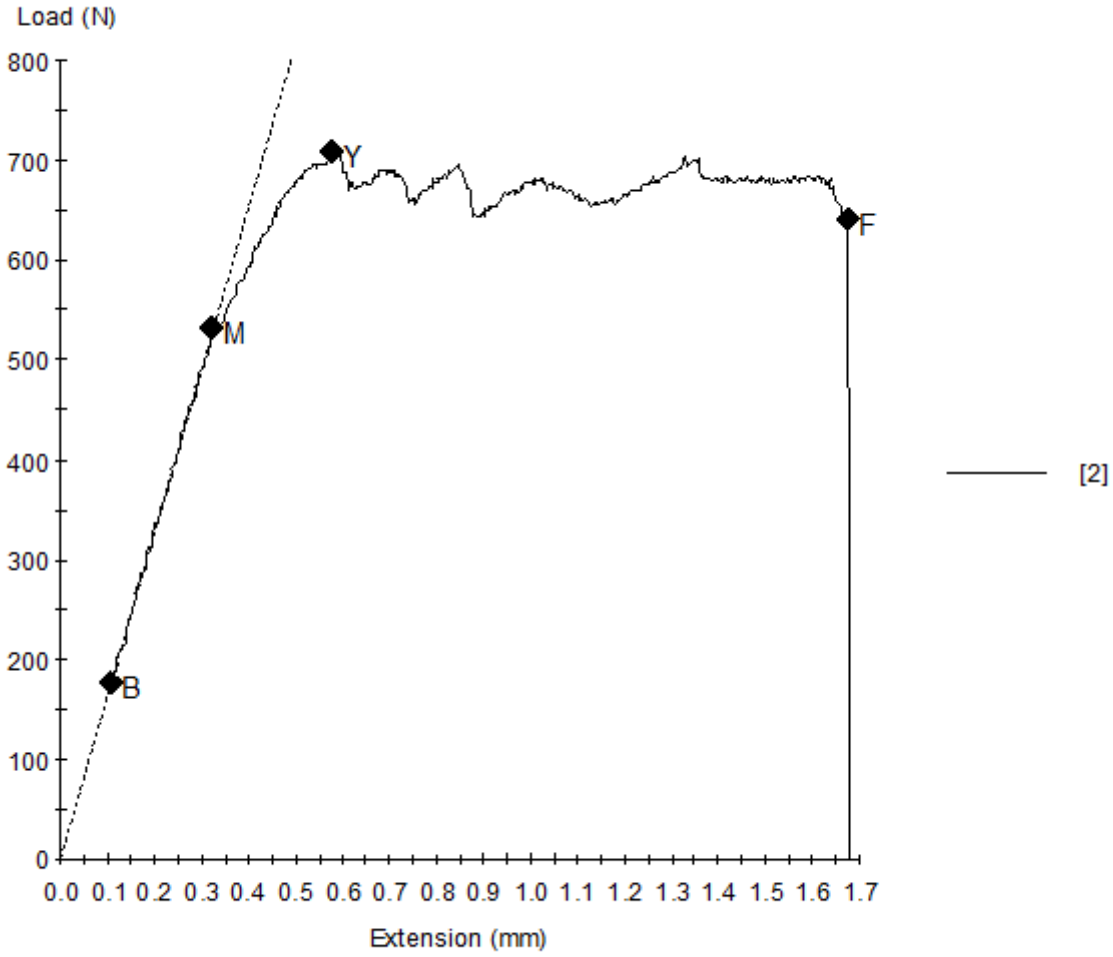

Specimen Results:

Name	Value	Units
Thickness	26.000	mm
Width	50.000	mm
Area	1300	mm^2
Peak Load	709	N
Peak Stress	0.55	MPa
Break Load	640	N
Break Stress	0.49	MPa
Elongation At Break	1.673	mm
Stress At Offset Yield	0.480	MPa
Load At Offset Yield	624.409	N

Sample ID: Geoff-35%G-3.mss
Specimen Number: 3
Tagged: False

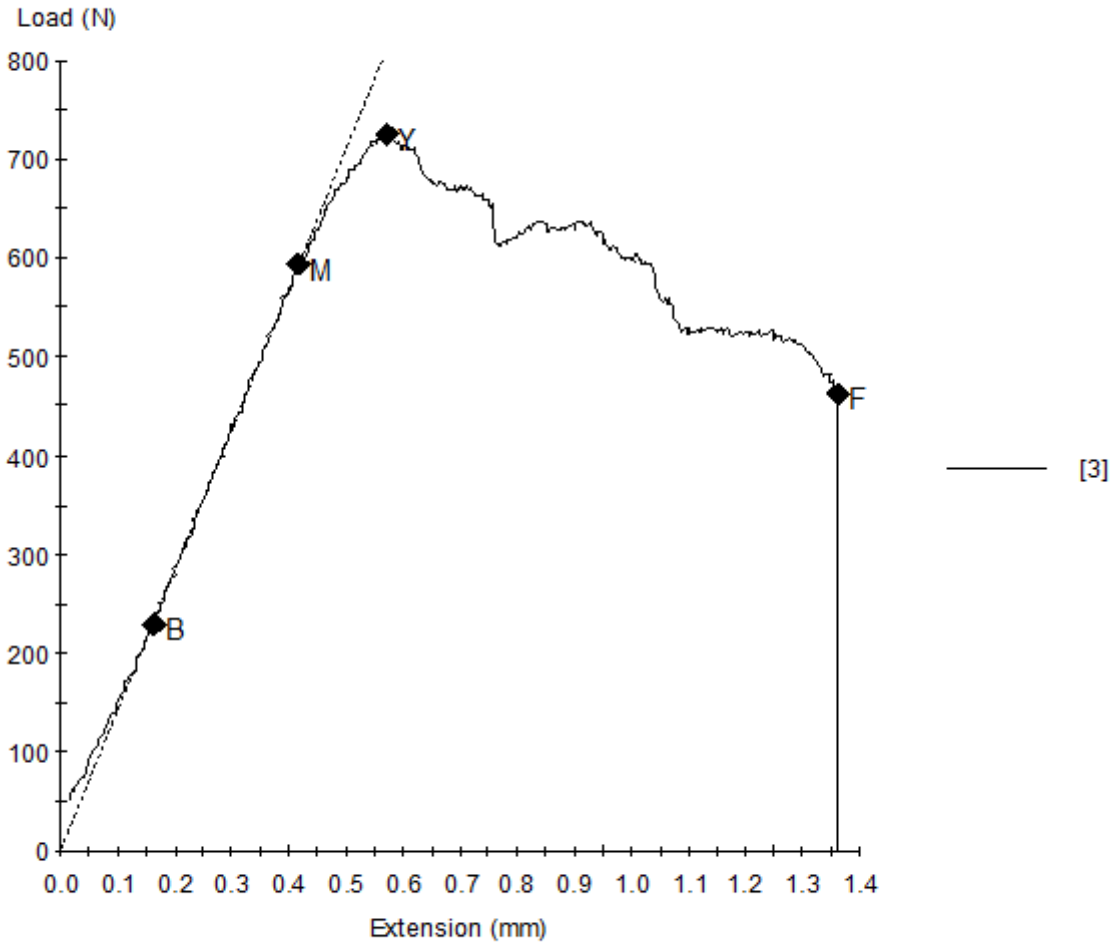

Specimen Results:

Name	Value	Units
Thickness	26.000	mm
Width	50.000	mm
Area	1300	mm^2
Peak Load	725	N
Peak Stress	0.56	MPa
Break Load	462	N
Break Stress	0.36	MPa
Elongation At Break	1.363	mm
Stress At Offset Yield	0.550	MPa
Load At Offset Yield	715.049	N

Sample ID: Geoff-35%G-4.mss
Specimen Number: 4
Tagged: False

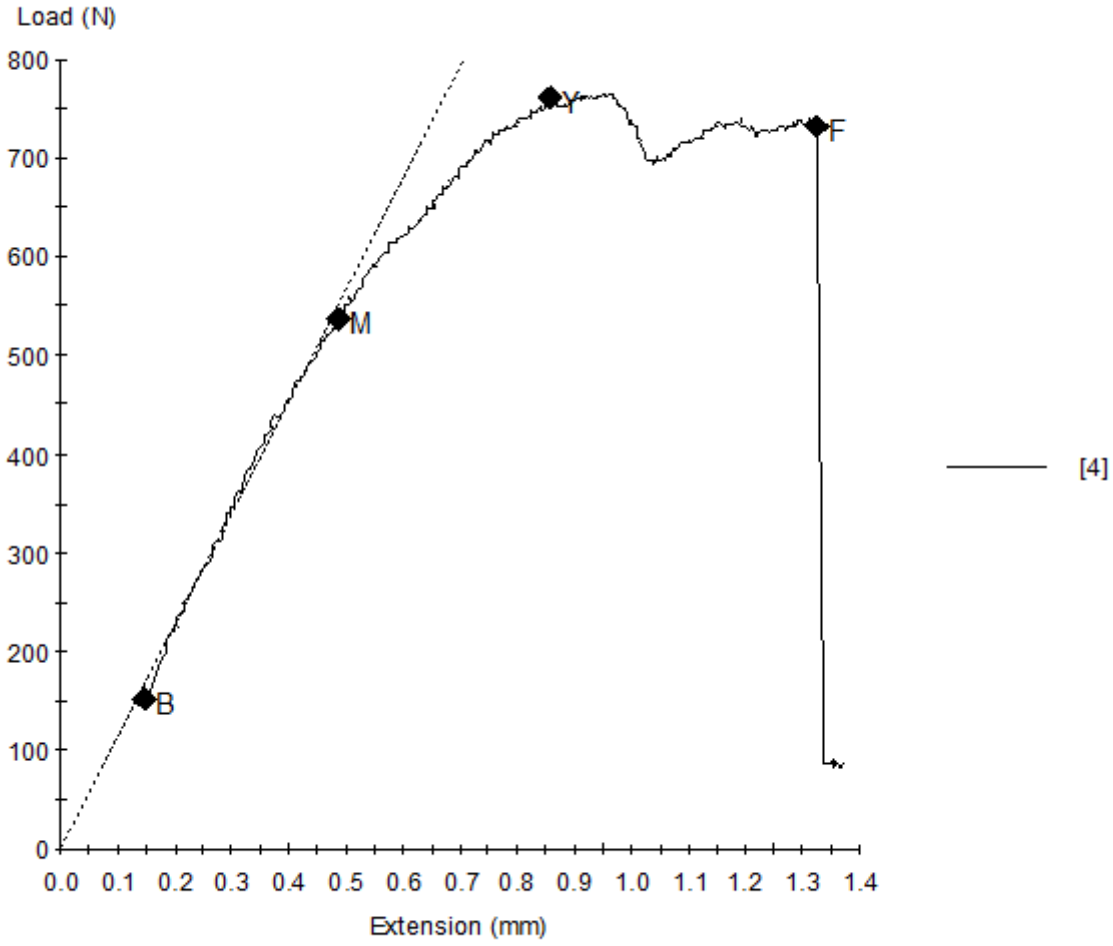

Specimen Results:

Name	Value	Units
Thickness	26.000	mm
Width	50.000	mm
Area	1300	mm^2
Peak Load	765	N
Peak Stress	0.59	MPa
Break Load	732	N
Break Stress	0.56	MPa
Elongation At Break	1.326	mm
Stress At Offset Yield	0.478	MPa
Load At Offset Yield	621.052	N

Sample ID: Geoff-35%G-5.mss
Specimen Number: 5
Tagged: False

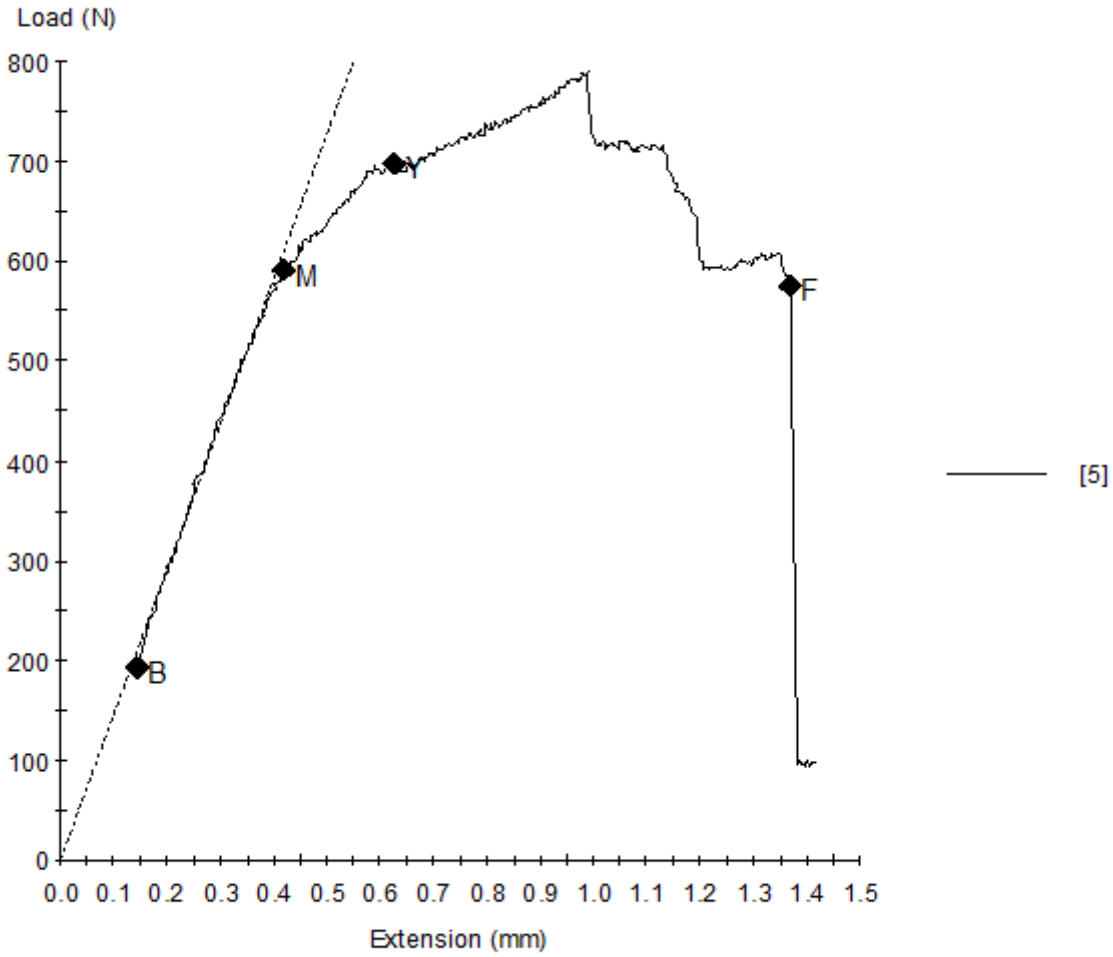

Specimen Results:

Name	Value	Units
Thickness	26.000	mm
Width	50.000	mm
Area	1300	mm^2
Peak Load	790	N
Peak Stress	0.61	MPa
Break Load	575	N
Break Stress	0.44	MPa
Elongation At Break	1.370	mm
Stress At Offset Yield	0.481	MPa
Load At Offset Yield	625.752	N

Sample ID: Geoff-35%G-6.mss
Specimen Number: 6
Tagged: False

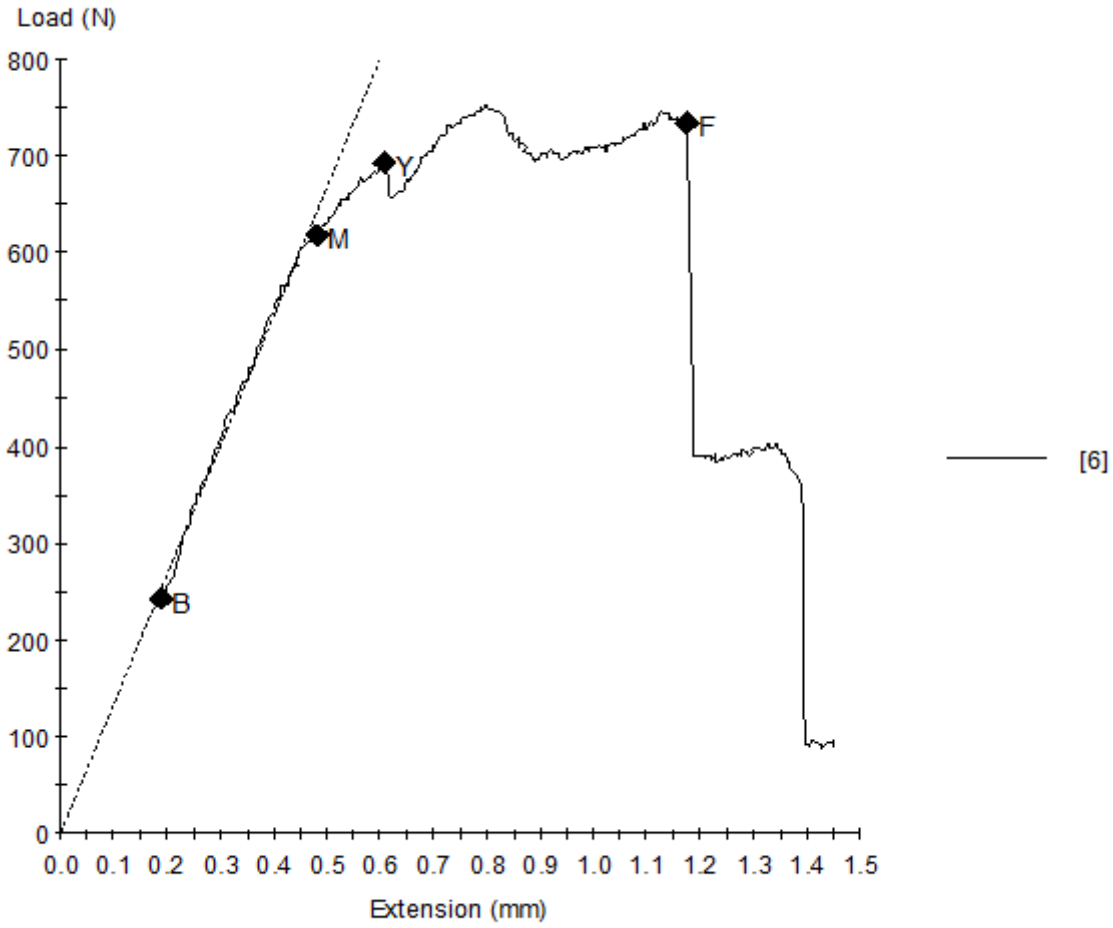

Specimen Results:

Name	Value	Units
Thickness	26.000	mm
Width	50.000	mm
Area	1300	mm^2
Peak Load	752	N
Peak Stress	0.58	MPa
Break Load	735	N
Break Stress	0.57	MPa
Elongation At Break	1.177	mm
Stress At Offset Yield	0.511	MPa
Load At Offset Yield	663.686	N

Geoff-35%G

Report Date: 26/02/2009

Test Date : 26/02/2009
Method : MMT fracture toughness Test .msm

Specimen Results:

Specimen #	Thickness mm	Width mm	Area mm^2	Peak Load N	Peak Stress MPa	Break Load N	Break Stress MPa
1	26.000	50.000	1300	796	0.61	457	0.35
2	26.000	50.000	1300	709	0.55	640	0.49
3	26.000	50.000	1300	725	0.56	462	0.36
4	26.000	50.000	1300	765	0.59	732	0.56
5	26.000	50.000	1300	790	0.61	575	0.44
6	26.000	50.000	1300	752	0.58	735	0.57
Mean	**26.000**	**50.000**	**1300**	**756**	**0.58**	**600**	**0.46**
Std Dev	**0.000**	**0.000**	**0**	**35**	**0.03**	**125**	**0.10**

Specimen #	Elongation At Break mm	Stress At Offset Yield MPa	Load At Offset Yield N				
1	1.574	0.573	745.262				
2	1.673	0.480	624.409				
3	1.363	0.550	715.049				
4	1.326	0.478	621.052				
5	1.370	0.481	625.752				
6	1.177	0.511	663.686				
Mean	**1.414**	**0.512**	**665.868**				
Std Dev	**0.180**	**0.041**	**53.035**				

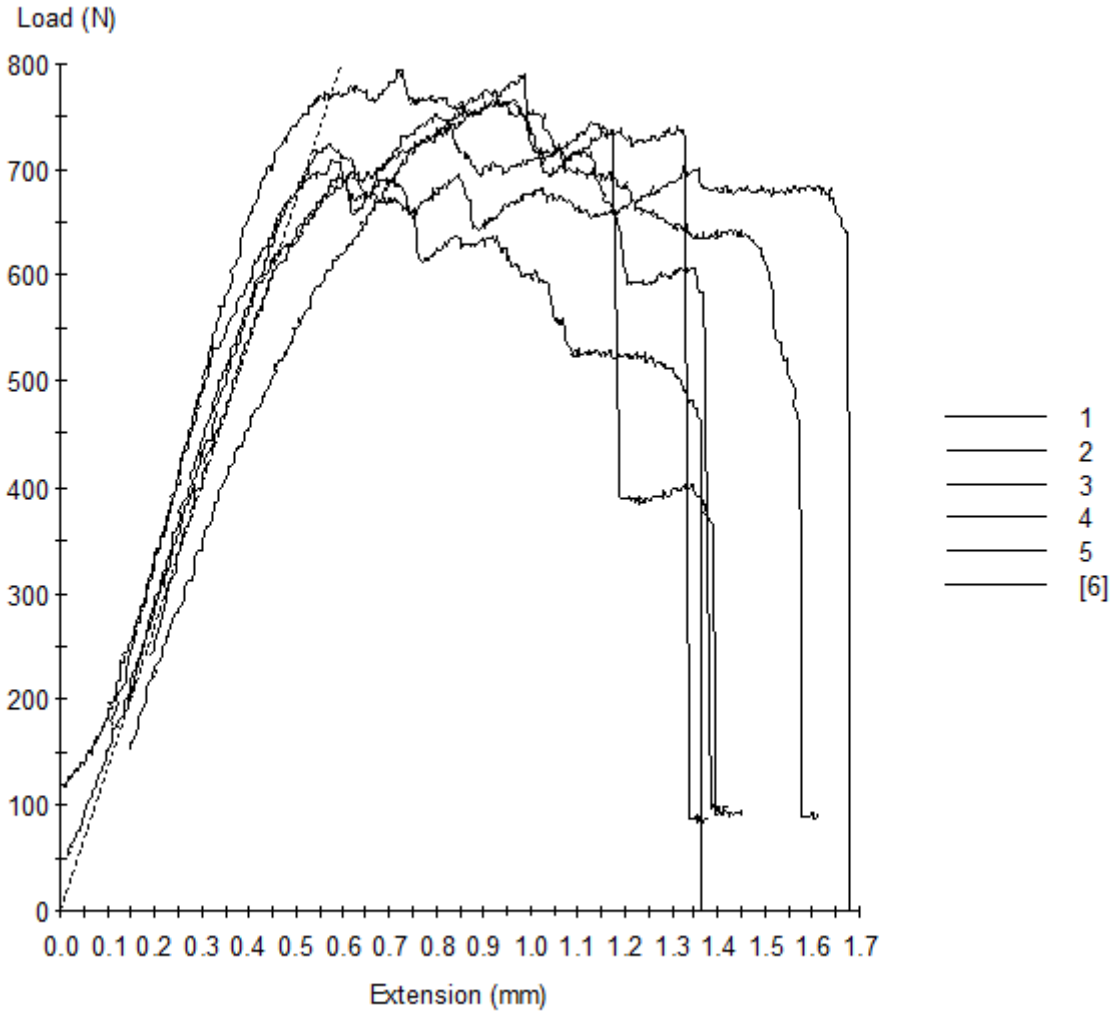
Load (N)
800
700
600
500
400
300
200
100
0
0.0 0.1 0.2 0.3 0.4 0.5 0.6 0.7 0.8 0.9 1.0 1.1 1.2 1.3 1.4 1.5 1.6 1.7
Extension (mm)
1
2
3
4
5
[6]

Appendix C – Data Analysis

Table C1: Peak Load

	F_{max} (N)							
Percentage	**0**	**5**	**10**	**15**	**20**	**25**	**30**	**35**
Specimen 1	557	757	755	943	853	829	806	796
Specimen 2	741	786	903	927	809	819	775	709
Specimen 3	505	829	765	856	846	802	762	725
Specimen 4	645	750	779	940	804	887	765	765
Specimen 5	615	783	792	953	809	943	761	790
Specimen 6	743	815	791	977	811	812	903	752

Dimensions By Design			**Actual Dimensions**	
B=		50	**B=**	48.5
W=	**1.5B =**	75	**W=**	74
H=	**0.87B =**	43.5	**H=**	38

a_1= 72

a_0= 26

ω=W/H= 1.95

$\alpha_0=a_o/W$= 0.35

$\alpha_1=a_1/W$= 0.97

Y_m*= (-0.36+5.48*ω+0.08*ω^2+(30.65-27.49*ω+7.46*ω)*B19...
...+(65.9+18.44*ω-9.76*ω)*α0^2)*((α1-α0)/(1-α0))^0.5
= 17.524

K_{ICSB}= Fmax*Ym*/B*√W

Table C2: Fracture Toughness

	K_{ICSB} (MPa√m)							
Percentage	**0**	**5**	**10**	**15**	**20**	**25**	**30**	**35**
Specimen 1		30.842	30.761	38.420	34.754	33.776	32.839	32.431
Specimen 2	30.190	32.024	-	37.768	32.961	33.368	31.576	-
Specimen 3		-	31.168	-	34.468	32.676	31.046	-
Specimen 4	26.279	30.557	31.739	38.298	32.757	-	31.168	31.168
Specimen 5		31.902	32.268	38.828	32.961	-	31.005	32.187
Specimen 6	30.272	33.205	32.227	39.806	33.042	33.083	-	30.639
Fracture Toughness	29.00	31.71	31.63	38.62	33.49	33.23	31.53	31.61
Standard Dev.	3.92	1.06	0.66	0.76	0.88	0.46	0.77	0.85

Appendix D – Eurotherm Controller Instructions

STERIDIUM

www.steridium.com sales@steridium.com

USER MANUAL

EUROTHERM 3200 SERIES CONTROLLERS

This manual covers the 3200 series of Eurotherm controllers. The images shown in the manual will vary and might not be the same as the controller installed on your Steridium product.

5.8.2 To Operate the Programmer

Operation of the programmer is the same as the timer.

Operation	Action	Indication
To Run a program	Press and quickly release ▼ + ▲	Beacon -- RUN = On Scrolling display - TIMER RUNNING
To Hold a program	Press and quickly release ▼ + ▲	Beacon -- RUN = Flashing Scrolling display - TIMER HOLD
To Reset a program	Press and hold ▼ + ▲ for more than 1 second	Beacon -- RUN = Off If End Type = Off then OFF will be displayed at the end of the program
	Program ended	Beacon -- RUN = Off SPX = On if End Type = SP2 Scrolling display - TIMER END
Repeat the above to Run the programmer again (Note: it is not essential to reset it after the End state is reached)		

Programs can also be operated from the '**T.STAT**' parameter found in the level 2 parameter list.

5.8.3 To Configure the Programmer

Select Access Level 2 – see section 5.1.

Operation	Action	Indication	Notes
Configure the Timer as a Programmer	Press ⟳ to select 'TM.CFG' Press ▼ or ▲ to 'ProG'		
Set the Resolution	Press ⟳ to select 'TM.RES' Press ▼ or ▲ to 'Hour or 'min"		In this example Dwell is set in hours and Rate in units/hour
Set the Threshold	Press ⟳ to select 'THRES' Press ▼ or ▲ to adjust		In this example the dwell periods will not start until the PV is within 5 units of the setpoint
Set the action when the programmer times out	Press ⟳ to select 'END.T' Press ▼ or ▲ to 'OFF' or 'SP2' or 'dwEll'		In this example the controller will continue to control indefinitely at the last setpoint. OFF will turn the output power off and SP2 will control at setpoint 2

5. Operator Level 2

Level 2 provides access to additional parameters. It is protected by a security code.

5.1 To Enter Level 2

1. From any display press and hold ⓟ.
2. After a few seconds the display will show:-

3. Release ⓟ.
   (If no button is pressed for 45 seconds the display returns to the HOME display)
4. Press ▲ or ▼ to choose LEu 2 (Level 2)

5. After 2 seconds the display will show:-

6. Press ▲ or ▼ to enter the pass code. Default = '2'

7. If an incorrect code is entered the controller reverts to Level 1.

5.2 To Return to Level 1

1. Press and hold ⓟ
2. Press ▼ to select LEu 1

The controller will return to the level 1 HOME display. Note: A pass code is not required when going from a higher level to a lower level.

5.3 Level 2 Parameters

Press ⓒ to step through the list of parameters. The mnemonic of the parameter is shown in the lower display. After five seconds a scrolling text description of the parameter appears.

The value of the parameter is shown in the upper display. Press ▲ or ▼ to adjust this value. If no key is pressed for 30 seconds the controller returns to the HOME display

Backscroll is achieved when you are in this list by pressing ▲ while holding down ⓒ.

The following table shows a list of parameters available in Level 2.